Packed-Bed Reactor Study of NETL Sample 196c for the Removal of Carbon Dioxide from Simulated Flue Gas Mixture

James S. Hoffman [1], Sonia Hammache [1, 2], McMahan L. Gray [1], Daniel J. Fauth [1], and Henry W. Pennline [1]

[1]U.S. Department of Energy
National Energy Technology Laboratory
P.O. Box 10940
Pittsburgh, PA 15236

[2]URS
PO Box 618
Library, PA 15129

Abstract

An amine-based solid sorbent process to remove CO_2 from flue gas has been investigated. The sorbent consists of polyethylenimine (PEI) immobilized onto silica (SiO_2) support. Experiments were conducted in a packed-bed reactor and exit gas composition was monitored using mass spectrometry. The effects of feed gas composition (CO_2 and H_2O), temperature, and simulated steam regeneration were examined for both the silica support as well as the PEI-based sorbent. The artifact of the empty reactor was also quantified. Sorbent CO_2 capacity loading was compared to thermogravimetric (TGA) results to further characterize adsorption isotherms and better define CO_2 working capacity. Sorbent stability was monitored by periodically repeating baseline conditions throughout the parametric testing and replacing with fresh sorbent as needed. The concept of the Basic Immobilized Amine Sorbent (BIAS) Process using this sorbent within a system where sorbent continuously flows between the absorber and regenerator was introduced. The basic tenet is to manipulate or control the level of moisture on the sorbent as it travels around the sorbent circulation path between absorption and regeneration stages to minimize its effect on regeneration heat duty.

Background/Introduction

Carbon Capture and Storage (CCS) is a viable alternative to reduce the emissions of the greenhouse gas carbon dioxide (CO_2) from large point sources. It holds the potential to provide deep reductions in greenhouse gas emissions. CCS is nominally a two-step process where the capture of carbon dioxide from a gas stream is followed by permanent storage. The capture step for carbon dioxide represents a major cost in the overall process.

Of particular interest are power generation point sources that use fossil fuels. Since nearly one-third of the anthropogenic CO_2 emissions are produced by these facilities, conventional coal-burning power plants present opportunities where carbon can be removed and then permanently stored. At the current time, pulverized coal-fired-base steam cycles have been the predominant electric power generation technology and will continue to be used in the near future. Post-combustion technologies for capturing CO_2 will need to be applied to new more efficient coal-fired facilities and will need to be retrofitted onto existing plants.

For coal-fired power plants, the conventional scrubbing system that is currently the comparative baseline for all other CO_2 capture technologies is monoethanolamine (MEA) scrubbing. This wet scrubbing process removes the CO_2 in an absorber and then regenerates the spent scrubbing liquor in a vessel by indirectly heating the solution with plant steam. Although there have been large scale commercial demonstrations of this technology, the process has several disadvantages, such as a high heat of reaction, low working capacity, corrosiveness of the solution, the susceptibility of being poisoned, and most notably, its need to be in an aqueous solution. This latter disadvantage results in a large energy need to regenerate the spent solution, especially the sensible heating of the water, which is about 70-wt% of the solution. The water is recognized as an inert carrier between the absorption and regeneration steps. Another energy loss while regenerating the spent MEA solution includes evaporative heat loss of vaporizing liquid water.

One type of novel CO_2 capture technology that can be applied to various gas streams has, as a basis, dry regenerable solid sorbents. Examples of these types of sorbents are zeolites, activated carbon, alkali/alkaline earth metals, immobilized amines, metal organic framework, etc. A specific sorbent class that shows significant advancement are amine-based solid sorbents, such as Basic Immobilized Amine Sorbents (BIAS). These sorbents consist of amines (primary, secondary, tertiary, or a combination thereof) deposited onto a porous substrate. The manner of deposition is important and can be random or structured deposition of the amine onto the support (silica, polymer, etc.). The sorbent process may act in a similar fashion to the wet scrubbing in that the sorbent would be transported between the absorption step and the regeneration step and in that the sorbent is regenerated by a temperature-swing application.

One of the main benefits in using the solid sorbent can be the elimination of the sensible heat for the liquid water as compared to aqueous MEA solution. A secondary benefit lies in the lower heat capacity for the solid versus the liquid solvent, also serving to lower the sensible heat. More CO_2 can be absorbed on a weight or volume basis with the amine-based solid sorbents, so the sorbent system is capable of a significant decrease in the heat duty for the regeneration step. A lower cost of energy service as compared to amine wet scrubbing may also result. Thus amine-based solid sorbents have the capability to improve the overall energetics of CO_2 capture.

Effective amine-based solid sorbent methodologies are needed for carbon dioxide capture, whether the capture occurs in combustion power generation systems, or in other applications, such as natural gas cleanup. Because of the high concentration of carbon dioxide in any of these feed streams, a large quantity of the gas will be reacting with the sorbent and thus produce considerable amounts of exothermic heat. This heat must be removed from the sorbent to prevent temperature instability within the reactor, to assure the sorbent will operate at optimum temperature, and to eliminate the potential degradation of the sorbent because of high temperature excursions. Reactor designs are available to eliminate heat problems. However, the presence of moisture in the various process gas streams can have a tremendous impact on the energetics of the system. Indirect/ direct steam regeneration will have a significant advantage in the regeneration step with respect to CO_2 regeneration with respect to some of these BIAS sorbents, and adsorption/ desorption, as related to water within the process steps, will potentially represent an energy loss unless controlled. It would be advantageous to provide a methodology whereby the CO_2 absorption and water adsorption of amine-based solid sorbents were effectively compensated for, and regeneration energy losses minimized.

Experimental

Sample preparation for several sorbents has been detailed in prior publications.(a-c) Various amines are physically immobilized onto a support using solvent (methanol) and then vacuum dried with a rotary evaporator device. In this study, sorbent was synthesized by impregnating polyethylenimine (PEI) onto silica (SiO_2) support. PEI (Mn-423) was supplied through Sigma-Aldrich USA. Reagent grade methanol was received from Sigma Aldrich USA. Both PEI and methanol were used as received in the preparation of the sorbent. The silica support was obtained from Fuji Silysia and is CARiACT G-10 high pore volume series (G-10 HPV, Lot # GH080702, particle size 75-500 µm, surface area 294 m^2/g, pore volume 1.77 ml/g, pore diameter 24.0 nm). In a typical synthesis, a homogeneous solution of PEI and methanol was added to SiO_2 to form a slurry. The slurry was then placed in a rotary evaporator set to 80°C and left to rotate for 1-2 hr. During rotation, methanol was removed with a vacuum pump and the resulting solid was refrigerated. The target PEI loading within the sample was 50wt%. The final immobilized amine sample bears the designation 196c and consists of approximately 45wt% PEI and 55wt% G-10 silica. For experimental consistency, a large homogenous batch of material was made and drawn from during the test campaign. As a follow-up effort to this study, this same material has been studied most recently to further evaluate the effect of steam regeneration.(d)

Experiments were conducted in a packed bed reactor, details of which have been described elsewhere (b) but are summarized here. A flow diagram of the unit appears in Figure 1. Photographs of the reactor with the clam shell furnace opened are shown in Figure 2. This furnace was utilized in the earliest sorbent studies but was more recently replaced with a flexible insulated blanket heater obtained from HTS/Amptek Company (HeatingJackets.com, model A510-USDE0309-32 with type K T/C, 110W, 120 V). Simulated flue gas mixtures consisted of carbon dioxide in balance helium using certified calibrated cylinder gases obtained from Butler Gas. Feed gas flow rate was established using calibrated mass flow controllers (Brooks 5850e). The feed gas could be passed through a sparger vessel to humidify the stream if desired, or it could simply bypass the sparger for dry feed conditions. The sparger was heat traced and insulated and had a Type K thermocouple inserted into the liquid reservoir to measure the bath temperature. A bypass on the reactor was also installed to allow steady state feed conditions to be obtained before subjecting the sorbent sample to the feed gas flow for either the absorption or desorption/regeneration stages.

One gram of dry sample was pre-weighed and loaded into the test section. Glass wool plugs encapsulated the loaded sample within the reactor tube (3/8" OD) to keep it stationary within the vertical tube. Gas flow passed vertically up through the bed. A Type K thermocouple (1/16" dia) was positioned immediately above the upper plug, representing the bed exit temperature. Gas composition was continuously measured downstream of the reactor using a Pfeiffer Omnistar® mass spectrometer (MS). Parent ions for helium, water, and carbon dioxide were scanned for identification and quantification. Carbon dioxide calibration was performed on a dry basis using the certified cylinder standard. Water calibration was performed using helium passed through the sparger and assuming equilibrium saturation for the measured sparger bath temperature and sparger pressure (approximated as the measured barometric pressure in the lab since negligible back pressure exists in the unit). The back pressure was monitored downstream of the MS sampling location using a pressure transmitter and typically was 0.1-0.2 psig. Upon cooling the exit gas flow to ambient temperature, a condensate pot was used to collect excess moisture prior to venting the gas to hood exhaust. All vessels and ductwork downstream of the sparger were heat traced and insulated to prevent condensation of elevated moisture in the gas stream.

Concentration versus time data acquired with the MS was exported into Excel spreadsheets. The breakthrough curves were integrated within the spreadsheets using discrete summation of the material balance equations to arrive at totalized gas amounts absorbed/desorbed from the sample. The material balance equations considered the effect of volume change across the reactor. The background carrier gas, helium, acts as a tracer since it does not absorb/desorb from the sample, and is used to account for change in total gas flow rate as a result of other components (CO_2, H_2O) absorbing or desorbing from the solid. Totalized gas amounts (reported in moles) were normalized by the weight of loaded sample, such that capacity is reported as moles of gas per kg of sample charged to the reactor.

The overall procedure generally used for experiments is hereby described, with specific variations in procedure detailed during the discussion of results. After the sample was charged to the reactor, it was dried and activated under helium purge near 105 °C. The sample was then cooled to the desired absorption temperature of interest, generally 60°C. The MS was calibrated for CO_2 using a standard gas blend of 10%CO_2/He. If the feed gas was to contain moisture, the MS was calibrated for H_2O using pure helium passed through a heated water bath. With the reactor off-line, a steady-state calibrated feed gas composition was established. The absorption stage would commence with manual valve switch to bring the reactor on-line. The absorption was typically held for 30-60 min, or longer as necessary, until the exit feed composition approached the inlet feed composition, signifying bed saturation. The reactor was then switched off-line, and the feed gas was switched to pure helium to purge residual CO_2 and H_2O from the system. Upon complete purge of residual gases, the reactor was switched on-line under pure helium flow to begin an isothermal desorption stage, typically for one hour. The desorption temperature was maintained the same as was used during the absorption stage, typically 60°C. The desorption stage represents an isothermal pressure swing desorption step. Upon completion of one hour desorption and while still under pure helium flow, the reactor temperature was ramped 2°C/min to 105°C and held for approximately 15 min at the upper temperature. This stage represents temperature swing regeneration. Upon completion of the sorbent regeneration, the reactor was switched off-line and cooled, signifying the completion of the cycle. Once cooled to the absorption temperature of interest for the next cycle, the reactor was briefly purged under pure helium and then switched off-line so as to establish the next absorption feed gas composition. Recalibration of the MS was conducted between cycles on an as-needed basis.

Discussion of Results

A series of parametric tests were conducted to elucidate the effects of various process parameters on the performance of sorbent 196c to capture CO_2 as well as its release via regeneration. To conserve sample, a sequence of tests would be performed with the same initial load of sample. A baseline condition(s) was established and repeated intermittently throughout the testing matrix so as to establish that sorbent performance was being maintained throughout the test sequence. If a noticeable drop-off in CO_2 loading capacity was observed, the testing was halted and a new sample was loaded into the system before commencing with additional tests. In the case of this particular sorbent having baseline CO_2 adsorption loadings near 3.2 moles CO_2/kg, new sample was substituted when loadings approached values around 2 moles CO_2/kg. Depending on the specific matrix of conditions examined, this substitution could occur after perhaps 6-12 cycles.

The baseline condition chosen used a feed gas of 10%CO_2 in balance helium under dry conditions (i.e., sparger was bypassed). The initial baseline absorption temperature was 45°C, but after some months of testing, it was further raised to 60°C. This was partially motivated by the desire to better match the post-combustion condition of the flue gas exiting a flue gas desulfurization unit in an actual electric utility. The feed gas flow was 100 sccm, both for the absorption and desorption/regeneration stages. The gas composition was 10%CO_2 in balance helium for absorption whereas pure helium was flowed for the desorption and regeneration stages.

Prior to conducting the absorption, the reactor would remain off-line and the CO_2 span gas was flowed through the system for about an hour in order to calibrate the MS. Calibrations were performed for mass tune, gas specific intensity, and offset on the MS. Shown in Figure 3 is an example baseline condition for sample 196c. The first cycle was conducted at 45°C absorption and the second cycle was conducted at 60°C absorption.

The absorption stage was typically held for approximately an hour or until the exit concentration closely matched the feed gas concentration. At this point, the reactor would be switched off-line and the feed gas flow was switched to pure helium. Once the residual CO_2 was purged from the system, the reactor was switched on-line to begin the desorption stage. The reactor was held isothermal (at the same temperature as the absorption temperature) for exactly one hour. This defines the desorption stage and represents a swing in partial pressure of CO_2 via helium gas sweep. After the 1-hr desorption stage, a temperature swing was initiated to begin the regeneration stage. The program temperature ramp (2°C/min) slowly raised the temperature to 105°C, followed by an isothermal hold period at 105°C. After completion of the first cycle, the reactor would be cooled back down under helium purge to the next desired absorption temperature to initiate another cycle.

As can be seen in Figure 3, CO_2 breaks through the bed after about 10-15 minutes but requires nearly an hour to reach complete absorption saturation. Some of the CO_2 is liberated during the desorption step but the temperature swing of regeneration appears necessary to liberate the remainder of the sorbed CO_2. This suggests that some sites weakly bond CO_2 whereas other sites more strongly bond CO_2 and require temperature swing to liberate.

The CO_2 absorption loading for the baseline condition tested intermittently during the parametric program is shown in Figure 4 for 45°C and Figure 5 for 60°C. The baseline absorption loading for 196c has typically been in the range of 3.2-3.3 moles CO_2/kg. Both figures denote when fresh sample was reloaded into the system, as well as the other non-baseline test conditions of interest that were performed throughout the testing periods. The non-baseline tests are discussed in further detail in subsequent sections, but the non-baseline conditions are listed to help elucidate any stability issues that may be apparent in the repeated baseline. It appears that testing with moisture, particularly high levels (90%H_2O) at 105°C to simulate steam sweep, leads to a significant degradation in CO_2 absorption loading. However, even thermal cycling under dry conditions can also lead to slight drop-off in CO_2 absorption loading. Reloading fresh sample into the system results in a return to initial CO_2 loading. It must be emphasized that the test program was planned and conducted with the aim of gathering performance information for various parameters systematically varied, rather than strictly evaluating sorbent stability.

Baseline material balances for CO_2 are plotted in Figure 6 for 45°C and Figure 7 for 60°C. CO_2 was totalized for the absorption, desorption, and regeneration stages. Summation of the desorption and regeneration quantities are denoted as the "Total" CO_2 liberated. Since numerous tests were conducted at 60°C and Figure 7 is visually congested, the data was replotted in Figure 8 showing only the absorption and total liberated quantities. Comparison of the absorption and total fragments demonstrate that good material balances were generally obtained throughout the testing, even when there was noticeable drop-off in CO_2 loading. This helps validates that the sorbent was indeed degraded at various times throughout the testing.

It appears that slightly higher CO_2 loadings are achieved at 60°C versus 45°C, but any apparent difference (on the order of several tenths of a mole/kg) could be considered within the scatter of data. Isotherm data that was obtained in a TGA is presented in a future section and helps validate that the 45°C and 60°C isotherm curves are indeed close, with the 60°C curve having slightly higher CO_2 loadings. However, the distribution of the liberated CO_2 is greatly affected when comparing 45°C versus 60°C data. Figure 6 shows that roughly one third is liberated by quasi-pressure swing (desorption under helium) at 45°C and the remaining two-thirds is liberated by temperature swing. However, the distribution is reversed at 60°C in Figure 7, with roughly two thirds liberated by pressure swing and the remaining one-third liberated by temperature swing.

Hence, the active sites for weakly bonded versus strongly bonded CO_2 are strongly influenced by just a small change in temperature from 45°C to 60°C.

Effect of absorption temperature

The effect of raising the adsorption temperature from 60°C to 105°C under dry conditions using 10%CO_2/He is shown in Figure 9. The first cycle represents the baseline condition at 60°C, and the next two cycles were performed isothermal at 105°C with switching of the feed gas between 10%CO_2/He and 100%He. It is visually apparent that the CO_2 breakthrough time is much shorter for the higher temperature cycles with a correspondingly lesser amount of CO_2 regenerated with pure helium sweep. The material balances for the three cycles are shown in Figure 10. The amount of CO_2 absorbed is in fairly good agreement with the amount of CO_2 desorbed for all cycles. However, the higher temperature of 105°C (i.e., the regeneration temperature) clearly shows that a significant amount of CO_2 will still absorb at this temperature, roughly 1.2 moles/kg, in the presence of 10%CO_2/He. The working capacity of the sorbent is defined as the difference in loading between the rich loading (i.e., the absorption capacity under flue gas conditions) and the lean loading (i.e., the absorption capacity under regeneration conditions). The type of sweep gas employed during regeneration, whether CO_2 recycle or inert gas sweep, will affect the lean loading attained during regeneration. Thus for the above example, the working capacity of the sorbent will be greatly reduced by about 40% when attempting to regenerate in a CO_2 partial pressure of 0.1 atm versus pure helium sweep regeneration. Results in subsequent sections show that regeneration under pure CO_2, an ideal regeneration scenario, would have a further reduction in working capacity for this particular sorbent.

Effect of CO_2 partial pressure and absorption temperature

The effect of raising the CO_2 partial pressure in the feed gas from 10%CO_2/He to 90%CO_2/He under dry conditions for various adsorption temperatures is shown in Figure 11. The first cycle is similar to the baseline condition at 45°C, only with higher CO_2 feed concentration. The same temperature programmed desorption and regeneration is employed for the remainder of the first cycle. The next two cycles were performed isothermal at 105°C with switching of the feed gas between 90%CO_2/He and 100%He.

The experimental procedure used for testing with 90%CO_2/He is described. The MS was initially calibrated using the lower span gas standard (10%CO_2/He). The feed gas was then switched to the higher span gas standard (90%CO_2/He). The mass flow controller was also calibrated for each gas standard to yield a desired feed flow of 100 sccm. It was generally found that the MS using high span gas standard was in very close agreement (typically indicated a CO_2 value around 89%) without recalibration. Hence it was concluded that the MS signal was highly linear over a large dynamic range and recalibration to the higher span standard was deemed not necessary. Thus the procedure was to calibrate at the low CO_2 standard and then utilize the high span gas for the remainder of the test day. This initial calibration is not shown in Figure 11.

Another consideration with using 90%CO_2/He concerns the dead gas volume of the reactor leg. A future section near the end of the discussion of results will describe in detail the artifact of the reactor under various conditions of temperature and feed gas concentration. To briefly summarize, the empty reactor has about 0.06 moles CO_2/kg when integrating the breakthrough curve using 10%CO_2/He. This was considered negligible when evaluating sorbents having CO_2 capacity in excess of 3 moles CO_2/kg, and hence no correction to the raw data was made for the low CO_2 span gas tests. However, when using a feed gas that is nine times more concentrated in CO_2, the dead volume of the reactor is no longer negligible in comparison to the raw data. This is logical just from an ideal gas law consideration, but the dead volume was independently measured and found to range around 0.50-0.55 moles CO_2/kg depending on temperature. This is consistent and roughly nine times larger than the low span gas capacity of 0.06 moles CO_2/kg.

The uncorrected material balances for the three cycles are shown in Figure 12. The amount of CO_2 absorbed is in fairly good agreement with the amount of CO_2 desorbed for the high temperature cycles, but lesser agreement was obtained for the 45°C cycle. The zero volume artifact was subtracted from the raw data and re-plotted in Figure 13. The correction factor was 0.55 moles CO_2/kg for the 45°C cycle and 0.5 moles CO_2/kg for the 105°C cycles. Note that in the case of the 45°C cycle having two stages of liberating CO_2, all of the subtracted artifact was apportioned to the pressure swing desorption stage since it occurred first before the temperature swing regeneration stage. It visually appears in Figure 11 that the absorption breakthrough times are shorter for the 90%CO_2/He feed versus the 10%CO_2/He feed cases (Figure 9). This is intuitively logical since a higher flux (flow rate) of CO_2 is being fed into the reactor, and therefore a shorter period of time should be required to occupy the available sites. When comparing conditions having the same temperature but different CO_2 feed levels in Figure 9 and Figure 11, the CO_2 loadings are higher with increased CO_2 feed levels. To help clarify the effects of temperature and CO_2 partial pressure on loadings, the following section was developed to systematically create adsorption isotherms.

Comparison of Packed-Bed Reactor CO_2 capacity data with TGA adsorption isotherms

A series of tests were previously conducted in a TGA reactor using sample 196c. (e) A prime goal of the testing was to create CO_2 adsorption isotherms at various partial pressures of CO_2 for a given constant temperature. The TGA has an upstream sparger that can deliver moisture into the feed gas, but only dry tests are presented in order to make comparisons with the dry packed-bed data. The intent of the TGA testing was to acquire a data base such that a kinetic model could be ultimately developed.

Given in Figure 14 are TGA isotherms acquired at five different CO_2 partial pressures and six different adsorption temperatures for sample 196c. The data points are curve-fitted using a logarithmic equation. As can be seen, higher partial pressure of CO_2 favors higher CO_2 capacity, with stronger dependence (i.e., slope) at lower partial pressure of CO_2. The temperature dependence of the isotherms passes through an optimum temperature near 60°C to achieve maximum CO_2 loading. This temperature is well suited to match the flue gas desulfurization exit temperature in an electric utility. As higher temperatures are examined, and are thus approaching reaction reversibility or regeneration, the CO_2 capacity is lower.

Since packed-bed tests were conducted at 45°C, 60°C, and 105°C, and TGA isotherms exist for slightly different temperatures, the TGA data was mathematically manipulated to create 45°C and 105°C isotherms. The 45°C isotherm was created by interpolation of the 40°C and 50°C isotherm data. The data was averaged to create 45°C data which was then logarithmically curve-fitted to form an isotherm. The 105°C isotherm was created by extrapolation of the 80°C and 100°C isotherm data, which was then curve-fitted. The addition of the two isotherms to the TGA data is shown in Figure 15. Figure 16 is the final subset of the three isotherms of interest at 45°C, 60°C, and 105°C to which packed bed results are compared.

Figure 17 show comparison of the packed-bed results with the TGA isotherms. Open symbols designate packed-bed measurements whereas closed symbols represent TGA data that was curve fitted (solid lines). Special emphasis is placed on capture of CO_2 from flue gas after a flue gas desulfurization unit. The process condition that closely matches this situation is the 60°C isotherm having a CO_2 partial pressure of 0.1 atm (i.e., 10 volume percent CO_2 in flue gas at atmospheric pressure). The packed bed and TGA data are generally in excellent agreement for this condition, having a CO_2 loading near 3.2-3.3 moles CO_2/kg. Lesser agreement is obtained for the 45°C and 105°C isotherms at 0.1 and 0.9 atm of CO_2. The packed bed data is lower in capacity than the TGA data, but the overall trends remain the same, with higher partial pressure of CO_2 favoring higher CO_2 loading. Reasons for the discrepancy are not obvious, but the important conclusion of both sets of data is that regenerating the sorbent near 105°C with a CO_2-containing sweep gas is going to be problematic and not practical. Much of the CO_2 working capacity of the sorbent is sacrificed because of appreciable CO_2 loading at regeneration temperature. This suggests that an inert sweep gas that is separable from the regenerator off-gas may be necessary, and since steam can be condensed and is in the temperature range of interest for regeneration, steam is the logical sweep gas to be considered for this sorbent. These and other process implications are further discussed in subsequent concluding summary sections.

Effect of moisture

Flue gas already contains some moisture as a result of the combustion process in an electric utility burning fossil fuel, and the level of moisture present is appreciable if it is passed through a downstream flue gas desulfurization unit in a commercial utility. The flue gas exiting the wet scrubber will be near saturation at temperatures in the vicinity of 55-60°C. Saturation of the flue gas at these conditions corresponds to the gas having approximately 15-17 mole percent moisture. In view of these considerations, a series of tests with sample 196c were conducted with moisture to elucidate its impact on CO_2 capture as well as other possible effects.

Given in Figures 18 through Figure 22 are a series of tests to simulate FGD exit conditions. Figure 18 is the dry baseline condition at 60°C using 10%CO_2/He feed that has been previously described. Figure 19 is a moisture-only test conducted with the same dry total flow of gas (100 sccm), which is then passed through the sparger at 55°C, resulting in the wet gas having roughly 16 mole percent H_2O. The absorption was performed at 60°C. Compared to the CO_2 breakthrough curve, a much longer period of time was required to achieve complete absorption of moisture onto the sorbent. Unless otherwise specified, under helium, the desorption (one hour isothermal) and regeneration (2 °C/min to 105 °C) phases were conducted in the same manner as was previously described for the dry CO_2 baseline condition. It is noteworthy that the H_2O is essentially completely liberated during the isothermal desorption phase, and little if any H_2O is liberated during the thermal regeneration phase. This suggests that the H_2O is more weakly bonded than the CO_2 since temperature swing is required to remove the remainder of the CO_2.

Figure 20 is the simultaneous combined CO_2/H_2O test for the sorbent. The presence of both CO_2 and H_2O in the packed-bed system presented additional operational challenges. The gas calibrations are not shown in Figure 20 but the calibration procedures are further described. The system was first calibrated using the 10%CO_2/He span gas. The system would then be calibrated for moisture only by passing the 100% He gas through the sparger. The 10%CO_2/He span gas was again rechecked and recalibrated as necessary, following again by the H_2O recalibration. The CO_2 and H_2O were individually calibrated and repeated as necessary until no further calibration shifts were observed. Once the binary gas calibrations were correctly proportioned, a three component feed gas was attained by passing the 10%CO_2/He span gas through the sparger. However, it needs to be emphasized that it is very important to have an independent reactor bypass leg designed into the reactor system. Significant additional time is necessary to achieve steady state gas composition exiting the sparger. Carbon dioxide is soluble, even in a heated water bath, and it takes up to an hour to achieve steady state exit composition out of the sparger. If the sparger and reactor are in the same combined leg with no independent bypass, the water bath will act as a sink for the CO_2 and will mask the performance of the sorbent in capturing CO_2. An analogous problem exists with the sparger following completion of the absorption phase. Just as additional time must be spent when passing 10%CO_2/He span gas through the sparger to achieve equilibrium CO_2 solubility, additional time must be spent to strip the CO_2 back out of solution when passing 100%He gas through the sparger.

Note that in Figure 20, one can check the accuracy of the binary gas calibrations by observing the degree of dilution of the 10%CO_2/He span gas when it is passed through the sparger. In this particular case where the feed gas is purported to have about 17% moisture, the 10%CO_2 dry level should be diluted down to 8.3% CO_2 on a wet basis, which is very close to what was experimentally observed. The perturbation observed in the H_2O curve after it begins to break through the bed is attributable to a similar dilution effect. The onset of CO_2 breakthrough occurs slightly after H_2O breakthrough, and the CO_2 serves to further dilute the H_2O in the product gas. Eventually CO_2 saturates the sorbent bed and ceases diluting the H_2O in the product gas, and the H_2O slowly continues rising toward the feed level. Again it is readily apparent that CO_2 attains equilibrium bed saturation much more quickly than H_2O.

Similar to the water-only case of Figure 19, essentially all of the water is liberated during the isothermal desorption phase and negligible water is liberated during the thermal regeneration phase in Figure 20. This occurs in spite of the presence of CO_2 being simultaneously liberated. The desorption/regeneration phases of CO_2 liberation appear very similar when comparing the dry CO_2 (Figure 18) and wet CO_2 (Figure 20) cases. This suggests that the uptake and evolution of the water is not in direct competition with the same sites responsible for CO_2 activity.

To more clearly compare the three cases, the curves were time shifted and plotted on a single graph, with time zero aligned to mark the start of absorption and the start of desorption/regeneration. The absorption curves are depicted in Figure 21 and the desorption/regeneration curves are depicted in Figure 22. Loading capacities are also listed on the plots for each of the phases. The material balances are generally in good agreement. The superimposed curves for the dry versus wet cases are exceedingly identical for both the absorption as well as the desorption/regeneration phases. There is a slight enhancement in CO_2 loading with moisture present (from 3.32 to 3.49 moles CO_2/kg), which is consistent with a 10-15% enhancement that has been historically observed during in-house research activities with these type sorbents.

The H_2O absorption loadings are an order of magnitude larger than the CO_2 loadings. A much longer period of time is required to achieve H_2O equilibrium absorption loadings. From a process standpoint, it appears advantageous to engineer the absorber reactor to have limited gas/solid contact time such that the majority of CO_2 loading is achieved but avoid the remainder of the H_2O from absorbing by restricting the contact time. The H_2O readily desorbs during the pressure swing desorption and does not require thermal temperature swing in Figure 22. The H_2O desorption is most likely endothermic and represents additional energy that must be inputted to the regenerator (i.e., regeneration heat duty). Mitigating additional heat duty can be partially accomplished by restricting the amount of water uptake during the absorption stage. These and other heat duty considerations are further discussed in summary and concluding remarks.

A similar battery of tests was conducted, but a lower moisture level near 8 mole percent H_2O was investigated. This would simulate cooling and partially drying the flue gas before performing the CO_2 capture, whether at a lower temperature or requiring flue gas reheat to the desired absorption temperature. Whether such a scenario would be technically and economically advantageous would require an in-depth system analysis, but the experiments were conducted to gain a sense of parametric sensitivity to moisture. In Figures 23 through Figure 27 are the five graphs for the reduced moisture situation. Figure 23 is the dry baseline condition at 60°C using 10%CO_2/He feed. Figure 24 is a moisture-only test conducted with the same dry total flow of gas (100 sccm), which is then passed through the sparger at 40°C, resulting in the wet gas having roughly 8 mole percent H_2O. The gas was then reheated in order to conduct the absorption at 60°C. Figure 25 is the combined CO_2/H_2O absorption test. Note that in Figure 25, the CO_2 dissolution into the sparger bath is shown, occurring before the absorption phase. This depicts the slow nature of achieving the equilibrium CO_2 solubility and the necessary time lapse that is required to achieve steady state sparger performance.

Features of the 8% H_2O case results are very similar in nature to the 16% H_2O case results. Compared to the CO_2 breakthrough curve, a much longer period of time was required to achieve complete absorption of moisture onto the sorbent. The H_2O is essentially completely liberated during the isothermal desorption phase, and little if any H_2O is liberated during the thermal regeneration phase, again indicative that the H_2O is more weakly bonded than the CO_2 since temperature swing is required to remove the remainder of the CO_2.

Superposition of the time shifted curves are depicted in Figure 26 for the absorption and Figure 27 for the desorption/regeneration. Loading capacities are also listed on the plots for each of the phases. The material balances are in fair agreement. However, the superimposed curves for the dry versus wet cases do not reproduce as well over one another for both the absorption and desorption/regeneration phases, unlike that of the 16% H_2O case study. Moisture enhancement on CO_2 removal is slightly more difficult to interpret, due to more ambiguity in the CO_2 material balance for the wet case. The CO_2 material balance for the dry case is very good, but the breakthrough curve for the wet CO_2 case was somewhat anomalous since there was substantial delay in attempting to reach the inlet CO_2 feed value. This is why the absorption phase for the wet case was allowed to proceed for a much longer period of time. The dilution shift in CO_2 from a dry to wet basis (from 10% to 9.37%) corresponds to a calculated moisture level of 6.33%, but the theoretical moisture level based on the sparger temperature was 7.79% H_2O. Depending on the various assumptions made for the inlet feed and final saturation level achieved, a range of CO_2 capacity is reported (4.1-4.8 moles CO_2/kg), and no zero volume adjustment was performed for this estimated range of CO_2 loading. Thus the absorber results suggest a much greater enhancement in CO_2 loading with 8% moisture present. However, the desorption/regeneration material balances are much more consistent between the dry and wet cases. Taking the sum of the desorption and regeneration phases, 3.25 moles CO_2/kg were liberated for the dry case versus 3.32 moles CO_2/kg for the wet case. Plus there is not much temporal difference in the CO_2 liberation curves between the dry and wet cases (Figure 27). It is for these reasons that more credence is placed on the regeneration loading versus the absorption loading, and only slight moisture enhancement in CO_2 loading is claimed for the 8% H_2O case.

The moisture material balances for the 8% H_2O cases are in fair agreement, but the prime difference between the 8% and 16% moisture cases is the much lower H_2O loading. Halving the moisture in the feed caused the absorber H_2O loading to drop by roughly 70% (from 30 to 9 moles H_2O/kg). This suggests that the equilibrium H_2O loading is highly sensitive to the partial pressure of H_2O. Even at lower H_2O loading, substantial contact time is still required to achieve H_2O equilibrium absorption loadings. Therefore it is still prudent to restrict the gas/solid contact time in the absorber to achieve maximal CO_2 performance but minimize H_2O pick-up, so as to mitigate regenerative heat duty losses in the regenerator from H_2O desorption.

Effect of steam (high moisture)

In anticipation of regenerating the sorbent with steam sweep gas in a commercial process so as to maintain sufficient CO_2 working capacity, the experimental capability of the packed-bed reactor system was extended to include attaining very high moisture levels (approximately 90% H_2O/He) exiting the sparger. Normal operating conditions customarily used a dry gas flow rate of 100 sccm, whether for absorption or regeneration. This yields an acceptable space velocity within the reactor and result in a reasonable breakthrough time for the CO_2 absorption curve. However, as the moisture level added to the dry gas flow rate exiting the sparger is increased, the total wet gas flow rate is correspondingly increased. Thus for a goal of 90% H_2O/He, the vaporized moisture flow will be nine times greater than the dry baseline helium flow of 100 sccm, resulting in a space velocity ten times greater than normal with a breakthrough time shortened proportionally. This condition was experimentally examined and numerical evaluation of the breakthrough curve was found to be problematic because of much fewer data points to integrate since the breakthrough curve occurred so quickly. There was also some indication that excessive gas flow rate was causing some back pressure in the system as measured by the pressure transducer downstream of the reactor near the exit of the system (Figure 1). Hence it was decided to lower the dry gas flow rate for absorption (just helium) to 12 sccm when humidifying the stream to simulate steam conditions (90% H_2O/He). This would serve to keep the reactor space velocity within a similar regime as the earlier experiments. The desorption/regeneration helium flow rate was still held at 100 sccm, similar to the other test conditions.

Given in Figure 28 is a 4-cycle test for sample 196c using simulated steam in the feed stream. No CO_2 was used in the feed gas when conducting steam absorptions, in part to simplify the experiments; to make interpretation of the H_2O breakthrough curve less complicated; and hopefully to make the H_2O material balance more straightforward. A secondary consideration was to avoid the possibility of generating excessive carbonic acid with the sparger bath operated much hotter and near the boiling point of water. The final chosen conditions consisted of heating the sparger to a target temperature of 96°C with the reactor held isothermal at 105°C.

Figure 28 illustrates the transient procedure used at the beginning of the experiment to establish 90% H_2O/He exiting the sparger. The MS was initially calibrated near 8% H_2O/He for a steady state condition of 100 sccm helium exiting the sparger held at 40°C. The sparger target temperature was gradually increased over roughly an hour to the final target of 96°C. The growth of the H_2O mole fraction (and corresponding decrease of the He) in the sparger exit gas is observed over this heating period. Eventually the H_2O signal reaches a plateau around 80%H_2O/He, which is lower than the predicted moisture level based on the sparger achieving equilibrium saturation at the measured sparger temperature. This is presumably due to insufficient gas/liquid contact time within the sparger to achieve equilibrium saturation. This is overcome by reducing the helium flow from 100 to 12 sccm, thus lengthening the gas/liquid contact time in the sparger. The H_2O signal rapidly increases at the onset of flow reduction, and eventually settles near 90% H_2O/He.

Four repeated cycles of absorption and regeneration were conducted isothermally at 105°C. The sparger fed approximately 90% H_2O/He with a dry helium flow of 12 sccm for the absorption phase, while 100 sccm dry helium flow was used during the regeneration phase. The reactor was held off-line when transitioning between the two feed flows. To help improve the visual clarity of the H_2O behavior, the 4-cycle test is replotted in Figure 29, minus the helium signal. The absorption breakthrough happens exceedingly fast, perhaps within a minute or so, but the absorption was typically held for at least 10 minutes so as to establish the baseline signal with the reactor on-line. The regeneration occurred more slowly, despite the higher helium sweep flowrate.

The material balances for the steam conditions proved to be problematic for several reasons. At very high moisture levels, there is typically a slight off-set in the H_2O feed level when the reactor is on-line, and the signal is often one to two mole percent less with the reactor on-line. If the original feed level was 90%, the absorption breakthrough curve would typically reach a plateau around 88-89% and would not return to the original feed value. Depending on which value is assumed as the input for the material balance, the numerical integration yielded different results that varied substantially. Hence the absorption capacity was reported using both feed values. The "minimum" value was calculated using the breakthrough plateau with the reactor on-line, whereas the "maximum" value was calculated using the initial sparger feed level with the reactor off-line. Material balances for the 4-cycle test are shown in Figure 30. Figure 30 also includes two additional cycles (#5 and #6) which were conducted on two other test days for the same conditions. They are included to help provide some additional statistical measure of variability. Note that the material balance uses the terms "desorption" and "regeneration" interchangeably in this example, even though no temperature swing was employed since both absorption and regeneration occurred at 105°C.

The desorption capacities lie intermediate between the minimum and maximum absorption capacities, and the desorption capacities appear more consistent, so more statistical confidence is lent to the desorption values. It is reasonable to conclude that the sorbent will achieve an equilibrium moisture loading of about 10-15 moles H_2O/kg when exposed to steam-like conditions of 90% H_2O/He at 105°C. However, the dead volume of the reactor is not accounted for in these measurements. As previously mentioned, the reactor dead volume becomes important when using high CO_2 calibration gas (90% CO_2/He), so it is reasonable to conclude that similar effects exist for high moisture tests. This is presented and discussed in further detail near the end of the results, but approximately 0.6-0.8 moles H_2O/kg capacity is measured for the reactor dead volume under these conditions, and therefore can be subtracted from the above reported H_2O values. Given the variability in the sorbent measurements under simulated steam, such correction was not implemented.

The process implications of the sorbent absorbing high levels of moisture during steam regeneration are hereby considered. Any desorption of moisture during regeneration represents an energy penalty on the regenerative heat duty since the desorption is likely to be endothermic. And since the absorption of water is relatively fast under steam sweep, it is very likely that the equilibrium moisture loading of 10-15 moles H_2O/kg will be achieved in the regenerator. The CO_2 equilibrium loading may or may not be achieved in the regenerator, depending on reactor design, but will most likely be slower to regenerate. Prior results have demonstrated that temperature swing is required to liberate all of the

CO_2 whereas isothermal pressure swing is sufficient to remove the H_2O without temperature swing, suggesting that the H_2O is more weakly bonded than CO_2.

It may be possible to design the absorber and regenerator in such a manner so as to manipulate the moisture loadings on the sorbent as it travels around the circulation loop. Balancing the moisture loadings is an attempt to mitigate moisture desorption in the regenerator. For instance, by appropriately restricting the contact time in the absorber so as to match the equilibrium moisture loading that will be attained in the regenerator under steam sweep, desorption of moisture in the regenerator will be lessened. However, some level of dehydration after the regenerator is probably necessary to avoid condensation of water onto the sorbent since it must be cooled back down to the absorption temperature to repeat the absorption cycle.

Effect of empty reactor ("zero" volume)

When interpreting sorbent breakthrough curves in a packed bed reactor, it is prudent to identify the contribution of the reactor's dead volume when empty. This effect can then be subtracted from the sorbent's breakthrough curve, and thus quantify the effect due to only the sorbent. Ideally, the bed of sorbent is replaced with an inert solid of similar particle size and is placed into the reactor to occupy the same bed volume. For the present case of zero volume determination, the reactor was completely empty without inert material and without quartz wool plugs that are normally used to hold the sample.

The contribution of the reactor volume when empty was characterized under various gas compositions. A step change in gas composition generates a breakthrough curve that can be integrated, similar to as if sorbent was present within the reactor. If the reactor was initially filled with helium and isolated, and a bypass flow of carbon dioxide/helium span gas was flowing in steady state, once the reactor was brought on-line, the slug of helium would flow downstream to the MS and a momentary reduction in CO_2 would be detected and then return to the CO_2 feed level. This situation is what is normally encountered during an absorption phase with sorbent loaded into the reactor. The opposite situation can also be envisioned, where the reactor is filled with carbon dioxide/helium span gas and isolated, and a bypass flow of helium gas is flowing at steady state. Once the reactor is brought on-line, the slug of CO_2/He span gas would flow downstream to the MS and a momentary increase in CO_2 would be detected, and then would return to the zero CO_2 value. This situation is what is normally encountered during a desorption phase with sorbent loaded into the reactor. The same two conditions can be established using a different tracer gas, such as H_2O, or even a multi-component mixture of CO_2 and H_2O.

The moles of gas that can occupy the dead volume of the reactor is a function not only of composition (mole fraction), but also temperature and pressure. These factors are interrelated through consideration of the ideal gas law. The pressure can be held constant by using the same flow rate of gas for the dead volume test as is used during the sorbent test. And it is a simple matter to establish the same reactor process temperature for both conditions. The material balance equations are simplified because there is no source or sink term in the empty reactor situation, unlike when sorbent is loaded.

Throughout the course of parametric sorbent testing, when the reactor was emptied of sorbent, it was sometimes convenient to conduct zero volume tests at particular conditions before refilling the reactor. The following results are compilations of zero volume reactor determinations under various gas compositions and temperature. Not all cycles were acquired within a single day, but over multiple and separate occasions. For a single condition, they are ordered chronologically.

In Figures 31 through Figure 33 are material balances for empty reactor tests using 10%CO_2/He span gas at three different absorption temperatures respectively (45°C, 60°C, and 105°C). The CO_2 balances are generally in good agreement between the absorption and regeneration loadings and the cycle variability is minimal. A rough visual average of the aggregate cycles shows that the zero volume loading decreases with increasing temperature, consistent with the ideal gas law. Assigning approximate mean values, the loadings are 0.068, 0.065, and 0.055 moles CO_2/kg respectively at 45°C, 60°C, and 105°C using 10%CO_2/He span gas. As mentioned earlier, these loadings were considered inconsequential compared to amine-sorbent loadings in excess of 3 moles CO_2/kg, and therefore no subtraction was performed.

In Figure 34 and Figure 35 are material balances for empty reactor tests using 90%CO_2/He span gas at two different absorption temperatures respectively (45°C and 105°C). The CO_2 balances are generally in good agreement between the absorption and regeneration loadings and the cycle variability is minimal. The zero volume loading decreases with increasing temperature, consistent with the ideal gas law. Assigning approximate mean values, the loadings are 0.55 and 0.50 moles CO_2/kg respectively at 45°C and 105°C using 90%CO_2/He span gas. However, as mentioned earlier, these loadings were not considered inconsequential compared to amine-sorbent loadings in excess of 3 moles CO_2/kg, and therefore subtraction was performed when the loadings were compared to TGA loadings in Figure 17.

Empty reactor tests were also conducted for H_2O feed gas mixtures. Figures 36 through Figure 38 respectively gives material balances for 8%H_2O/He at 45°C, 16%H_2O/He at 60°C, and 90%H_2O/He at 105°C. Compared to CO_2, the moisture zero volume results exhibit somewhat more cycle to cycle variability. The material balances generally agree between the absorption and regeneration quantity for any one cycle, with the exception of the steam tests in Figure 38. Negligible zero volume is measured for 8%H_2O/He at 45°C, roughly 0.1 moles H_2O/kg. However, higher zero volume is measure for 16%H_2O/He at 60°C, roughly 0.2-0.4 moles H_2O/kg. The cycle variability makes it difficult to assign an average loading. This is the experimental condition used to simulate FGD exit composition. However, since moisture loadings for 196c were in the range of 30 moles H_2O/kg for the FGD simulated condition, the zero volume was considered small and no subtraction was performed for zero volume for this condition. The steam simulated tests of 90%H_2O/He at 105°C (Figure 38) has zero volume moisture loadings between 0.6-0.8 moles H_2O/kg. These are roughly an order of magnitude larger than the 8%H_2O/He zero volume loading at 45°C (0.1 moles H_2O/kg). This ratio is fairly consistent based on 8%H_2O versus 90% H_2O. Since moisture loadings for 196c were in the range of 10-15 moles H_2O/kg for the steam simulated condition (90%H_2O/He at 105°C), the zero volume was considered negligible and no zero volume subtraction was performed for this condition.

Effect of silica substrate

Since the silica-based amine sorbent (196c) was shown to have high affinity towards both CO_2 and H_2O, and the sorbent contained approximately 45wt% amine with the remainder being silica, the support was examined individually for its reactivity towards CO_2 and H_2O. The silica support was obtained from Fuji Silysia. The support is CARiACT G-10 high pore volume series (G-10 HPV). The same total mass of silica sample (1 gram) was loaded into the reactor, just as with sample 196c, but in order for capacity results to be compared on an equivalent basis, the amine loading should be taken into account for sample 196c. For instance, in order to partition the effect due only to the silica on 196c, the substrate capacity measurement for the G-10 can be multiplied by 55%. This normalized silica value can then be compared to the capacity measurement for sample 196c, and any difference can be attributed to the presence of the amine. This procedure assumes that the effects of the amine and the support are independent and additive, rather than synergistic.

In Figure 39 and Figure 40 respectively are the material balances at 60°C and 105°C using 10%CO_2/He span gas. The CO_2 loading are miniscule, roughly 0.08 and 0.07 moles CO_2/kg at 60°C and 105°C, respectively. In fact, when compared to the zero volume reactor results of Figure 32 and Figure 33 (0.065 and 0.055 moles CO_2/kg), much of the apparent loading is due to the empty reactor volume, and therefore the silica has virtually no affinity to absorb CO_2.

Similar to tests with sample 196c, tests with G-10 silica were conducted with dry 10%CO_2/He span gas, H_2O at 8 and 16 mole percent moisture, and combined CO_2/H_2O feed. The absorption temperature was 60°C and the regeneration was conducted stepwise with 1-hr isothermal desorption followed by temperature swing regeneration. Graphs of the individual cases are omitted for brevity. To more clearly compare the three cases, the curves were time shifted and plotted on a single graph, with time zero aligned to mark the start of absorption and, alternately, the start of desorption/regeneration.

The absorption curves are depicted in Figure 41 and the desorption/regeneration curves are depicted in Figure 42 for the 8 mole percent moisture case family. Analogous results for the 16 mole percent moisture family (simulating FGD conditions) are shown in Figure 43 and Figure 44 for absorption and desorption/regeneration respectively. Loading capacities are also listed on the plots for each of the phases. The material balances are generally in good agreement. The superimposed curves for the dry versus wet cases are exceedingly identical for both the absorption as well as the desorption/regeneration phases. The 10%CO_2 dry level is diluted down to a lower level for the wet case. The amount of CO_2 dilution is in proportion to the amount of moisture added to the feed gas and was consistent with the H_2O calibrated feed value. The G-10 has negligible CO_2 absorption, whether under dry or wet conditions, and can be considered benign with respect to CO_2. The G-10 does have some affinity to absorb moisture, but there does not appear to be any influence by the presence of CO_2 on the level of moisture pickup.

Roughly 2.5 and 5.0 moles H_2O/kg loadings are achieved at 8% and 16%H_2O, respectively, a doubling of capacity that is in proportion to the doubling of the feed moisture. However, these moisture capacities were not corrected for zero volume, recalling that for 16%H_2O/He at 60°C, roughly 0.2-0.4 moles H_2O/kg was estimated for the zero volume, which is still well below the G-10 H_2O loadings. The H_2O is essentially completely liberated during the isothermal desorption phase, and little if any H_2O is liberated during the thermal regeneration phase, again indicative that the H_2O is more weakly bonded than the CO_2 since temperature swing is required in the case of sample 196C to remove the remainder of the CO_2.

When comparing moisture loadings for G-10 versus 196c, after accounting for 55wt% silica within 196c, it is dramatically obvious that the silica plays a minor role in moisture absorption. Sample 196c had moisture loadings near 30 moles H_2O/kg under FGD conditions whereas the G-10 silica has apportioned values around 2.5 moles H_2O/kg. Rather, it is the presence of the amine that plays the dominant role in attracting water. Although the exact mechanism is not known, one plausible explanation is that the moisture is attracted to the amine through hydrogen bonding. Although it may be possible to engineer a sorbent having a hydrophobic support, the presence of the amine could still dominate and make the sorbent overall hydrophilic.

The effect of simulated steam (90% H_2O/He) was performed on G-10 silica. The same methodology as described for 196c was utilized. Four repeated cycles of absorption and regeneration were conducted isothermally at 105°C, shown in Figure 45. The sparger fed approximately 90% H_2O/He with a dry helium flow of 12 sccm for the absorption phase, while 100 sccm dry helium flow was used during the regeneration phase. The reactor was held off-line when transitioning between the two feed flows. To help improve the visual clarity of the H_2O behavior, the 4-cycle test is replotted in Figure 46, minus the helium signal. The absorption breakthrough happens exceedingly fast, perhaps within a minute or so, but the absorption was typically held for at least 10 minutes so as to establish the baseline signal with the reactor on-line. The regeneration occurred slightly slower than the absorption, despite the higher helium sweep flowrate.

As was the case for sample 196c under simulated steam, the G-10 material balances using simulated steam were problematic for similar aforementioned reasons, namely a slight off-set in the H_2O feed level when the reactor is on-line versus off-line. Hence the absorption capacity is reported using both feed values. The “minimum” value was calculated using the breakthrough plateau with the reactor on-line, whereas the “maximum” value was calculated using the initial sparger feed level with the reactor off-line. Material balances for the 4-cycle test are shown in Figure 47. Note that the material balance uses the terms “desorption” and “regeneration” interchangeably in this example, even though no temperature swing was employed.

The desorption capacities for G-10 are in good agreement with the “minimum” absorption values, and there is good cycle repeatability. However, the “maximum” absorption values are much greater in value and therefore deemed less credible. These G-10 results differ from sample 196c in which the desorption values ranged intermediate between the minimum and maximum values. The G-10 silica has a moisture loading of roughly 4 moles H_2O/kg when exposed to simulated steam conditions of 90% H_2O/He at 105°C. The reactor dead volume under these conditions (0.6-0.8 moles H_2O/kg capacity) has not been subtracted from this loading.

When comparing moisture loadings for G-10 silica versus sample 196c under simulated steam conditions, one can again conclude that the support plays a minor role in moisture pick-up. This observation is consistent with comparative tests at lower moisture feeds of 8% and 16%H_2O. After accounting for 55wt% silica within 196c, the G-10 silica has apportioned values around 2 moles H_2O/kg whereas sample 196c had moisture loadings near 10-15 moles H_2O/kg. Hence the amine plays the dominant role in attracting water, even under simulated steam sweep regeneration. Such process implications should be considered when designing the absorber and regenerator so as to minimize moisture desorption within the regenerator which negatively impacts regenerator heat duty.

Conceptual BIAS Process

Based on the findings of this study using an amine-based sorbent for CO_2 removal from flue gas, the following discussion centers on proposing a conceptualized CO_2 removal process with this type sorbent. The Basic Immobilized Amine Sorbent (BIAS) Process has been submitted as a non-provisional patent application (f) and is hereby described. The basic tenet is to manipulate or control the level of moisture on the sorbent as it travels around the sorbent circulation path between absorption and regeneration stages.

The absorption step at simulated conditions that represent the gas composition after the flue gas desulfurization unit with subsequent regeneration was initially presented in Figures 18-22. It is desirable to achieve large CO_2 loading while minimizing H_2O loading during the absorption step so as to mitigate moisture desorption during regeneration. Figure 21 originally presented the three feed gas cases (dry CO_2, H_2O, and combined CO_2/H_2O) with time-shifted axes marking the beginning of absorption. Figure 48 shows the initial breakthrough curves with the time axis expanded for the first 30 minutes. The cumulative loadings as a function of time are shown in Figure 49. Both Figure 48 and Figure 49 show the cumulative loadings at 7 min (the onset of CO_2 breaking through the bed) and 10 min (the onset of CO_2 reaching a plateau near the feed value). After approximately 10-15 minutes, there is minimal gain in CO_2 loading but the H_2O loading continues increasing towards its equilibrium loading, near 30 moles H_2O/kg. Therefore the gas/solid contact time in the absorber should be engineered (i.e., restricted) so as to achieve acceptable CO_2 loading but avoid excess contact time in reaching the equilibrium H_2O loading. For this initial restricted time regime, the H_2O loading is roughly twice the CO_2 loading. So for the BIAS concept, the assumption is made that for achieving a CO_2 loading near 3.5 moles CO_2/kg, an H_2O loading of 7 moles H_2O/kg will be absorbed.

Figure 50 shows a conceptual layout of the BIAS process in one embodiment envisioned within the patent application. (f) The sorbent is circulated between absorption and regeneration vessels while removing CO_2 from flue gas and thereby recovering a concentrated CO_2 off-gas from the regenerator. Both CO_2 and H_2O loadings, as determined for sample 196c, are depicted along the sorbent circulation loop. To maintain maximum driving force for gas/solid transfer, the absorber and regenerator are configured for counter-flow operation using moving bed reactors, with sorbent traveling downward under gravity flow and upward flow of gas.

A major key to successful implementation of the BIAS process is effective integration of heat management. Appreciable chemical heats of reaction are encountered during CO_2 absorption, and conversely, regeneration. Within a conventional bed of sorbent, the resulting exotherm will be significant and due to poor heat transfer within the bed, the bed will likely overheat. The opposite effect will occur in the regenerator, with the resulting endotherm cooling the bed. Although the specifics are not detailed in Figure 50, both vessels will require internal heat exchangers with a circulating fluid. In the case of the absorber, the likely fluid to dissipate the heat is cooling water, whereas in the case of the regenerator, indirect steam is a suitable fluid to heat the regenerator. The indirect steam for regeneration is well suited since its temperature closely matches the temperature required for thermal regeneration of the sorbent. The regenerator would most likely rely on using a condensing steam heat exchanger since the latent heat of phase change of steam is large and would input considerable heat into the bed of sorbent. The heat removed from the absorber should be recovered as low grade heat within the integrated power plant, such as preheating water for steam generation, etc. Similarly, a condenser is used to separate the moisture from the regenerator off-gas, and this low grade heat is also recoverable, such as water preheat, etc.

The above heat considerations account for the chemical energy of removing CO_2, namely the heats of reaction. However, there are additional terms that contribute to the overall energy needed to regenerate the sorbent, commonly termed as the regenerative heat duty. Since temperature swing is employed for regeneration in the BIAS process, with the absorber at 60°C and the regenerator at 105°C, a sensible energy term of the sorbent must be accounted for. This term involves the heat capacity of the sorbent, the CO_2 working capacity of the sorbent, as well as the delta temperature swing. To minimize this sensible term, a solid-solid cross flow heat exchanger is shown in Figure 50, whereby the hotter CO_2-lean sorbent exiting the regenerator indirectly contacts the cooler CO_2-rich sorbent exiting the absorber and exchanges the sensible heat. This method is similar to the cross-flow heat exchange commonly employed in liquid MEA scrubbing.

Based on the experimental findings with 196c and the required use of steam sweep gas to maintain sufficient CO_2 working capacity, a direct steam sweep gas is fed into the bottom of the regenerator in Figure 50. The amount of sweep gas required is currently not known, but a minimum steam flux will be necessary to allow the exiting sorbent to be in equilibrium with essentially zero partial pressure of CO_2 surrounding the sorbent, and thus achieve a maximum level of regeneration and CO_2 working capacity. Based on experimental findings using simulated steam, sample 196c is expected to achieve an equilibrium moisture loading of approximately 15 moles H_2O/kg within the regenerator. It is desired that moisture desorption be minimized/avoided in the regenerator, to lessen its impact on increasing the regenerator heat duty. Therefore, the sorbent entering the regenerator (or equivalently exiting the absorber), should have the same moisture level of near 15 moles H_2O/kg so as to keep the moisture level constant across the regenerator.

If the absorber is designed correctly for the appropriate gas-solid contact time, the sorbent will absorb roughly 3.5 moles CO_2/kg and 7 moles H_2O/kg from the flue gas. Since the regenerator requires an input of 15 moles H_2O/kg that exits the absorber, the recycled sorbent entering the absorber should have a moisture loading of 8 moles H_2O/kg. Assuming the sorbent moisture content is additive, the moisture loading on the sorbent will increase from an entrance level of 8 moles H_2O/kg to an exit level of 15 moles H_2O/kg across the absorber while in contact with moist flue gas (approximately 17 volume percent moisture) for a restricted period of time.

The sorbent exiting the regenerator will have an equilibrium water loading of 15 moles H_2O/kg at 105°C by being contacted with steam sweep gas. Equilibrium with respect to moisture is reasonable since sorbent residence time in the regenerator will be large as compared to the absorber. It is necessary to cool the sorbent back down to 60°C to repeat the absorption cycle. However, such cooling could cause condensation of absorbed water on or within the sorbent. It is also conceivable that residual steam within the pore structure could also condense with cooling. This should be avoided from the perspective of sorbent stability, given that liquid water could possibly impact the amine in the substrate matrix. Thus a dehydration step is first incorporated before lowering the sorbent temperature so as to avoid the possibility of moisture condensation.

A sample conditioner is depicted in Figure 50 to accomplish partial dehydration of the sorbent exiting the regenerator. Any inert sweep gas could be used, and it could need to be preheated to avoid contacting the hot sorbent with sweep gas at ambient temperature causing condensation on the sorbent. If the sorbent is stable with respect to oxygen at elevated temperature, then preheated dry air can be used as the sweep gas. The contact time in the sample conditioner should be designed to achieve partial drying of the sorbent such that 7 moles H_2O/kg are removed from the sorbent and transferred to the air sweep gas. This will balance the moisture loading on the sorbent around the circulation loop, by lowering the moisture loading from 15 moles H_2O/kg to 8 moles H_2O/kg across the conditioner.

From a thermodynamic perspective, the BIAS process avoids moisture desorption within the regenerator but instead results in partial moisture desorption within the conditioner. The desorption of water will be endothermic regardless of which location it occurs and is an energy penalty on the heat duty. However, the enthalpy of the sweep gas needs to be considered. In the case of the regenerator, the sweep gas is steam. In the case of the conditioner, the sweep gas is preheated air. The steam has higher heat value (enthalpy) than preheated air and is therefore more valuable (or costly) to produce and use. Therefore the use of sweep air in the conditioner is more preferable to control the moisture loading. It should also be noted that most of the experimental results are for one sorbent (196c) and that more recent sorbents adsorb considerably less moisture in the absorber and regenerator.

Summary/Conclusions

An amine-based sorbent has been investigated in support of developing a CO_2 removal process to remove CO_2 from flue gas. The sorbent is composed of PEI immobilized onto a silica support. The performance of the sorbent was characterized in a packed-bed reactor and compared to TGA data. In the packed bed system, exit gas analysis was performed using mass spectrometry, yielding conventional breakthrough curves that were integrated to yield loading capacity. Simulated flue gas was fed to the reactor, composed of $CO_2/H_2O/He$ mixtures. The effect of simulated steam sweep for regeneration was also investigated. Sorbent stability was monitored during parametric testing by periodically repeating the same baseline condition and noting any drop-off in CO_2 loading. In addition to the immobilized amine sorbent, the silica support was individually examined for its performance. Empty reactor tests were also conducted without sorbent loaded to characterize the empty volume contribution to the breakthrough curves.

Parametric tests identified the effects of temperature, CO_2 partial pressure, H_2O partial pressure, and simulated steam on adsorption and regeneration performance of the sorbent and individual substrate. The baseline absorption loading for sample 196c is typically in the range of 3.2-3.3 moles CO_2/kg at 60°C using dry 10%CO_2/He feed. The baseline adsorption loading at 45°C using dry 10%CO_2/He feed is slightly lower, near 3.0 moles CO_2/kg. Regeneration under helium sweep gas was conducted stage-wise, with one hour isothermal desorption followed by temperature swing desorption to 105°C. The two-stage regeneration suggests both weakly bonded and strongly bonded CO_2 sites are present. The two baseline conditions were repeated intermittently throughout the parametric testing and new sample was loaded into the reactor when apparent drop-off in CO_2 loading was noted. Slight loss in loading capacity was observed with thermal swing regeneration, but the degradation was greater with very high moisture (i.e., simulated steam) in the feed gas.

Good material balances were obtained for the baseline tests when comparing the absorption and total desorption/regeneration fragments, even when there was noticeable drop-off in CO_2 loading. This helps validates that the sorbent was indeed degraded at various times throughout the testing. However, the distribution of the liberated CO_2 is greatly affected when comparing 45°C versus 60°C data. Roughly one third is liberated by quasi-pressure swing (desorption under helium) at 45°C and the remaining two-thirds is liberated by temperature swing. However, the distribution is reversed at 60°C with roughly two thirds liberated by pressure swing and the remaining one-third liberated by temperature swing. Hence, the active sites for weakly bonded versus strongly bonded CO_2 are strongly influenced by just a small change in temperature from 45°C to 60°C.

The effect of raising the adsorption temperature from 60°C to 105°C under dry conditions using 10%CO_2/He shows that a significant amount of CO_2 will still absorb at this temperature, roughly 1.2 moles/kg, in the presence of 10%CO_2/He. The 105°C temperature represents the ceiling temperature attained during temperature swing regeneration. The working capacity of the sorbent is defined as the difference in loading between the rich loading (i.e., the absorption capacity under flue gas conditions) and the lean loading (i.e., the absorption capacity under regeneration conditions). The type of sweep gas employed during regeneration, whether CO_2 recycle or inert gas sweep, will affect the lean loading attained during regeneration. Thus for the above example, the working capacity of the sorbent will be greatly reduced by about 40% when attempting to regenerate in a CO_2 partial pressure of 0.1 atm versus pure helium sweep regeneration. Attempting to regenerate under higher partial pressures of CO_2 will further reduce the working capacity for this particular sorbent.

The effect of high CO_2 partial pressure (0.9 atm) was examined at low temperature (45^{o}C) for absorption conditions as well as high temperature (105^{o}C) for regeneration conditions. Because the reactor dead volume is not negligible under high CO_2 feed concentration, a correction factor of 0.55 moles CO_2/kg for the 45^{o}C cycle and 0.5 moles CO_2/kg for the 105^{o}C cycles was respectively employed for measured sorbent capacities. Under 0.9 atm CO_2, the sorbent absorbs significant loadings (corrected) of CO_2, roughly 3.5-4 moles CO_2/kg for 45^{o}C and 2.9-3.0 moles CO_2/kg for 105^{o}C. Hence, the CO_2 capacity is increased by roughly 0.5 moles CO_2/kg when comparing 0.1 atm CO_2 versus 0.9 atm CO_2 under same absorption temperatures. However, when comparing the loading at 60 ^{o}C and 0.1 atm CO_2 (3.2-3.3 moles CO_2/kg) versus 105 ^{o}C at 0.9 atm CO_2 (2.9-3.0 moles CO_2/kg), a very low working capacity of about 0.3 moles CO_2/kg is obtained. Hence these results again affirm that attempting to regenerate under high partial pressures of CO_2 yields unacceptably low CO_2 working capacity for this particular sorbent.

To further validate the effects of temperature and CO_2 partial pressure on CO_2 adsorption loading capacity, packed-bed results were compared to adsorption isotherms obtained using a TGA. Both data sets were acquired without moisture in the feed gas. The TGA data were curve-fitted using a logarithmic equation, with the intent of eventually developing a kinetic model. Higher partial pressure of CO_2 favors higher CO_2 capacity, with stronger dependence (i.e., slope) at lower partial pressure of CO_2. The temperature dependence of the isotherms passes through an optimum temperature near 60^{o}C to achieve maximum CO_2 loading. This temperature is well suited to match the flue gas desulfurization exit temperature in an electric utility. As higher temperatures are examined, and are thus approaching reaction reversibility or regeneration, the CO_2 capacity is lower. Special emphasis is placed on capture of CO_2 from flue gas after a flue gas desulfurization unit. The process condition that closely matches this situation is the 60^{o}C isotherm having a CO_2 partial pressure of 0.1 atm (i.e., 10 volume percent CO_2 in flue gas at atmospheric pressure). The packed bed and TGA data agree exceedingly well for this condition, having a CO_2 loading near 3.2-3.3 moles CO_2/kg. Lesser agreement is obtained for the 45^{o}C and 105^{o}C isotherms at 0.1 and 0.9 atm of CO_2. The packed bed data is lower in capacity than the TGA data, but the overall trends remain the same, with higher partial pressure of CO_2 favoring higher CO_2 loading. The major conclusion of both sets of data is that regenerating the sorbent near 105^{o}C with a CO_2-containing sweep gas is problematic and not practical. Much of the CO_2 working capacity of the sorbent is sacrificed because of appreciable CO_2 loading at regeneration temperature. This suggests that an inert sweep gas that is separable from the regenerator off-gas will be necessary. Since steam can be condensed and is in the temperature range of interest for regeneration, steam is the logical sweep gas under consideration.

The effect of moisture was examined, both by itself and in combination with CO_2 in the feed gas. Since the sorbent process is targeted to be located downstream of the flue gas desulfurization unit in a commercial electric utility, H_2O levels near 8% and 16% were established in the feed gas. To simulate the effect of regenerating with steam sweep gas, H_2O levels near 90% were also established in the gas.

Some general observations for the lower moisture cases are hereby summarized. Although equilibrium CO_2 loadings are attained within 15-30 minutes, a much longer period of time is required to achieve equilibrium H_2O loadings, of the order of 3 to 4 or more hours. This has the effect of equilibrium H_2O loadings being much greater than CO_2 loadings, by as much as a factor of 10 for FGD simulated conditions. However, this effect can be lessened by engineering the absorber to restrict the solid contact time. For this particular sorbent and within 10-15 minutes initial contact time, the H_2O loading will be approximately twice the CO_2 loading. The effect of moisture on CO_2 loadings is minimal at best, perhaps enhancing CO_2 loadings by 10 to 15 percent. In the case of FGD simulated conditions, the CO_2 loading increased from approximately 3.3 to 3.5 moles CO_2/kg under dry versus wet conditions, respectively. When the dry and wet cases are superimposed on top of one another, there is little difference in the time histories of the absorption breakthrough curves and desorption/regeneration breakthrough curves. This suggests that there is little competition for adsorption sites between CO_2 and H_2O. Reactivation or regeneration of the sorbent was sometimes conducted in two stages, a one-hour isothermal pressure swing desorption under pure helium purge, followed by temperature swing (2°C /min) regeneration. With respect to H_2O, the first stage of pressure swing desorption was sufficient to liberate the adsorbed H_2O. However, with respect to CO_2, both stages (pressure swing and temperature swing) were required to liberate the adsorbed CO_2. These results suggest that both weakly bonded and strongly bonded CO_2 sites are present, whereas only weakly bonded H_2O sites are present. Halving the moisture in the feed (from 16% to 8%) caused the absorber H_2O loading to drop by roughly 70% (from 30 to 9 moles H_2O/kg). This suggests that the equilibrium H_2O loading is highly sensitive to the partial pressure of H_2O. Even at lower H_2O loading, substantial contact time is still required to achieve H_2O equilibrium absorption loadings. Therefore it is still prudent to restrict the solid contact time in the absorber to achieve maximal CO_2 performance but minimize H_2O pick-up, so as to mitigate regenerative heat duty losses in the regenerator from H_2O desorption.

The effect of simulated steam (0.9 atm H_2O) on sorbent regeneration was examined. However, because of the high moisture content in the feed gas, it was necessary to reduce the dry helium flow rate in the feed gas from 100 sccm to 12 sccm in order to keep the total gas flow (and hence space velocity through the reactor) within a similar regime as the dry cases. The helium flow rate was kept at 100 sccm for the isothermal pressure swing desorption step. Multi-cycle tests were conducted at 105°C and the H_2O breakthrough curves occur exceedingly fast, reaching equilibrium capacity within several minutes. The regeneration curve with pure helium is slightly slower despite the higher helium sweep flow rate. Both results suggest that when the regenerator is designed to achieve adequate CO_2 regeneration, because of the very fast nature of the H_2O

adsorption, the sorbent will quickly achieve equilibrium moisture loadings when a sweep of steam gas is employed in the regenerator. The H_2O material balances were slightly more problematic due to signal shift in the H_2O feed value when switching the reactor on-line or bypassed. However, best estimates conclude that the sorbent will achieve an equilibrium moisture loading of about 10-15 moles H_2O/kg when exposed to steam-like conditions of 90% H_2O/He at 105°C. This equilibrium moisture estimate does not consider the dead volume of the reactor under these conditions (approximately 0.6-0.8 moles H_2O/kg capacity) and therefore can be subtracted from the above reported H_2O values. However, given the variability in the sorbent measurements under simulated steam, such correction was not implemented. Seeking to avoid any desorption of water within the regenerator that would thereby raise the regenerator heat duty, manipulation of moisture loadings between the absorber and regenerator is described in greater length while introducing the concept of the BIAS process. Sorbent stability tests suggest that steam contacting the sorbent can cause degradation in the baseline CO_2 loading capacity.

The experimental "artifact" or "empty-volume" of the reactor was measured over multiple cycles for specific temperatures and gas compositions of interest used during sorbent evaluation. The CO_2 loadings are 0.068, 0.065, and 0.055 moles CO_2/kg respectively at 45°C, 60°C, and 105°C using 10%CO_2/He span gas. These loadings were considered inconsequential compared to amine-sorbent loadings in excess of 3 moles CO_2/kg, and therefore no subtraction was performed. The CO_2 loadings are 0.55 and 0.50 moles CO_2/kg respectively at 45°C and 105°C using 90%CO_2/He span gas. However, these loadings were not considered inconsequential compared to amine-sorbent loadings in excess of 3 moles CO_2/kg, and therefore subtraction was performed when the loadings were compared to TGA loadings. Empty reactor tests were also conducted for H_2O feed gas mixtures. Negligible zero volume is measured for 8%H_2O/He at 45°C, roughly 0.1 moles H_2O/kg. However, higher zero volume is measure for 16%H_2O/He at 60°C, roughly 0.2-0.4 moles H_2O/kg. However, since moisture loadings for 196c were in the range of 30 moles H_2O/kg for the FGD simulated condition, the zero volume was considered small and no subtraction was performed for zero volume for this condition. The steam simulated tests of 90%H_2O/He at 105°C has zero volume moisture loadings between 0.6-0.8 moles H_2O/kg. These are roughly an order of magnitude larger than the 8%H_2O/He zero volume loading at 45°C (0.1 moles H_2O/kg). This ratio is fairly consistent based on 8%H_2O versus 90% H_2O. Since moisture loadings for 196c were in the range of 10-15 moles H_2O/kg for the steam simulated condition (90%H_2O/He at 105°C), the zero volume was considered negligible and no zero volume subtraction was performed for this condition.

The silica support (G-10, HPV) was also examined for its affinity towards CO_2 and H_2O, both individually and in combination. Bearing in mind that sample 196c consisted of approximately 45wt% PEI and therefore 55wt% silica, the loadings must be put on a "per-gram" silica basis before direct comparisons are made between the sorbent and support. This procedure assumes that the effects of the amine and the support are independent and additive, rather than synergistic. For instance, in order to partition the effect due only to the silica on 196c, the substrate capacity measurement for the G-10 can be multiplied by 55%. This normalized silica value can then be compared to the capacity measurement for sample 196c, and any difference can be attributed to the presence of the amine.

G-10 silica was found to have virtually no affinity for CO_2 at 60°C and 105°C using 10%CO_2/He span gas, respectively having loadings of approximately 0.08 and 0.07 moles CO_2/kg. These values are barely above the zero volume reactor results (0.065 and 0.055 moles CO_2/kg) and therefore much of the apparent loading is due to the empty reactor artifact. The effect of moisture was examined, both by itself and in combination with CO_2 in the feed gas. The test conditions mirrored those performed with sample 196c for simulated FGD conditions, namely H_2O levels near 8% and 16% were established in the feed gas for 60°C absorption. The silica does have some affinity to absorb H_2O, but there is the same very low CO_2 loading due to reactor artifact even when moisture is present in the feed gas. The adsorption and desorption/regeneration curves virtually lie on top of one another, again indicating that the presence of CO_2 in the feed gas makes no difference in the substrates affinity for H_2O. Roughly 2.5 and 5.0 moles H_2O/kg loadings are achieved at 8% and 16%H_2O, respectively, a doubling of capacity that is in proportion to the doubling of the feed moisture. However, these moisture capacities were not corrected for zero volume, recalling that for 16%H_2O/He at 60°C, roughly 0.2-0.4 moles H_2O/kg was estimated for the zero volume, which is still well below the G-10 H_2O loadings. The H_2O is essentially completely liberated during the isothermal desorption phase, and little if any H_2O is liberated during the thermal regeneration phase, again indicative that the H_2O is more weakly bonded than the CO_2 since temperature swing is required in the case of sample 196C to remove the remainder of the CO_2. Although the substrate does have some affinity to attract H_2O, it is obvious that the silica plays a lesser role in moisture absorption compared to the amine. After correcting for silica weight fraction, sample 196c had moisture loadings near 30 moles H_2O/kg under FGD conditions whereas the G-10 silica has apportioned values around 2.5 moles H_2O/kg. Thus it is the presence of the amine that plays the dominant role in attracting water, presumably through hydrogen bonding. Although it may be possible to engineer a sorbent having a hydrophobic support, the presence of the amine could still dominate and make the sorbent overall hydrophilic.

The effect of simulated steam on the silica support yields similar conclusions regarding the hydrophilic character of the amine outweighing that of the support. The G-10 silica has a moisture loading of roughly 4 moles H_2O/kg when exposed to simulated steam conditions of 90% H_2O/He at 105°C. The reactor dead volume under these conditions (0.6-0.8 moles H_2O/kg capacity) has not been subtracted from this loading. Correcting for silica weight fraction, the G-10 silica has apportioned values around 2 moles H_2O/kg whereas sample 196c had moisture loadings near 10-15 moles H_2O/kg. Hence the amine plays the dominant role in attracting water, even under simulated steam sweep regeneration. Such process implications should be considered when designing the absorber and regenerator so as to minimize moisture desorption within the regenerator which negatively impacts regenerator heat duty.

The concept of the Basic Immobilized Amine Sorbent ("BIAS") Process using an amine-based sorbent for CO_2 removal from flue gas was introduced, and the reader is referred to that specific section for a more detailed description of the process. The basic tenet is to manipulate or control the level of moisture on the sorbent as it travels around the sorbent circulation path between absorption and regeneration stages. Gas/solid contact time is restricted in the absorber to achieve near equilibrium CO_2 loadings while avoiding excessive H_2O loadings. The sensible heat required for temperature swing is minimized with heat recovery using solids cross flow heat exchange. Sorbent regeneration is accomplished through the use of direct steam sweep gas, yielding higher CO_2 working capacity. A sample conditioner partially dehydrates the regenerated sorbent before cooling the sorbent back down to absorption temperature. These and other considerations combine to lessen the regenerator heat duty necessary to reactivate the sorbent and liberate a pure stream of CO_2 off-gas, after moisture is condensed from the off-gas.

References

(a) Ebner, A. D.; Gray, M. L.; Chisholm, N. G.; Black, Q. T.; Mumford, D. D.; Nicholson, M. A.; Ritter, J. A. Suitability of a Solid Amine Sorbent for CO_2 Capture by Pressure Swing Adsorption. Ind. Eng. Chem. Res. 2011, 50, 5634.
(b) Gray, M. L.; Hoffman, J. S.; Hreha, D. C.; Fauth, D. J.; Hedges, S. W.; Champagne, K. J.; Pennline, H. W. Parametric Study of Solid Amine Sorbents for the Capture of Carbon Dioxide. Energy Fuels 2009, 23, 4840.
(c) Gray, M. L.; Soong, Y.; Champagne, K. J.; Pennline, H.; Baltrus, J. P.; Stevens, R. W.; Khatri, R.; Chuang, S. S. C.; Filburn, T. Improved immobilized carbon dioxide capture sorbents. Fuel Process. Technol. 2005, 86, 1449.
(d) Hammache, S.; Hoffman, J. S.; Gray, M. L.; Fauth, D. J.; Pennline, H. W. Impact of Steam Regeneration on the Performance of Amine-Based CO_2 Sorbents. Prepr. Pap.-Am. Chem. Soc., Div. Fuel Chem. 2011, 55 (1), xxxx.
(e) Mebane, D. S.; Fauth, D. J.; Gray, M. L. A Rigorous Yet Scalable Kinetic Model for the Uptake of CO_2 by Silica-Supported, PEI-Impregnated Sorbents. Twenty-Eighth Annual International Pittsburgh Coal Conference, September 12 - 15, 2011, Pittsburgh, PA.
(f) Pennline, H. W.; Hoffman, J. S.; Gray, M. L.; Fauth, D. J.; Resnik, K. P. Regenerable Sorbent Technique for Capturing CO_2 Using Immobilized Amine Sorbents. U.S. Non-Provisional Patent Application S-119419. 2011.

Disclaimer

Figure 1

Laboratory Scale Reactor

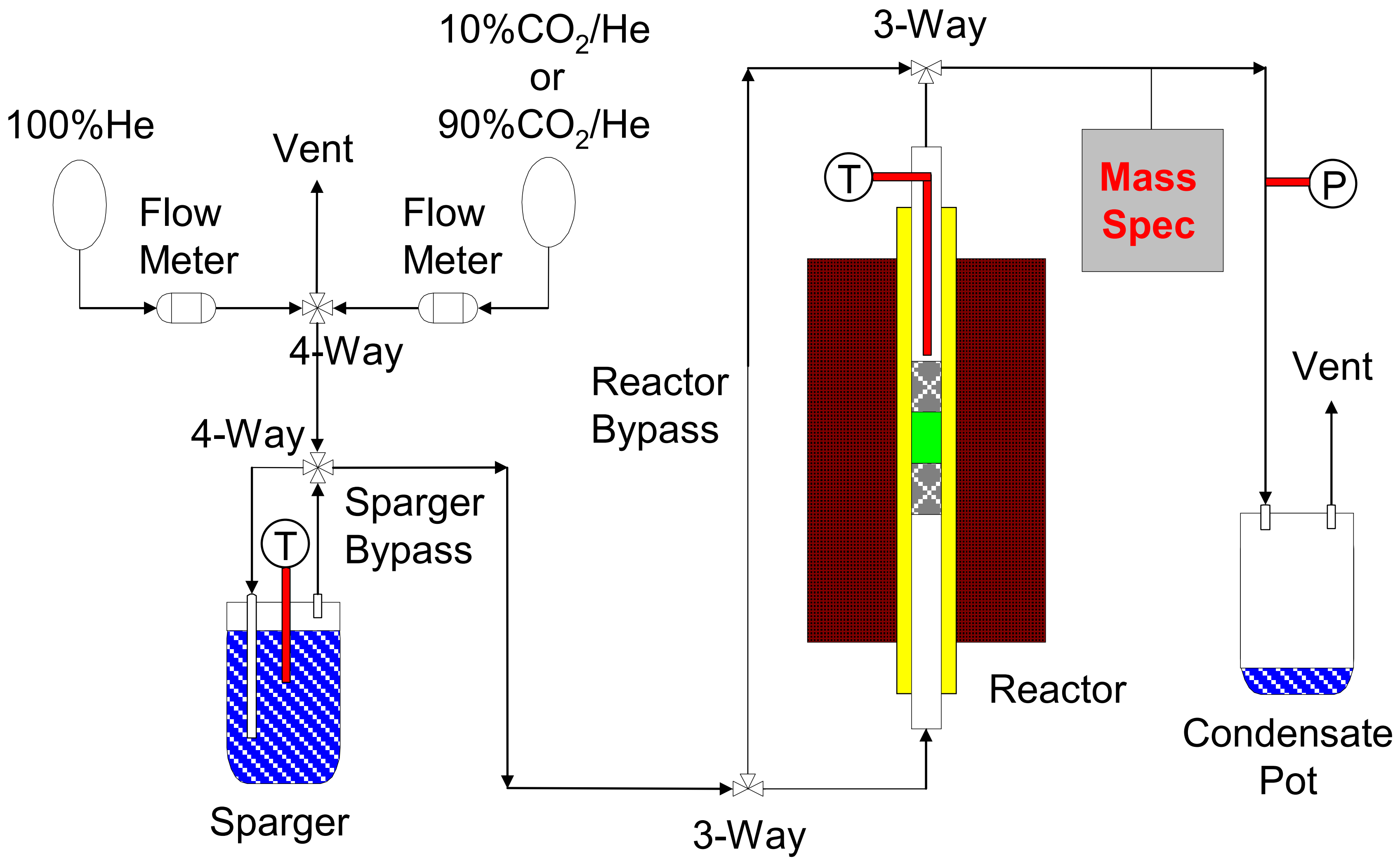

Figure 2

Laboratory Scale Reactor

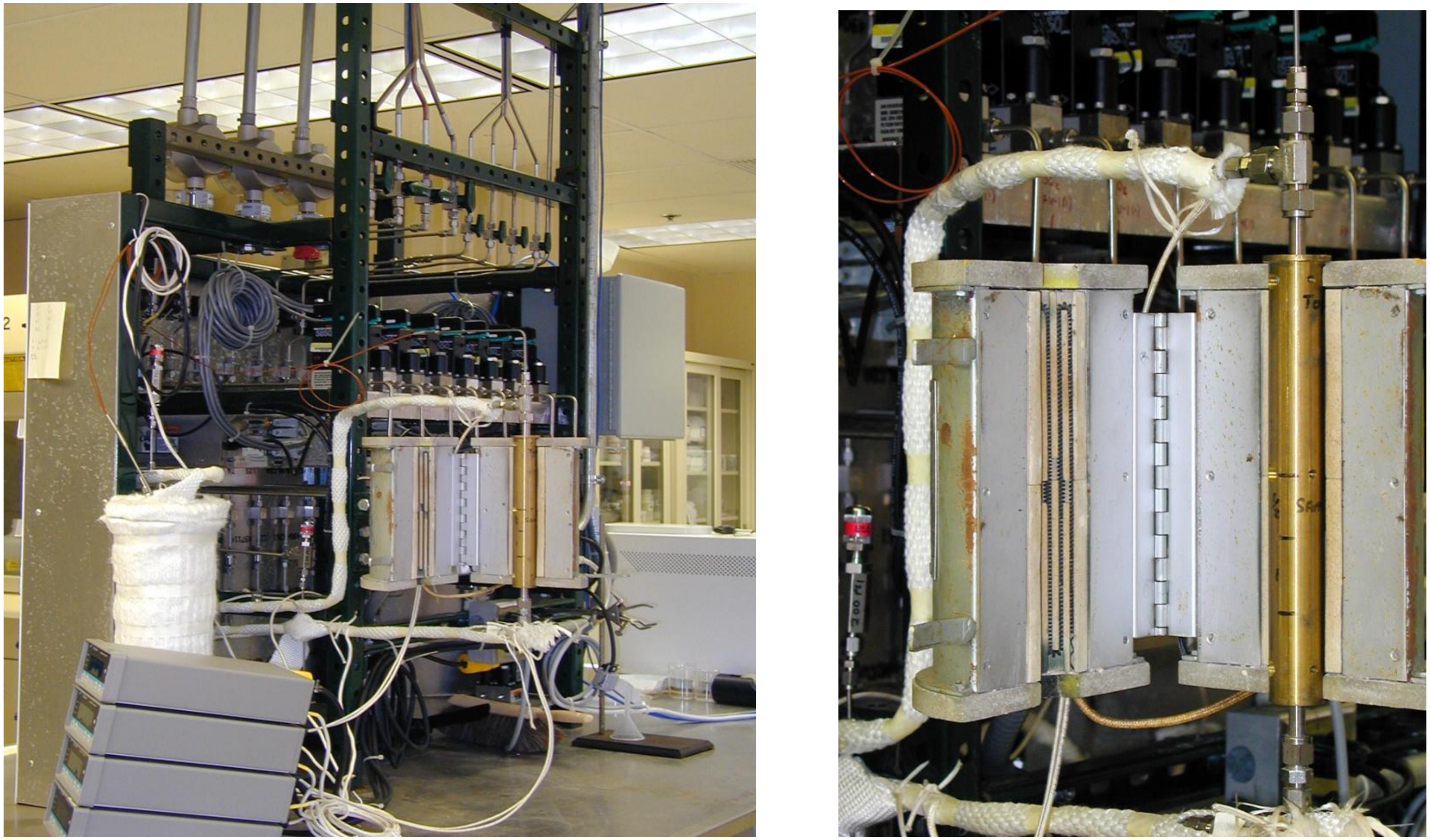

Figure 3

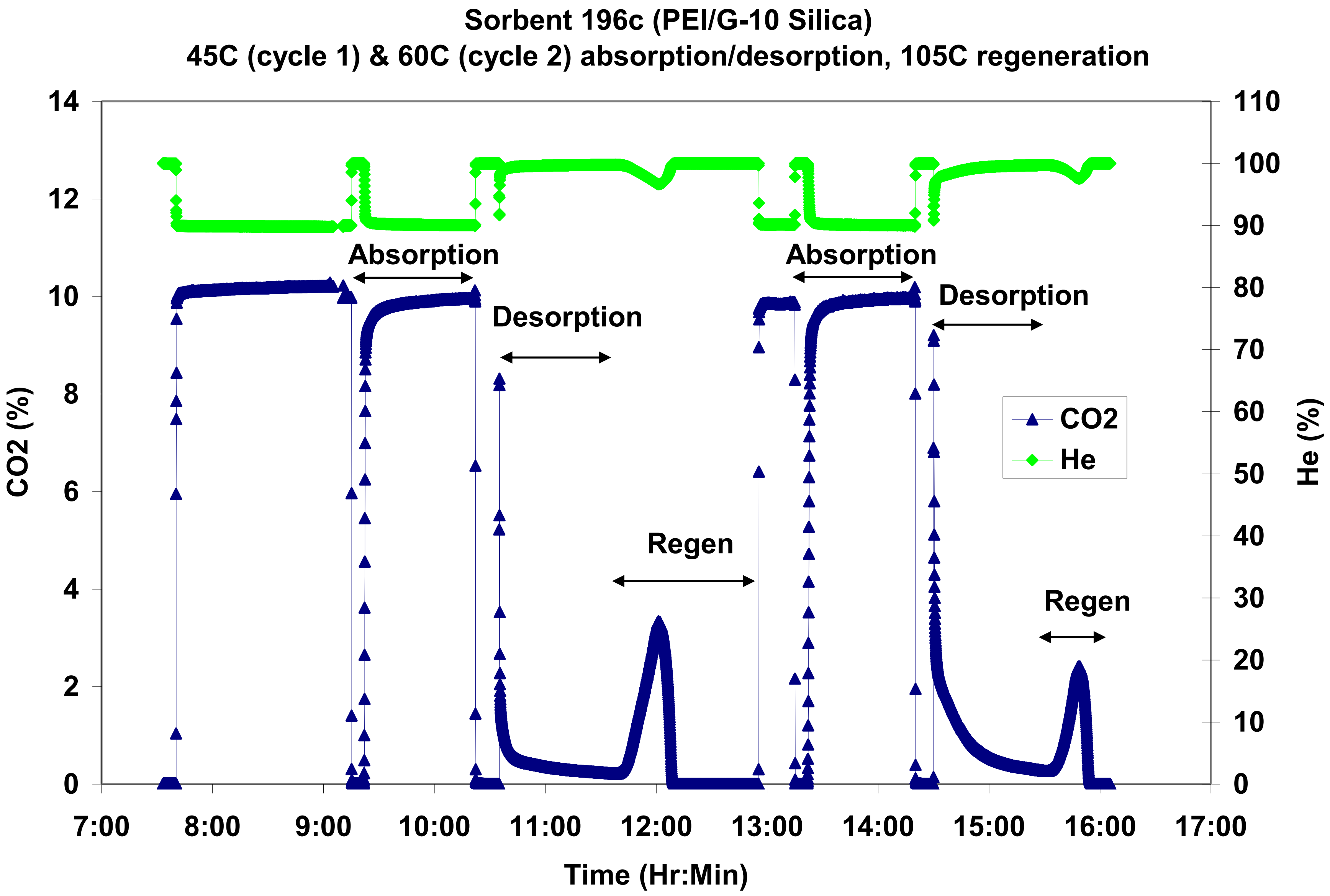
Sorbent 196c (PEI/G-10 Silica)
45C (cycle 1) & 60C (cycle 2) absorption/desorption, 105C regeneration
Absorption
Desorption
Absorption
Desorption
Regen
Regen
CO2
He
CO2 (%)
He (%)
Time (Hr:Min)
0
2
4
6
8
10
12
14
0
10
20
30
40
50
60
70
80
90
100
110
7:00
8:00
9:00
10:00
11:00
12:00
13:00
14:00
15:00
16:00
17:00

Figure 4

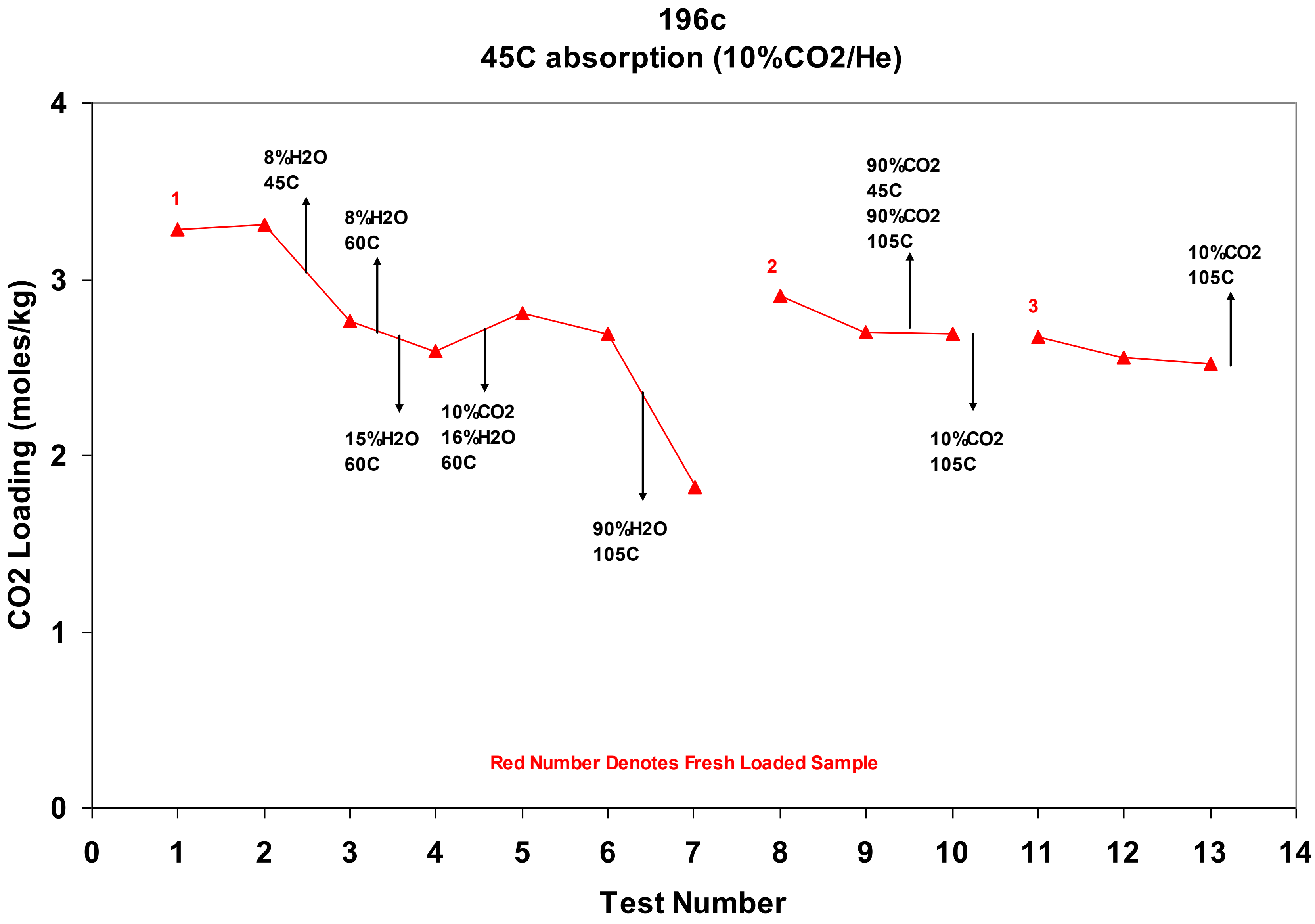
196c
45C absorption (10%CO2/He)
CO2 Loading (moles/kg)
Test Number
0
1
2
3
4
0
1
2
3
4
5
6
7
8
9
10
11
12
13
14
1
2
3
8%H2O
45C
8%H2O
60C
15%H2O
60C
10%CO2
16%H2O
60C
90%H2O
105C
90%CO2
45C
90%CO2
105C
10%CO2
105C
10%CO2
105C
Red Number Denotes Fresh Loaded Sample

Figure 5

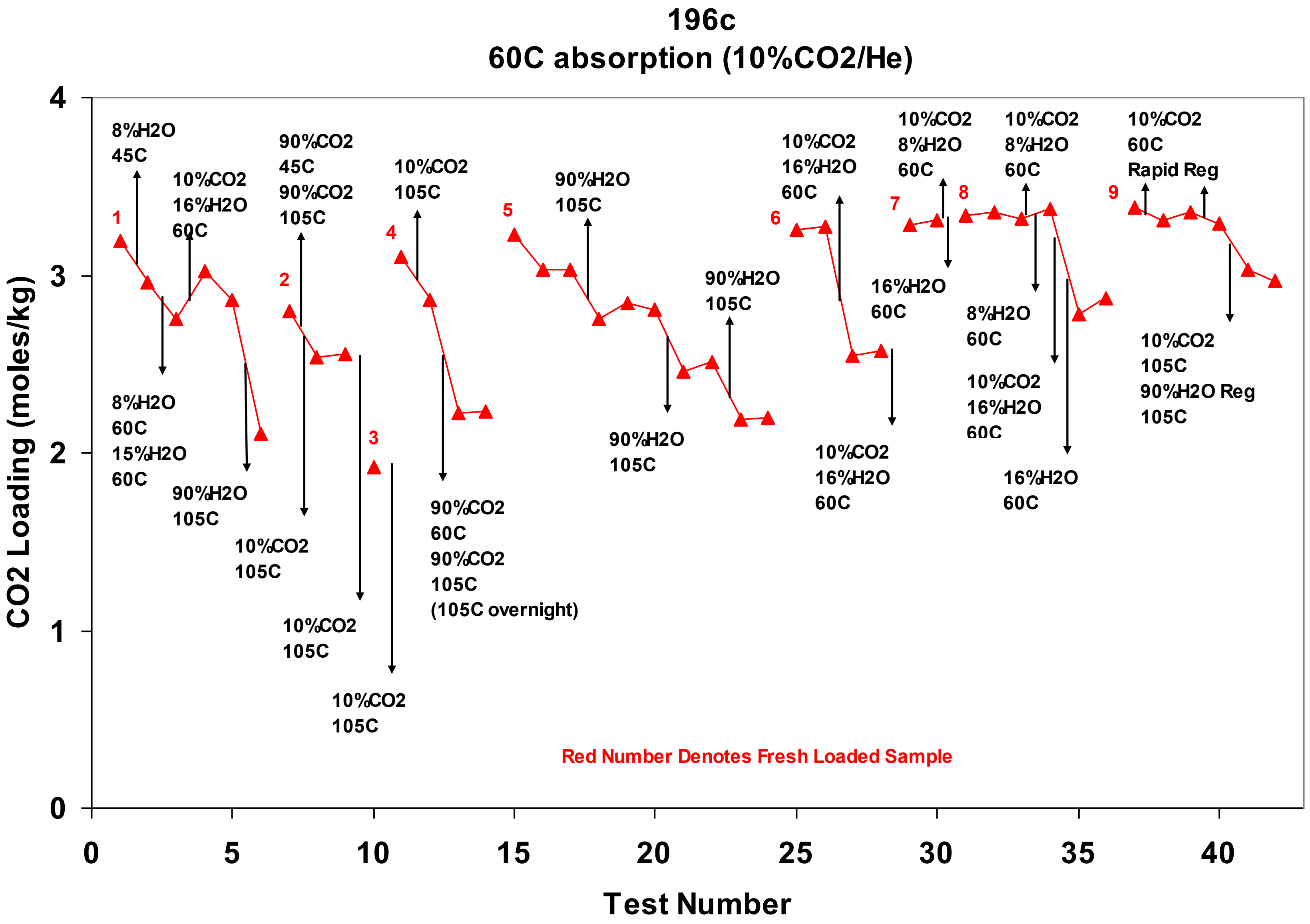
196c
60C absorption (10%CO2/He)
CO2 Loading (moles/kg)
Test Number
0
1
2
3
4
0
5
10
15
20
25
30
35
40
1
2
3
4
5
6
7
8
9
8%H2O
45C
10%CO2
16%H2O
60C
8%H2O
60C
15%H2O
60C
90%H2O
105C
90%CO2
45C
90%CO2
105C
10%CO2
105C
10%CO2
105C
10%CO2
105C
10%CO2
105C
90%CO2
60C
90%CO2
105C
(105C overnight)
90%H2O
105C
90%H2O
105C
90%H2O
105C
10%CO2
16%H2O
60C
10%CO2
16%H2O
60C
10%CO2
8%H2O
60C
16%H2O
60C
10%CO2
8%H2O
60C
8%H2O
60C
10%CO2
16%H2O
60C
16%H2O
60C
10%CO2
60C
Rapid Reg
10%CO2
105C
90%H2O Reg
105C
Red Number Denotes Fresh Loaded Sample

Figure 6

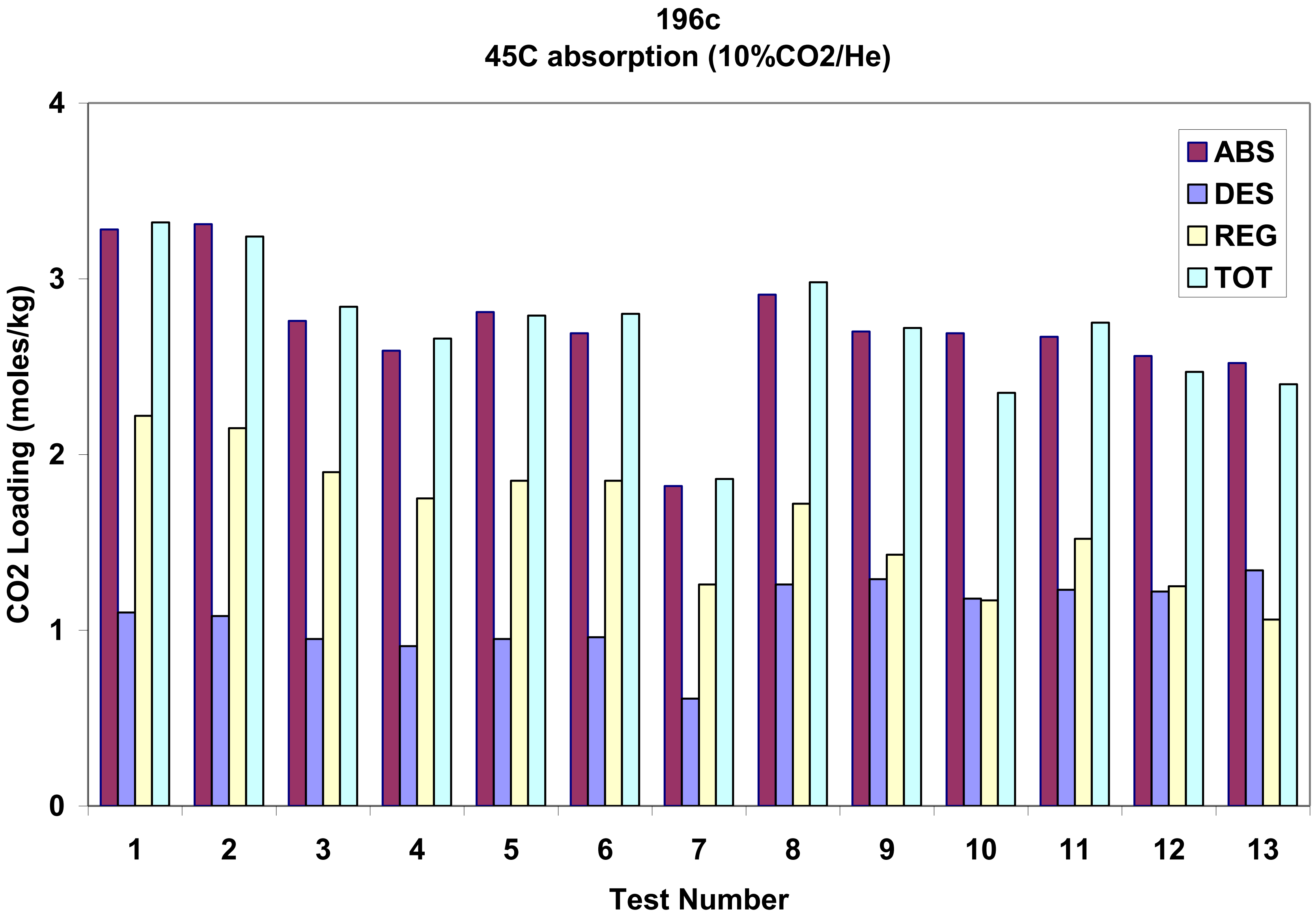
196c
45C absorption (10%CO2/He)
CO2 Loading (moles/kg)
0
1
2
3
4
ABS
DES
REG
TOT
1
2
3
4
5
6
7
8
9
10
11
12
13
Test Number

Figure 7

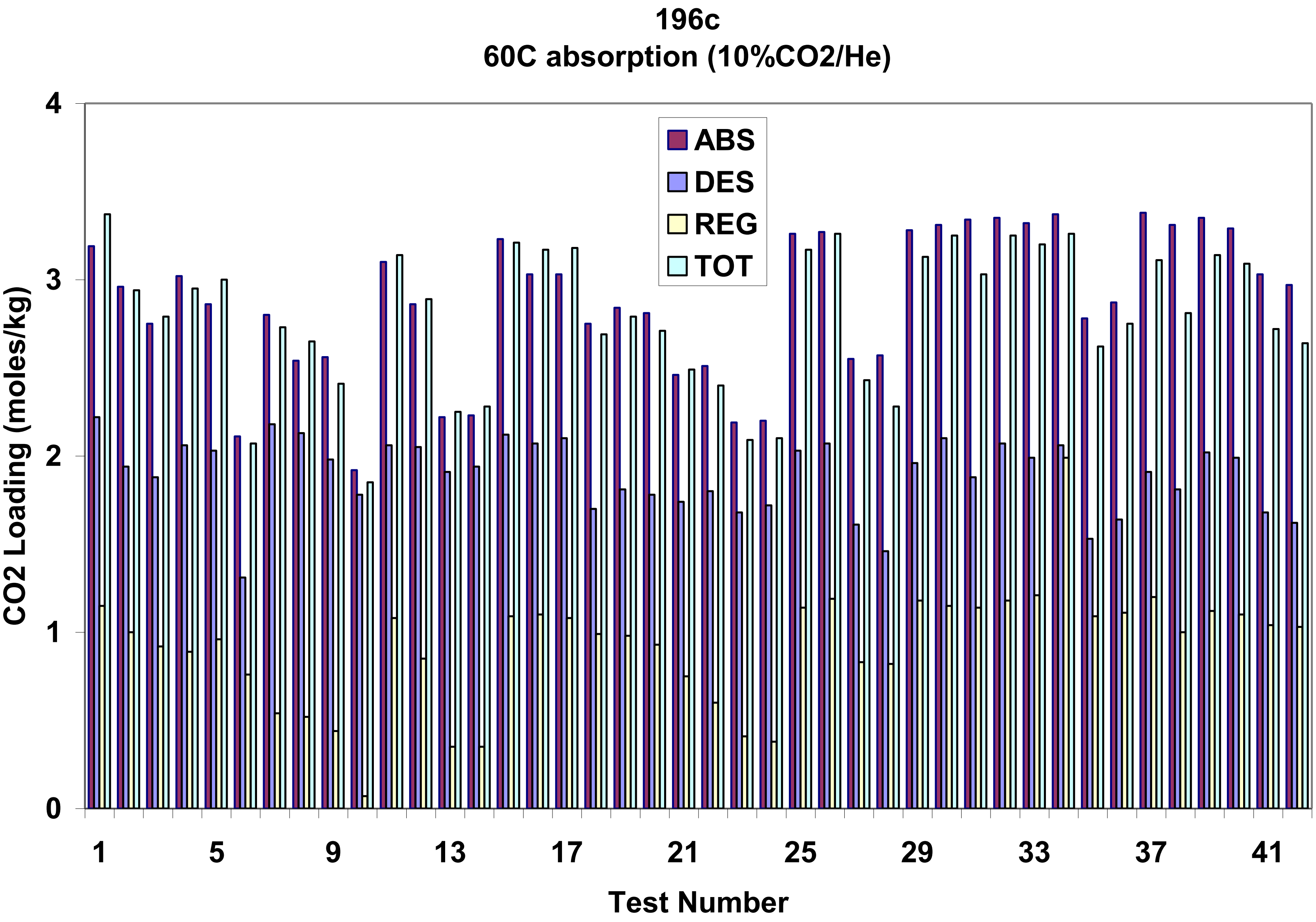
196c
60C absorption (10%CO2/He)
ABS
DES
REG
TOT
CO2 Loading (moles/kg)
0
1
2
3
4
1
5
9
13
17
21
25
29
33
37
41
Test Number

Figure 8

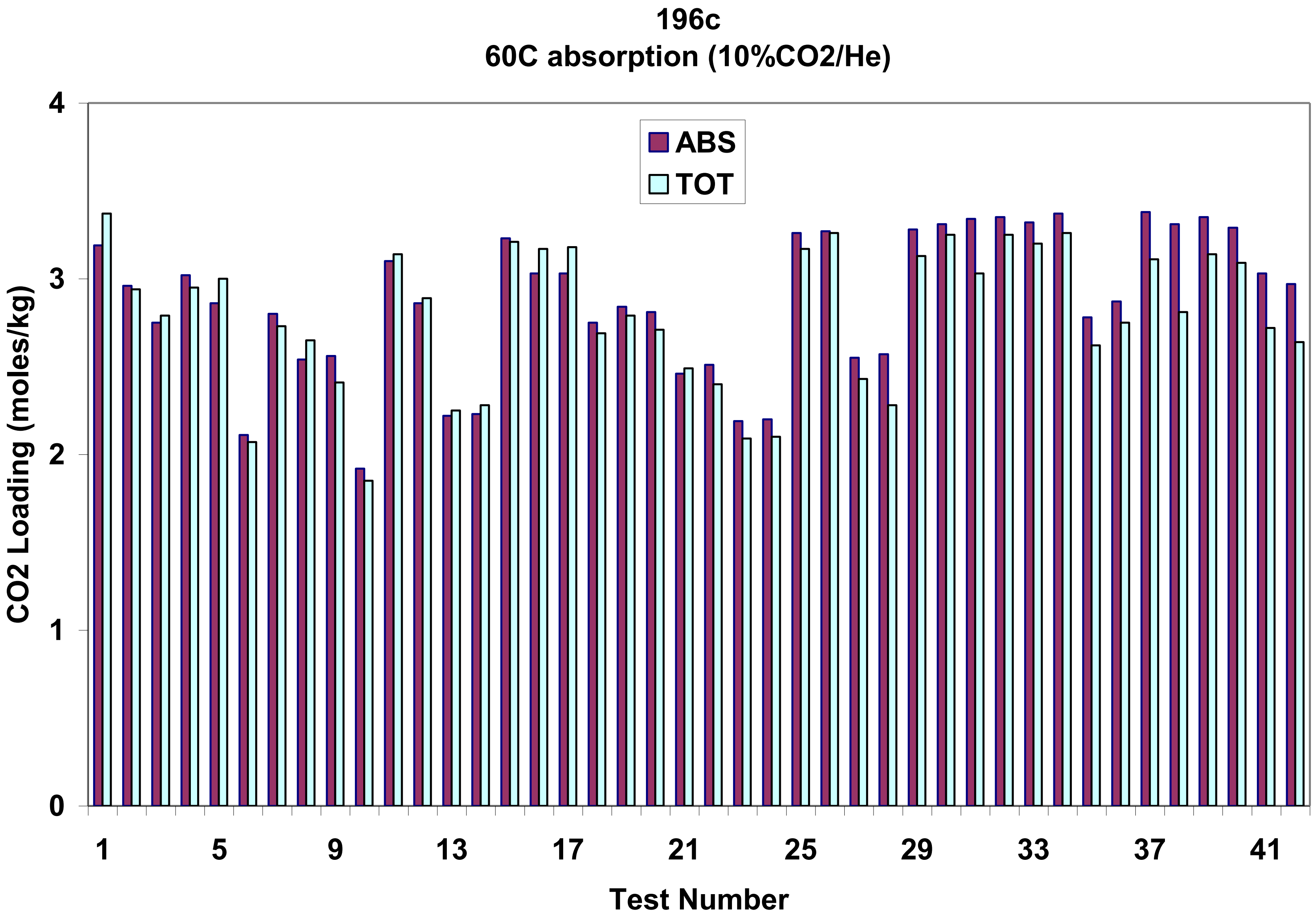

196c
60C absorption (10%CO2/He)

Figure 9

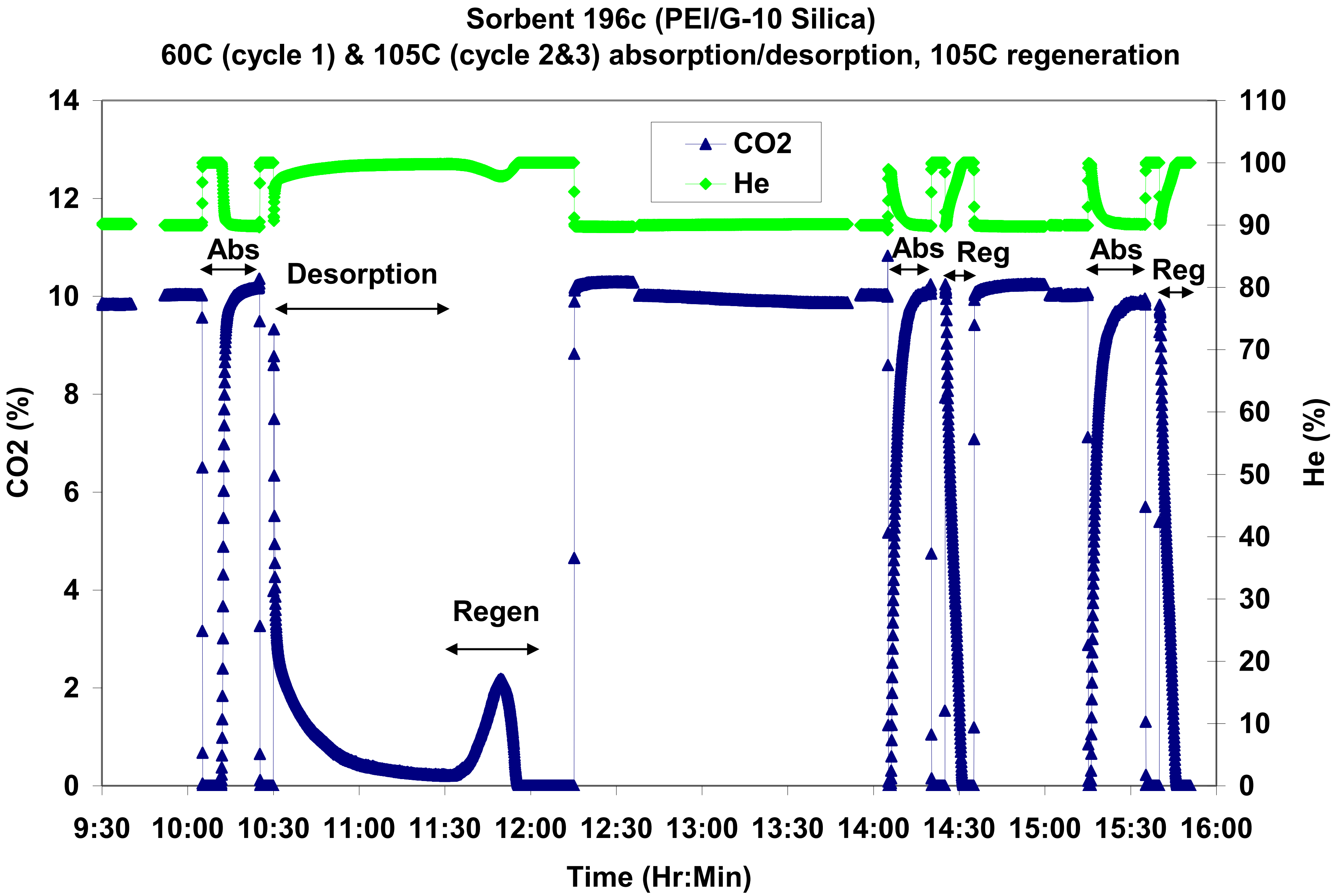
Sorbent 196c (PEI/G-10 Silica)
60C (cycle 1) & 105C (cycle 2&3) absorption/desorption, 105C regeneration
CO2
He
Abs
Desorption
Regen
Abs
Reg
Abs
Reg
14
12
10
8
6
4
2
0
CO2 (%)
110
100
90
80
70
60
50
40
30
20
10
0
He (%)
9:30
10:00
10:30
11:00
11:30
12:00
12:30
13:00
13:30
14:00
14:30
15:00
15:30
16:00
Time (Hr:Min)

Figure 10

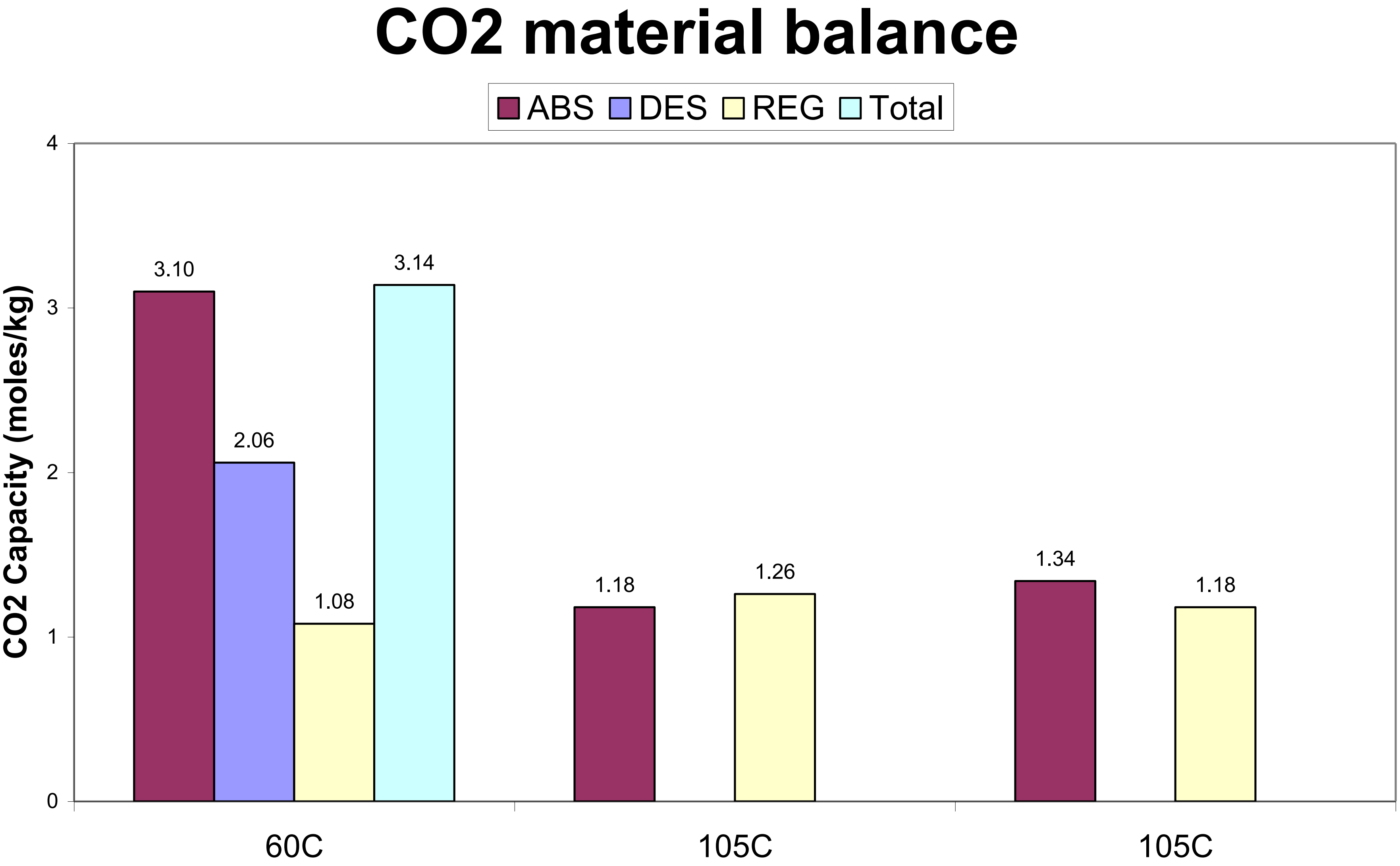
CO2 material balance
ABS
DES
REG
Total
CO2 Capacity (moles/kg)
0
1
2
3
4
3.10
2.06
1.08
3.14
1.18
1.26
1.34
1.18
60C
105C
105C

Figure 11

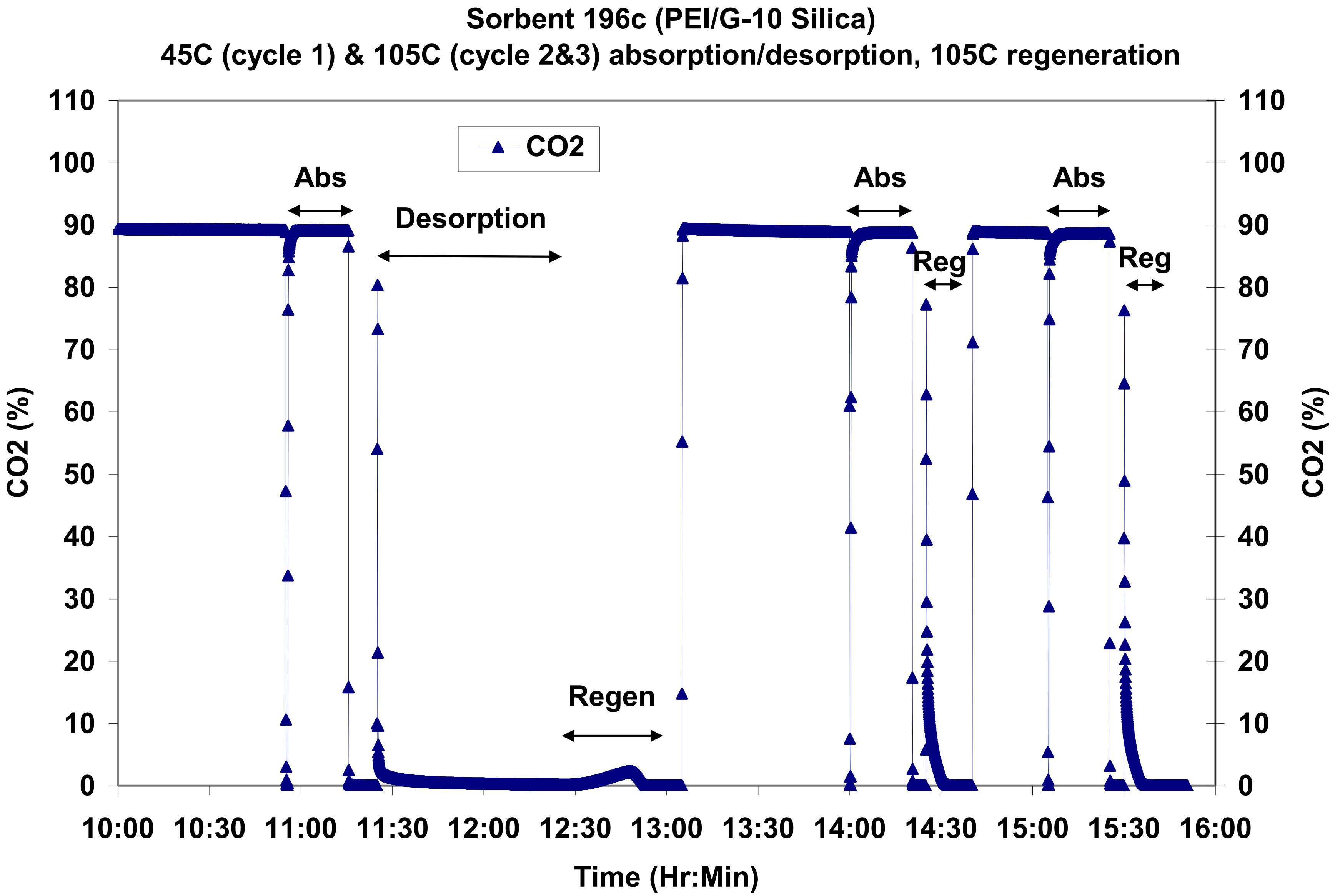
Sorbent 196c (PEI/G-10 Silica)
45C (cycle 1) & 105C (cycle 2&3) absorption/desorption, 105C regeneration
CO2
Abs
Desorption
Regen
Abs
Reg
Abs
Reg
CO2 (%)
CO2 (%)
110
100
90
80
70
60
50
40
30
20
10
0
10:00
10:30
11:00
11:30
12:00
12:30
13:00
13:30
14:00
14:30
15:00
15:30
16:00
Time (Hr:Min)

Figure 12

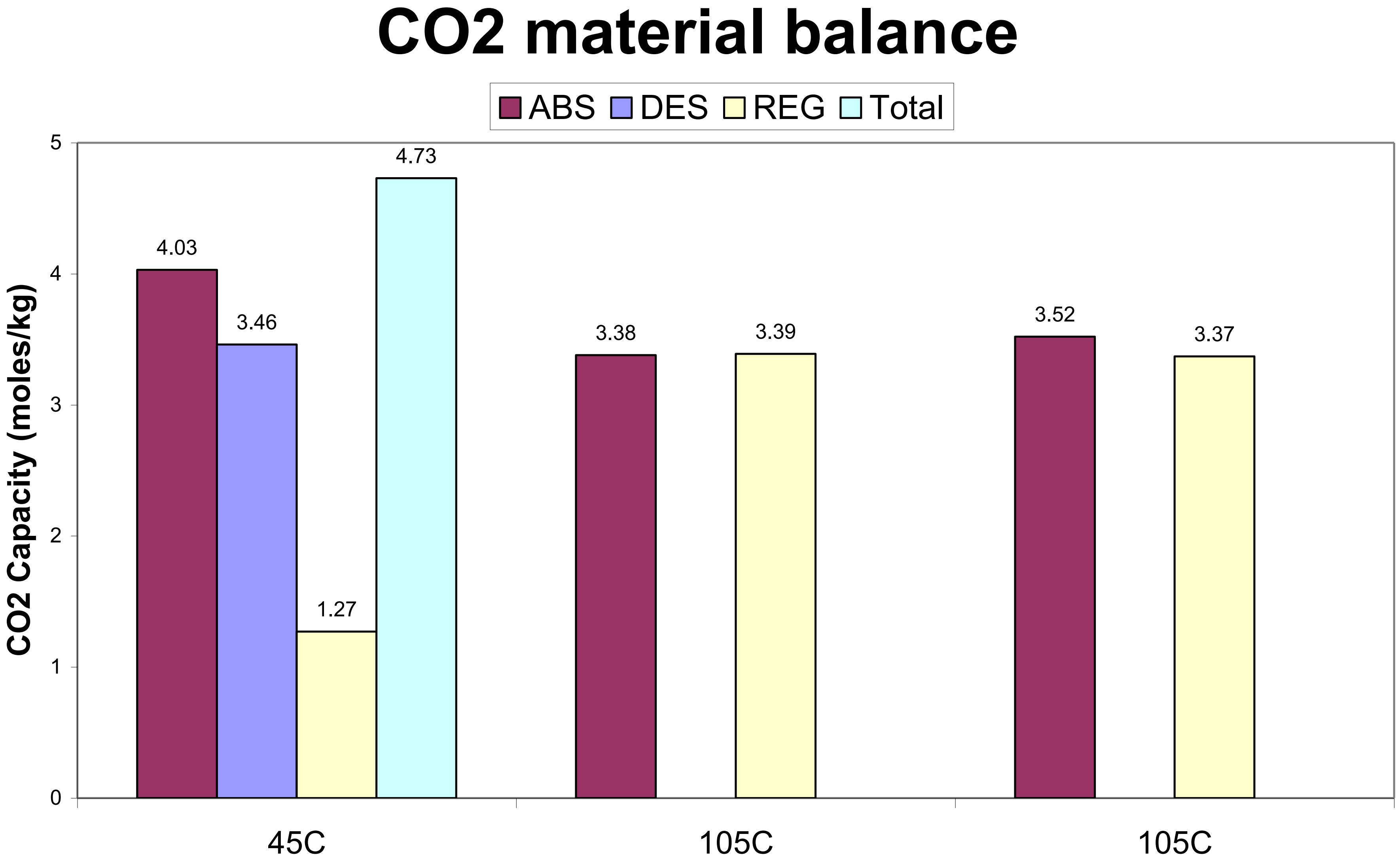
CO2 material balance
ABS
DES
REG
Total
CO2 Capacity (moles/kg)
5
4
3
2
1
0
4.03
3.46
1.27
4.73
3.38
3.39
3.52
3.37
45C
105C
105C

Figure 13

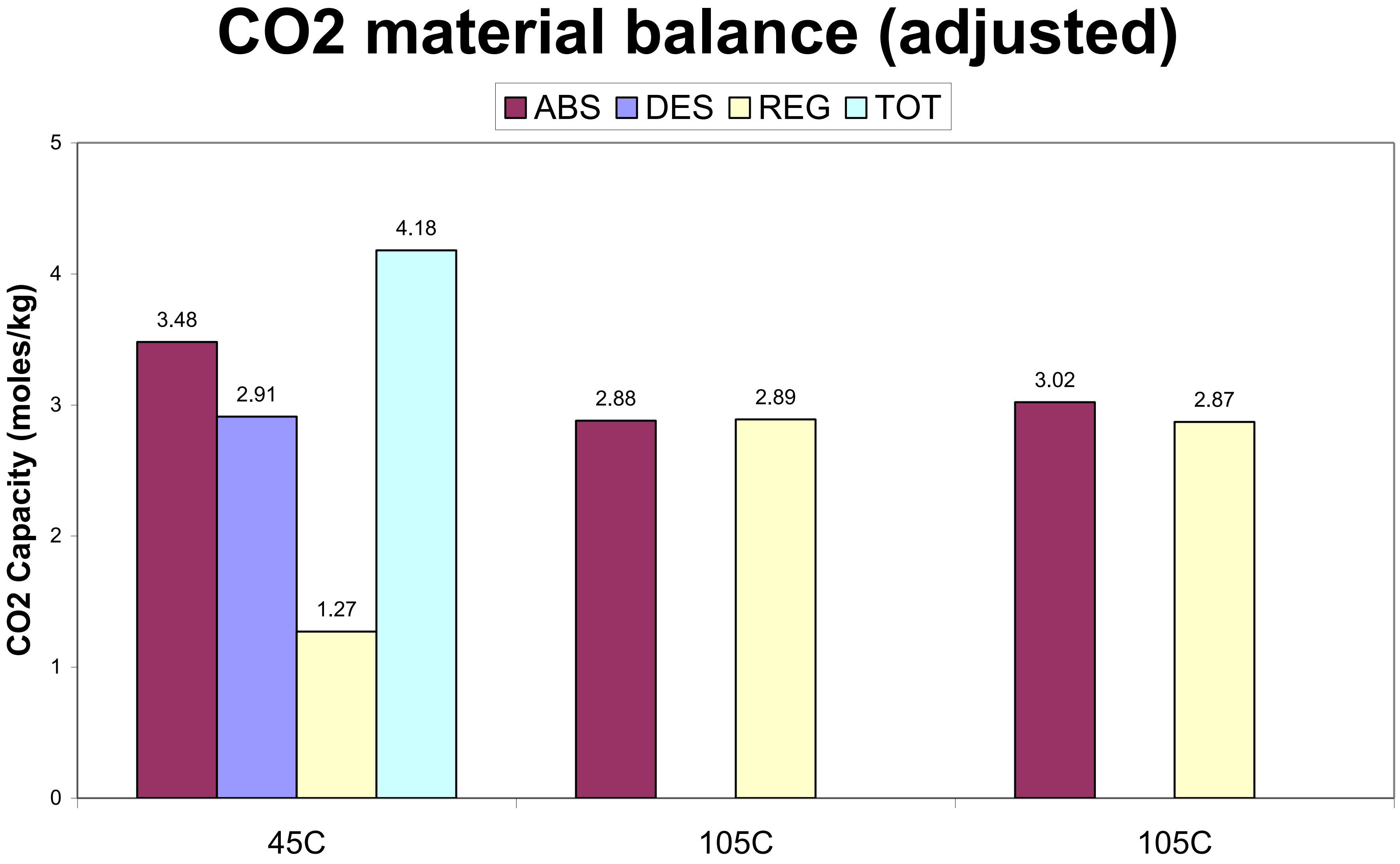
CO2 material balance (adjusted)
ABS
DES
REG
TOT
CO2 Capacity (moles/kg)
0
1
2
3
4
5
3.48
2.91
1.27
4.18
2.88
2.89
3.02
2.87
45C
105C
105C

Figure 14

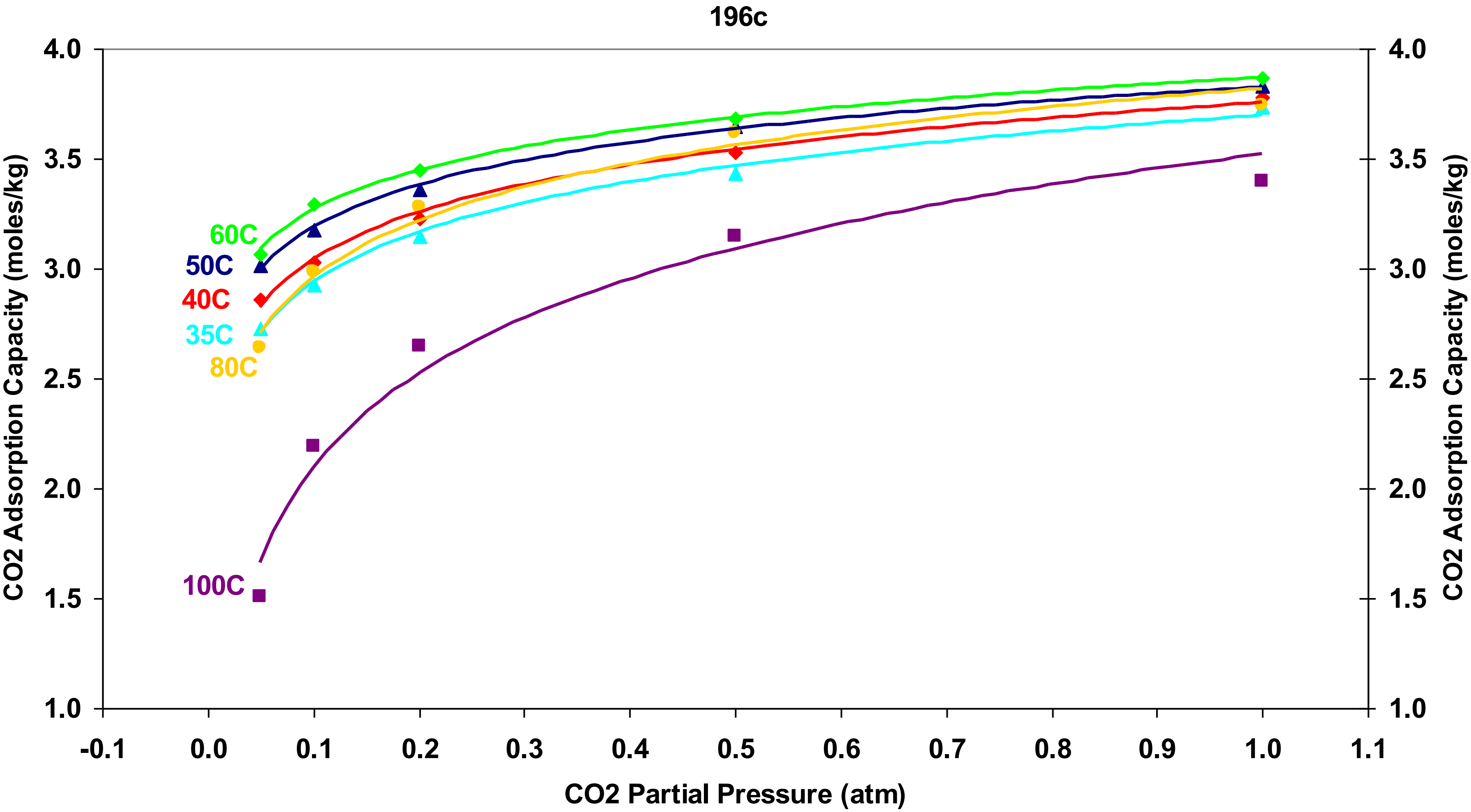
196c
CO2 Adsorption Capacity (moles/kg)
4.0
3.5
3.0
2.5
2.0
1.5
1.0
60C
50C
40C
35C
80C
100C
-0.1
0.0
0.1
0.2
0.3
0.4
0.5
0.6
0.7
0.8
0.9
1.0
1.1
CO2 Partial Pressure (atm)
CO2 Adsorption Capacity (moles/kg)

Figure 15

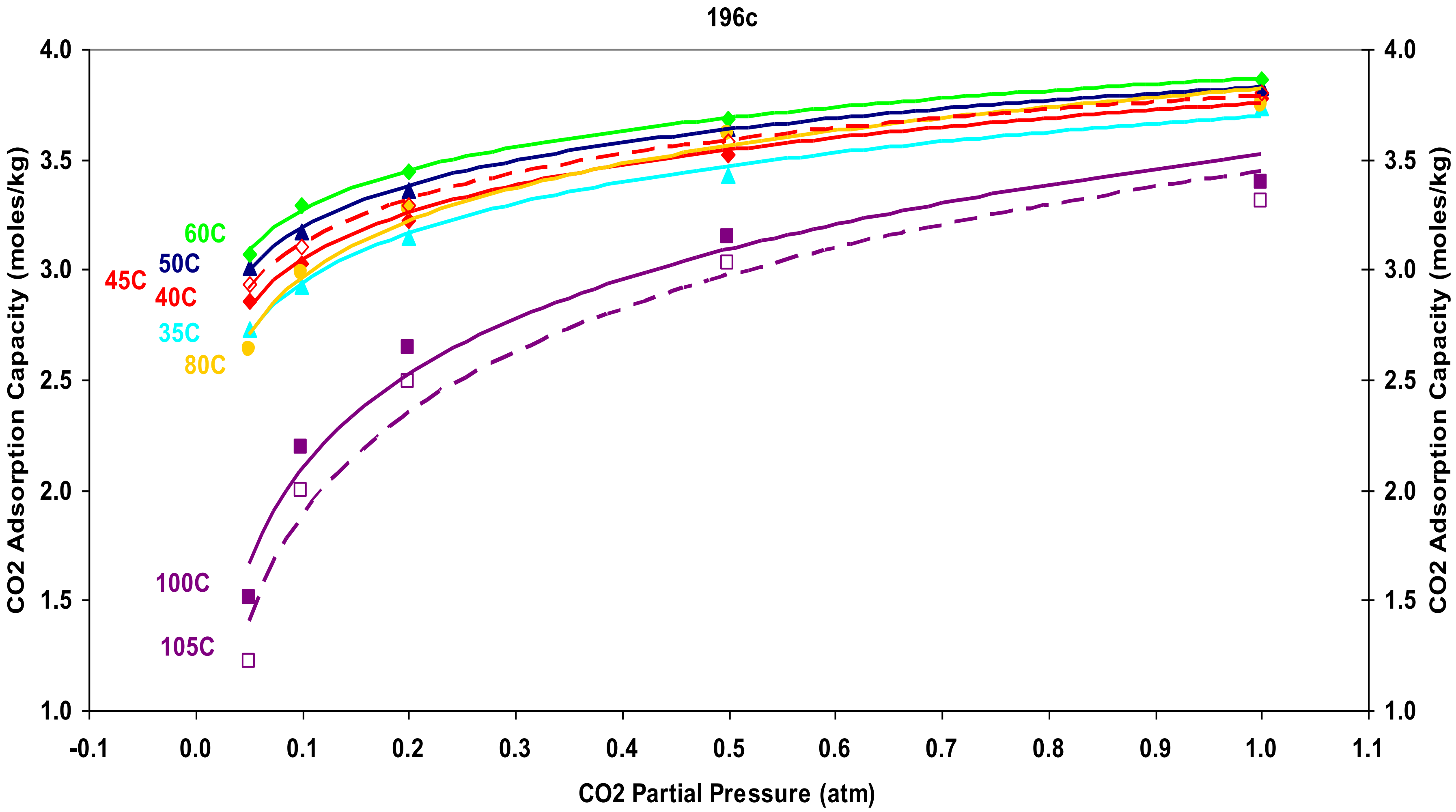

196c
CO2 Adsorption Capacity (moles/kg)
4.0
3.5
3.0
2.5
2.0
1.5
1.0
60C
50C
45C
40C
35C
80C
100C
105C
-0.1
0.0
0.1
0.2
0.3
0.4
0.5
0.6
0.7
0.8
0.9
1.0
1.1
CO2 Partial Pressure (atm)

Figure 16

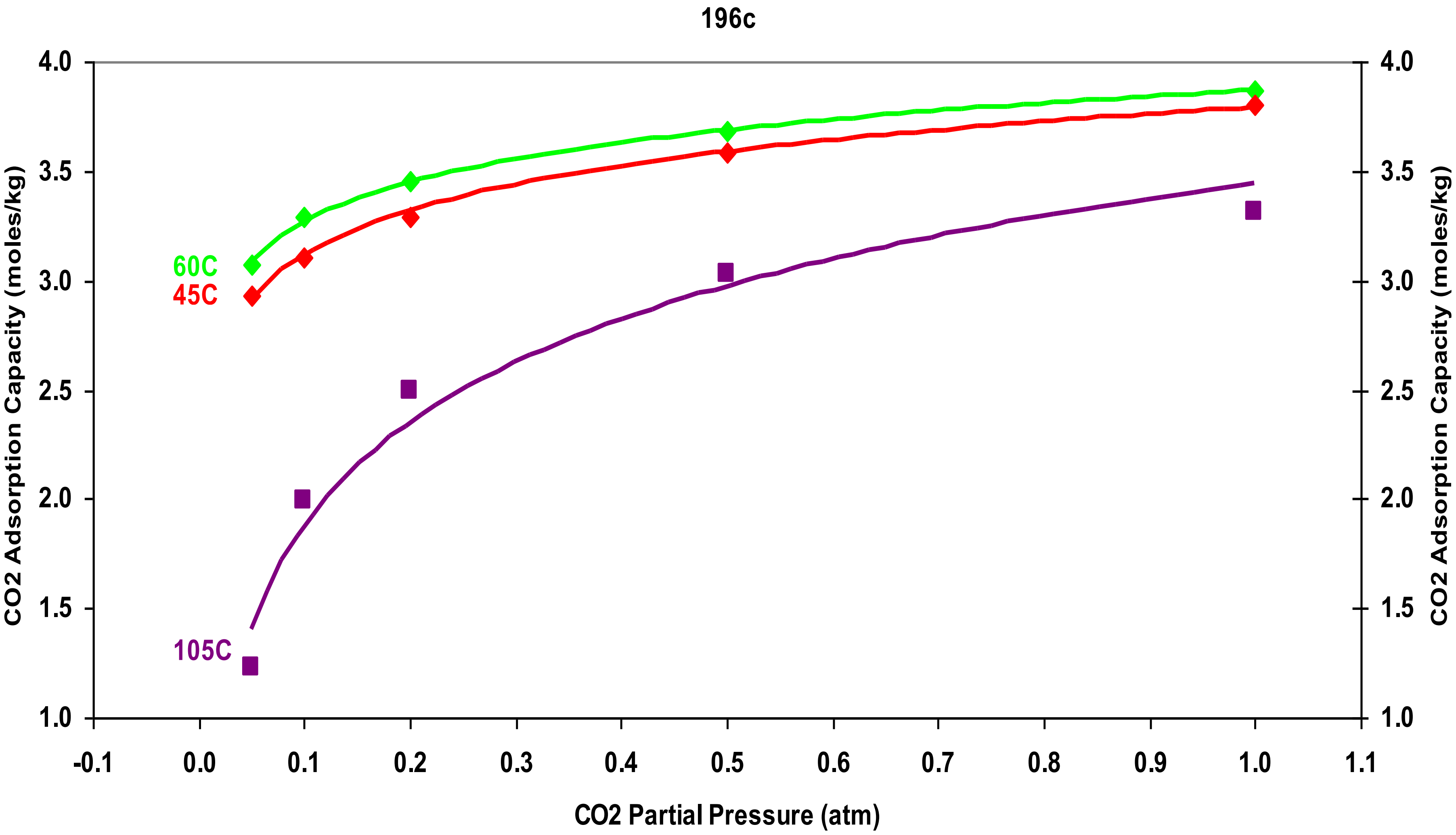
196c
4.0
3.5
3.0
2.5
2.0
1.5
1.0
CO2 Adsorption Capacity (moles/kg)
60C
45C
105C
-0.1
0.0
0.1
0.2
0.3
0.4
0.5
0.6
0.7
0.8
0.9
1.0
1.1
CO2 Partial Pressure (atm)
4.0
3.5
3.0
2.5
2.0
1.5
1.0
CO2 Adsorption Capacity (moles/kg)

Figure 17

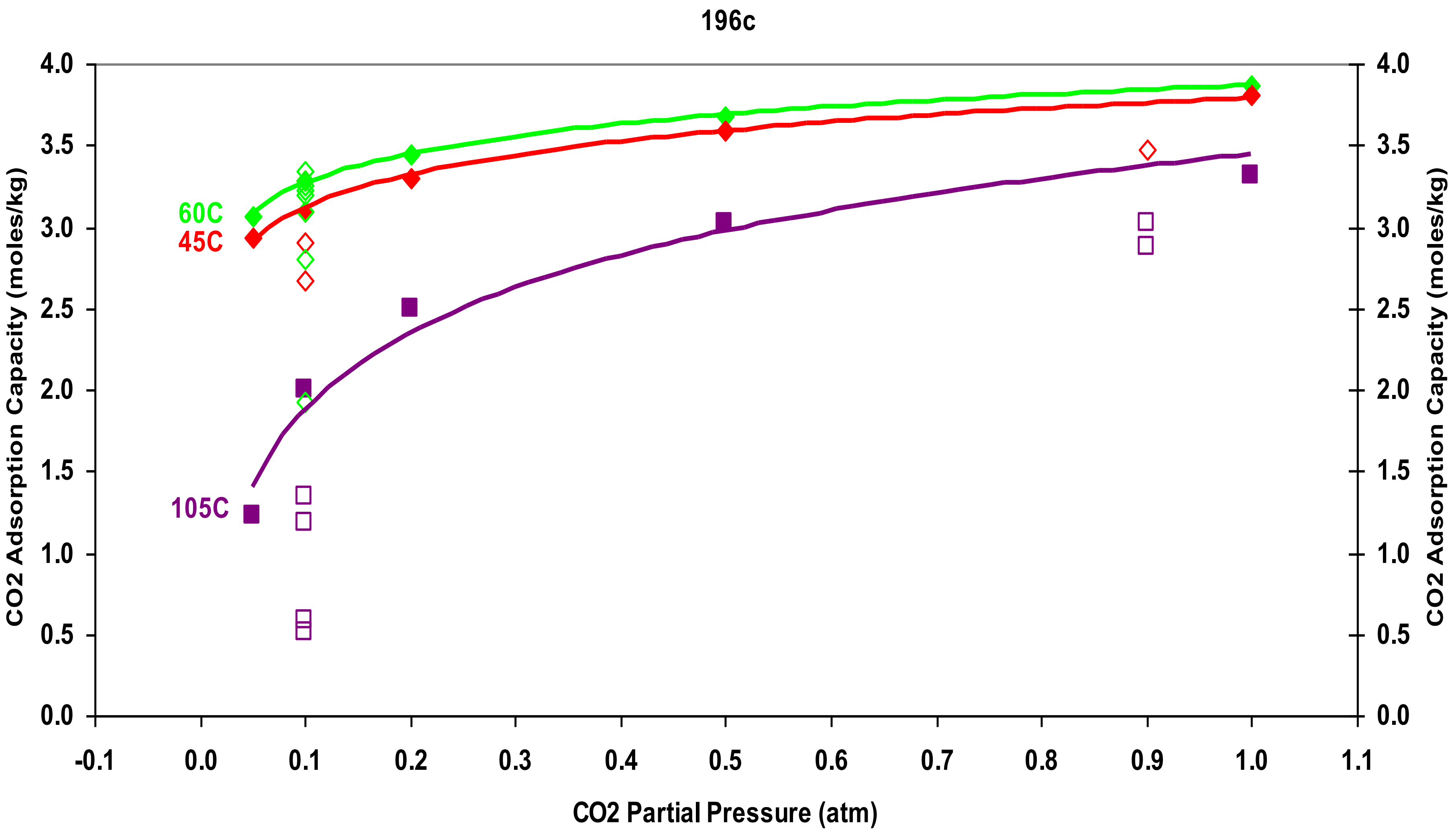
196c
60C
45C
105C
CO2 Adsorption Capacity (moles/kg)
CO2 Adsorption Capacity (moles/kg)
4.0
3.5
3.0
2.5
2.0
1.5
1.0
0.5
0.0
-0.1
0.0
0.1
0.2
0.3
0.4
0.5
0.6
0.7
0.8
0.9
1.0
1.1
CO2 Partial Pressure (atm)

Figure 18

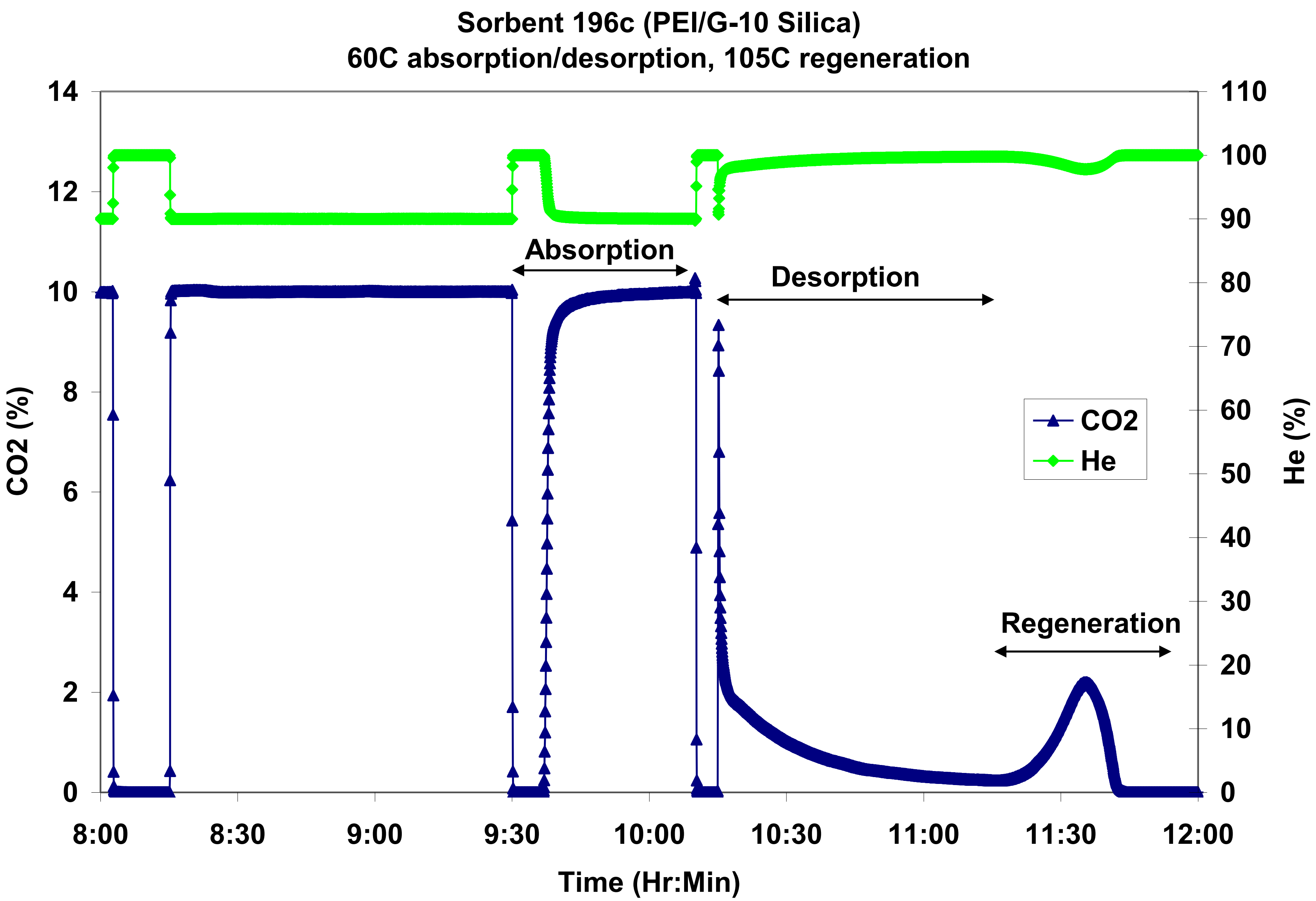
Sorbent 196c (PEI/G-10 Silica)
60C absorption/desorption, 105C regeneration
14
12
10
8
6
4
2
0
CO2 (%)
110
100
90
80
70
60
50
40
30
20
10
0
He (%)
8:00
8:30
9:00
9:30
10:00
10:30
11:00
11:30
12:00
Time (Hr:Min)
Absorption
Desorption
Regeneration
CO2
He

Figure 19

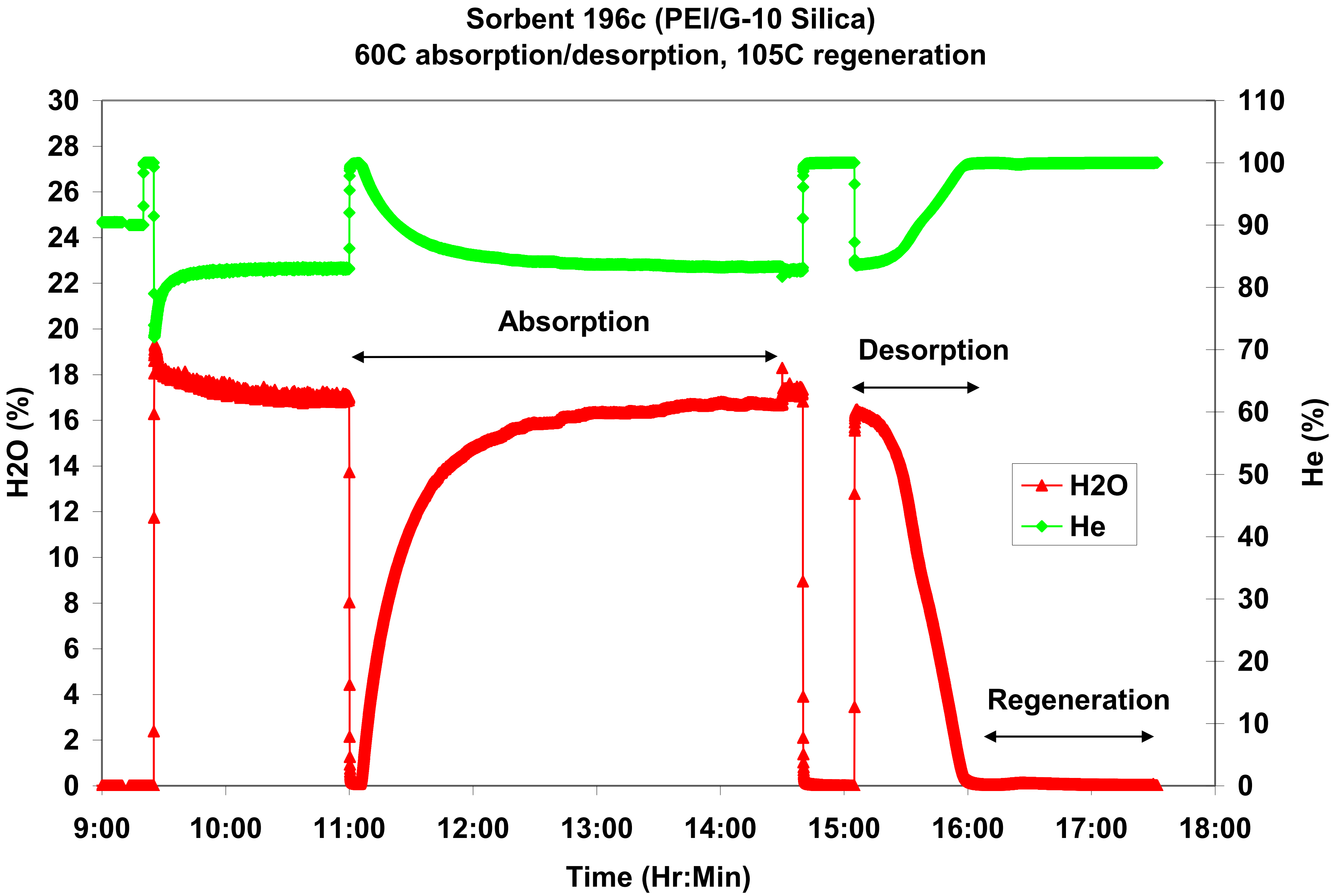
Sorbent 196c (PEI/G-10 Silica)
60C absorption/desorption, 105C regeneration
H2O (%)
He (%)
Time (Hr:Min)
30
28
26
24
22
20
18
16
14
12
10
8
6
4
2
0
110
100
90
80
70
60
50
40
30
20
10
0
9:00
10:00
11:00
12:00
13:00
14:00
15:00
16:00
17:00
18:00
Absorption
Desorption
Regeneration
H2O
He

Figure 20

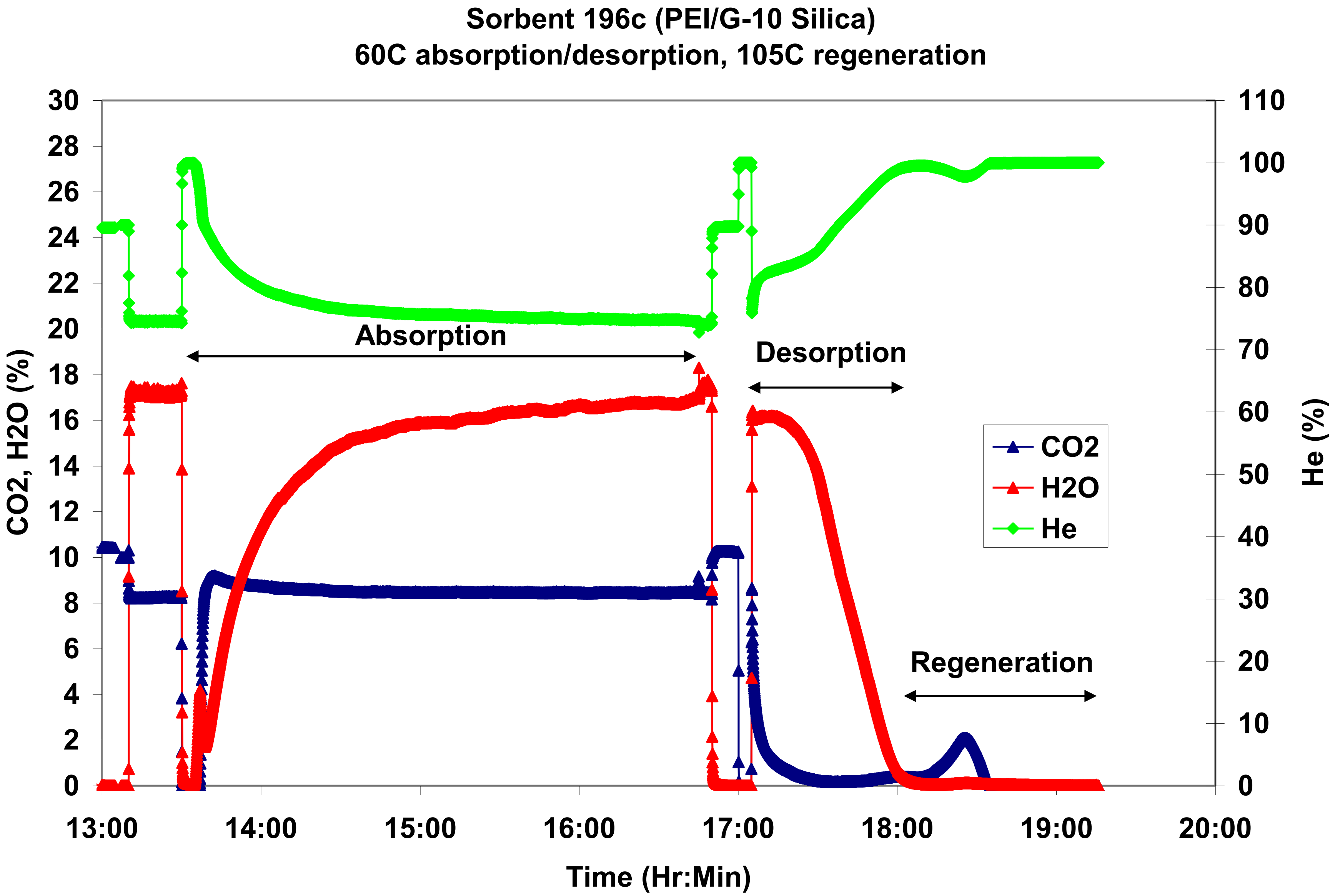
Sorbent 196c (PEI/G-10 Silica)
60C absorption/desorption, 105C regeneration
30
28
26
24
22
20
18
16
14
12
10
8
6
4
2
0
CO2, H2O (%)
110
100
90
80
70
60
50
40
30
20
10
0
He (%)
13:00
14:00
15:00
16:00
17:00
18:00
19:00
20:00
Time (Hr:Min)
Absorption
Desorption
Regeneration
CO2
H2O
He

Figure 21

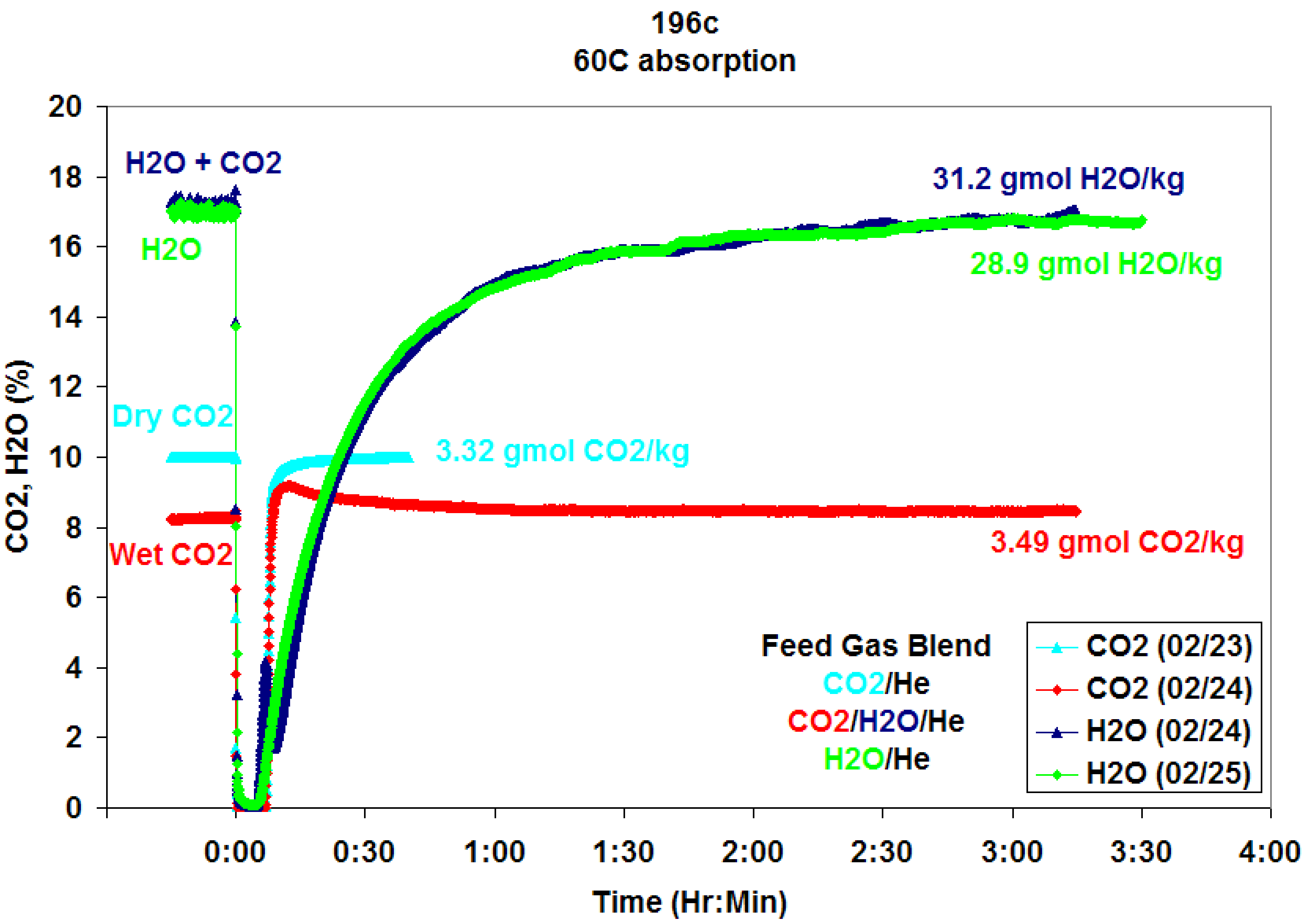

196c
60C absorption
H2O + CO2
H2O
Dry CO2
Wet CO2
31.2 gmol H2O/kg
28.9 gmol H2O/kg
3.32 gmol CO2/kg
3.49 gmol CO2/kg
Feed Gas Blend
CO2/He
CO2/H2O/He
H2O/He
CO2 (02/23)
CO2 (02/24)
H2O (02/24)
H2O (02/25)
CO2, H2O (%)
0
2
4
6
8
10
12
14
16
18
20
0:00
0:30
1:00
1:30
2:00
2:30
3:00
3:30
4:00
Time (Hr:Min)

Figure 22

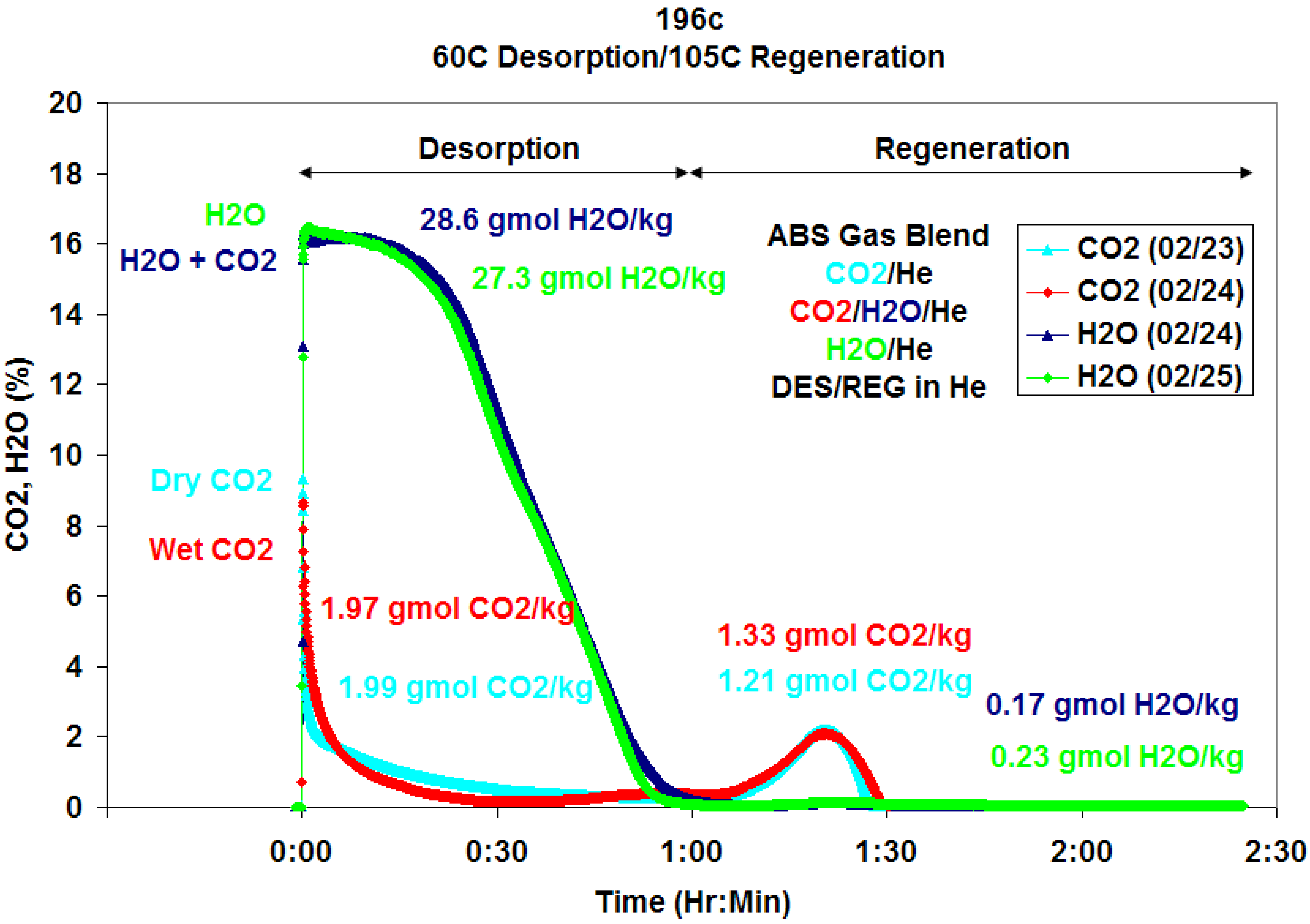
196c
60C Desorption/105C Regeneration
Desorption
Regeneration
H2O
H2O + CO2
28.6 gmol H2O/kg
27.3 gmol H2O/kg
ABS Gas Blend
CO2/He
CO2/H2O/He
H2O/He
DES/REG in He
CO2 (02/23)
CO2 (02/24)
H2O (02/24)
H2O (02/25)
Dry CO2
Wet CO2
1.97 gmol CO2/kg
1.99 gmol CO2/kg
1.33 gmol CO2/kg
1.21 gmol CO2/kg
0.17 gmol H2O/kg
0.23 gmol H2O/kg
CO2, H2O (%)
20
18
16
14
12
10
8
6
4
2
0
0:00
0:30
1:00
1:30
2:00
2:30
Time (Hr:Min)

Figure 23

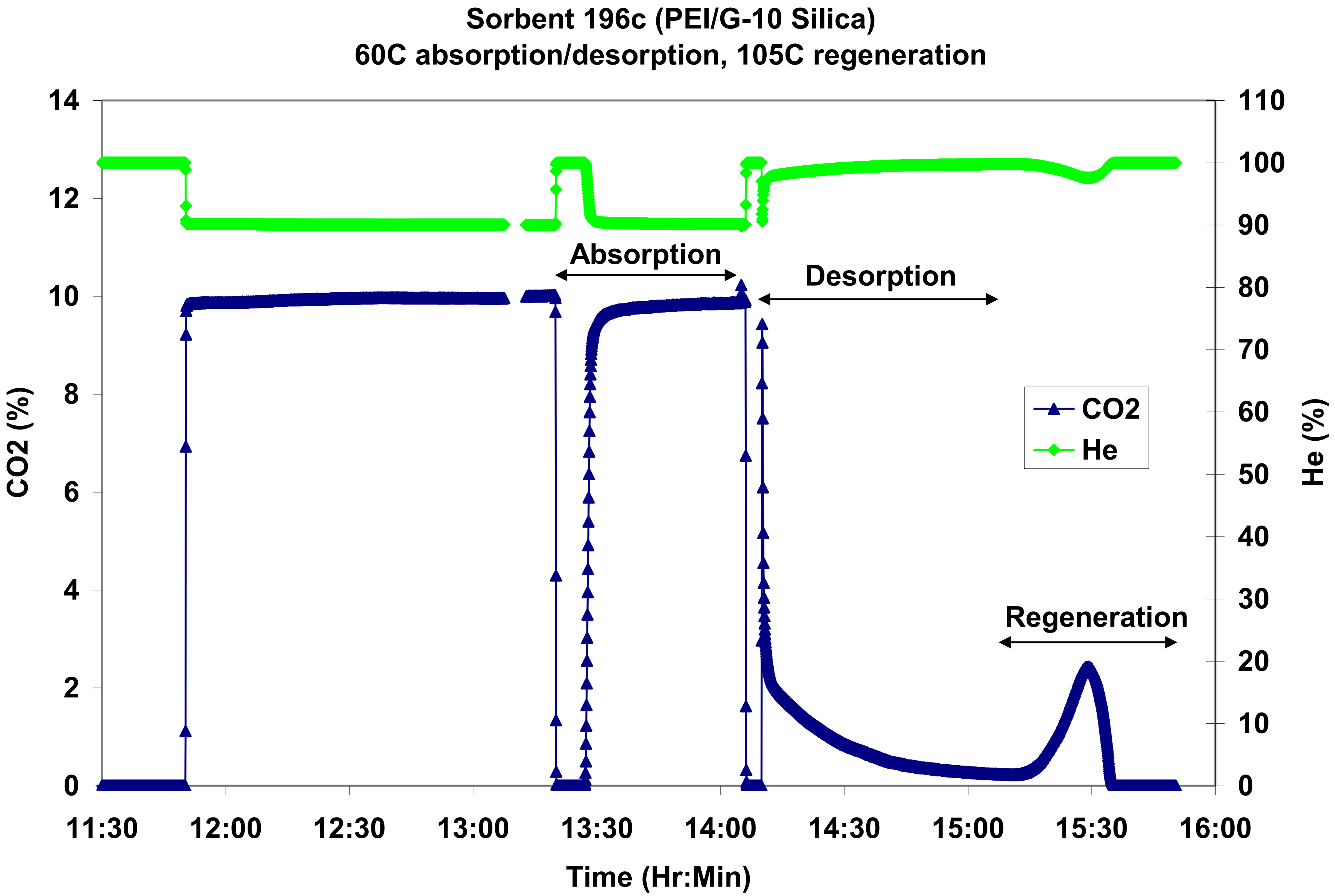
Sorbent 196c (PEI/G-10 Silica)
60C absorption/desorption, 105C regeneration
CO2 (%)
He (%)
Time (Hr:Min)
0
2
4
6
8
10
12
14
0
10
20
30
40
50
60
70
80
90
100
110
11:30
12:00
12:30
13:00
13:30
14:00
14:30
15:00
15:30
16:00
Absorption
Desorption
Regeneration
CO2
He

Figure 24

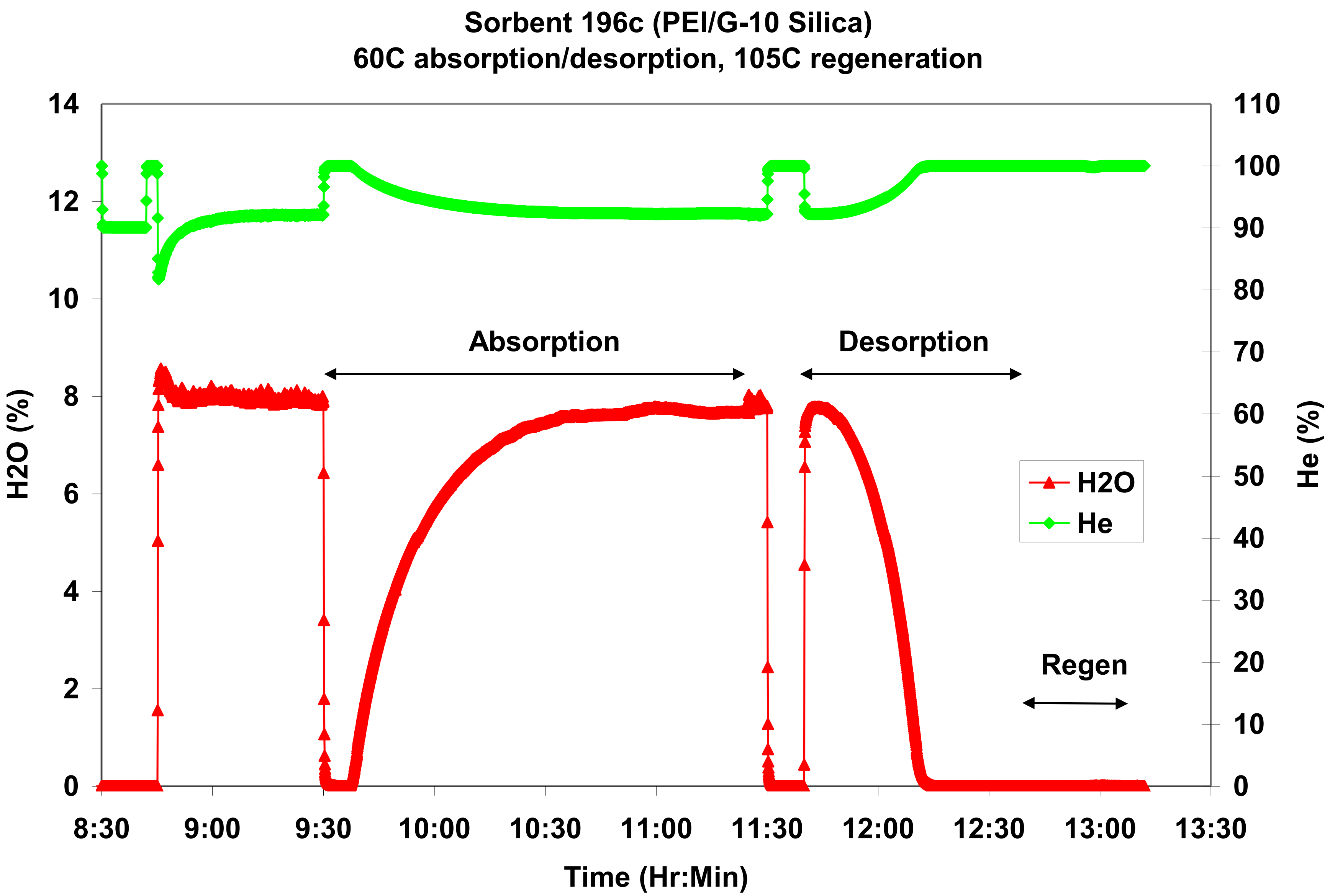

Sorbent 196c (PEI/G-10 Silica)
60C absorption/desorption, 105C regeneration
H2O (%)
He (%)
Time (Hr:Min)
0
2
4
6
8
10
12
14
0
10
20
30
40
50
60
70
80
90
100
110
8:30
9:00
9:30
10:00
10:30
11:00
11:30
12:00
12:30
13:00
13:30
Absorption
Desorption
Regen
H2O
He

Figure 25

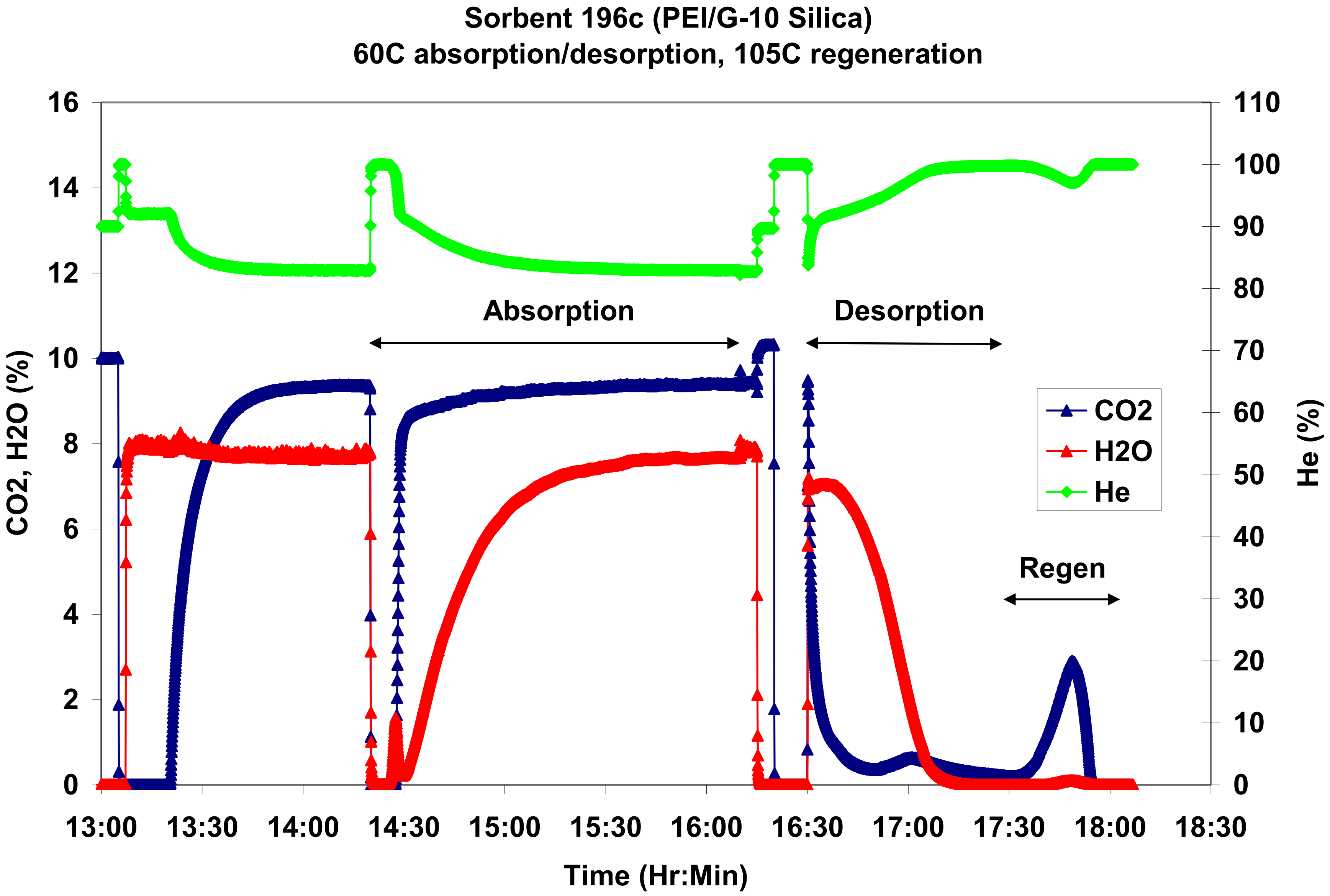
Sorbent 196c (PEI/G-10 Silica)
60C absorption/desorption, 105C regeneration
CO2, H2O (%)
16
14
12
10
8
6
4
2
0
He (%)
110
100
90
80
70
60
50
40
30
20
10
0
Absorption
Desorption
Regen
CO2
H2O
He
13:00
13:30
14:00
14:30
15:00
15:30
16:00
16:30
17:00
17:30
18:00
18:30
Time (Hr:Min)

Figure 26

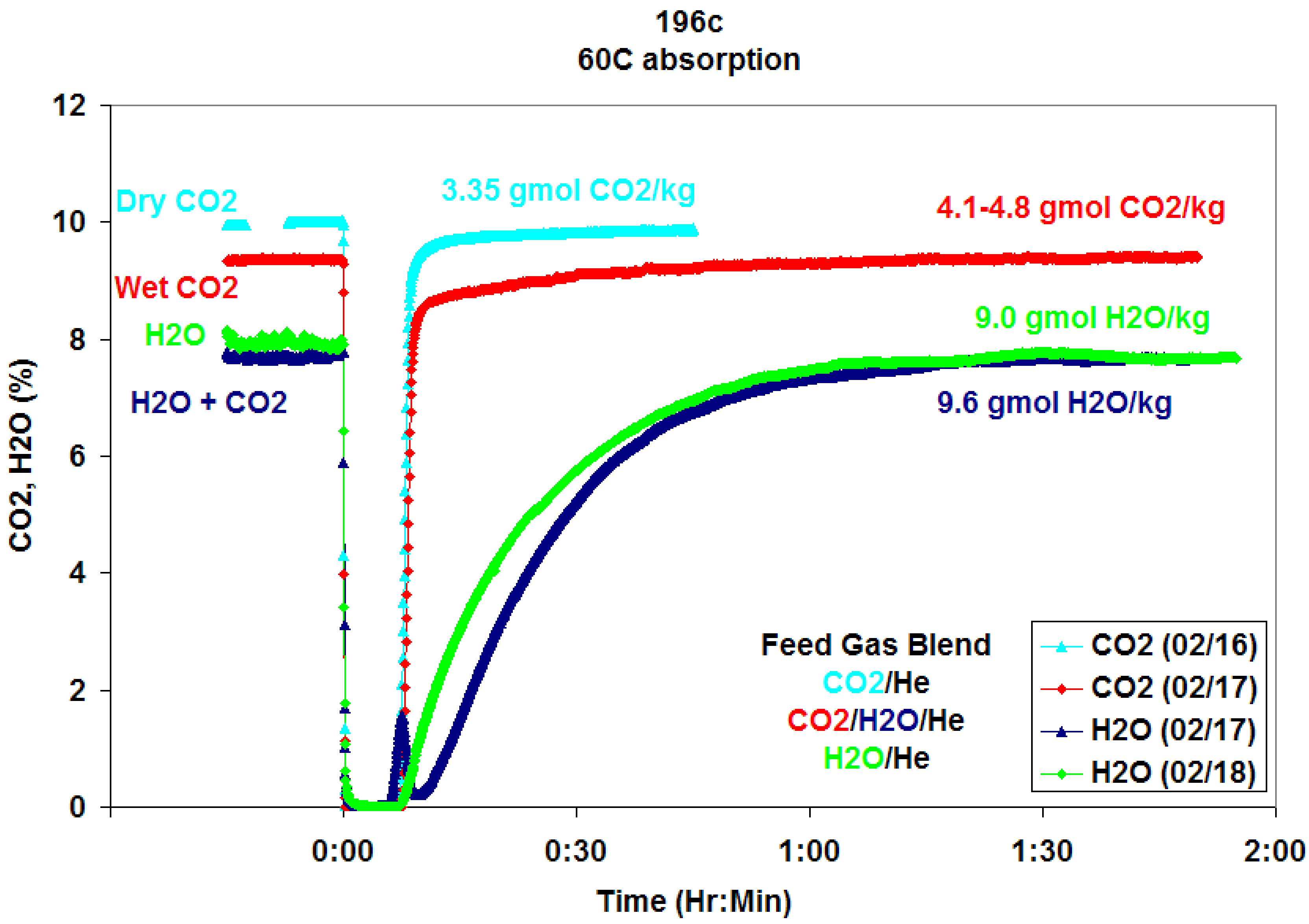

196c
60C absorption
12
10
8
6
4
2
0
CO2, H2O (%)
Dry CO2
Wet CO2
H2O
H2O + CO2
3.35 gmol CO2/kg
4.1-4.8 gmol CO2/kg
9.0 gmol H2O/kg
9.6 gmol H2O/kg
Feed Gas Blend
CO2/He
CO2/H2O/He
H2O/He
CO2 (02/16)
CO2 (02/17)
H2O (02/17)
H2O (02/18)
0:00
0:30
1:00
1:30
2:00
Time (Hr:Min)

Figure 27

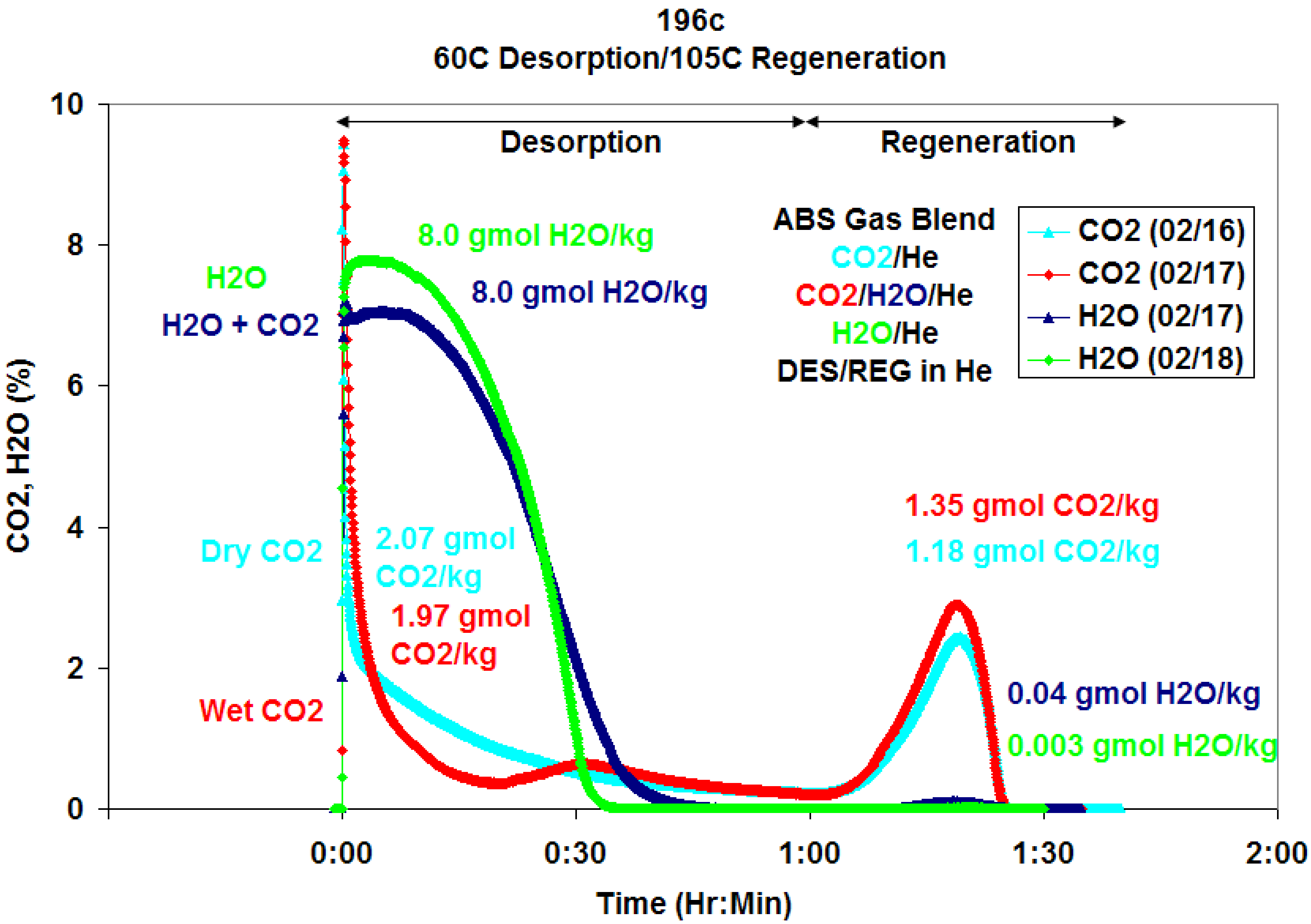
196c
60C Desorption/105C Regeneration
Desorption
Regeneration
ABS Gas Blend
CO2/He
CO2/H2O/He
H2O/He
DES/REG in He
CO2 (02/16)
CO2 (02/17)
H2O (02/17)
H2O (02/18)
8.0 gmol H2O/kg
8.0 gmol H2O/kg
H2O
H2O + CO2
Dry CO2
2.07 gmol CO2/kg
1.97 gmol CO2/kg
Wet CO2
1.35 gmol CO2/kg
1.18 gmol CO2/kg
0.04 gmol H2O/kg
0.003 gmol H2O/kg
CO2, H2O (%)
10
8
6
4
2
0
0:00
0:30
1:00
1:30
2:00
Time (Hr:Min)

Figure 28

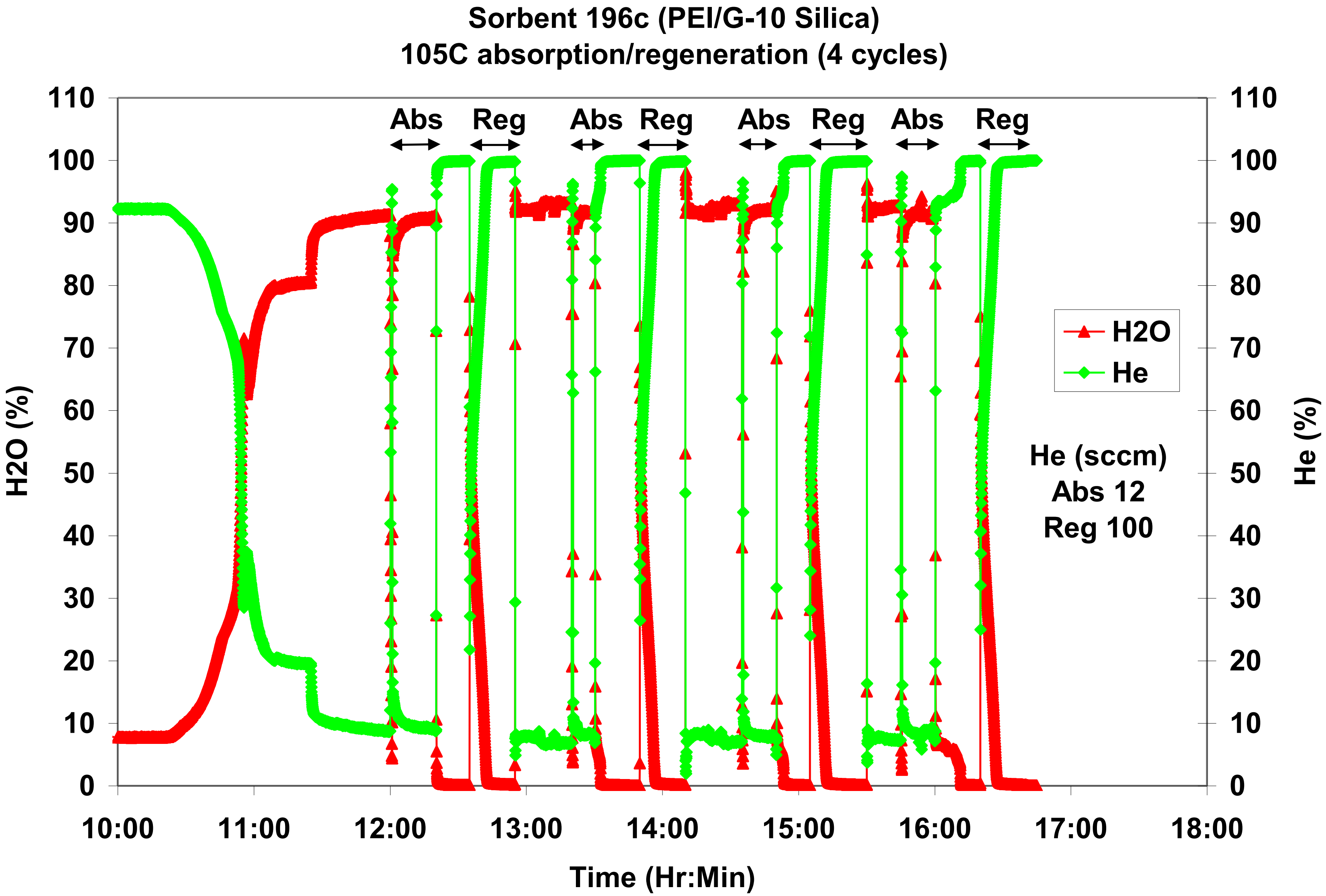

Sorbent 196c (PEI/G-10 Silica)
105C absorption/regeneration (4 cycles)
H2O (%)
He (%)
Time (Hr:Min)
Abs
Reg
Abs
Reg
Abs
Reg
Abs
Reg
H2O
He
He (sccm)
Abs 12
Reg 100
110
100
90
80
70
60
50
40
30
20
10
0
10:00
11:00
12:00
13:00
14:00
15:00
16:00
17:00
18:00

Figure 29

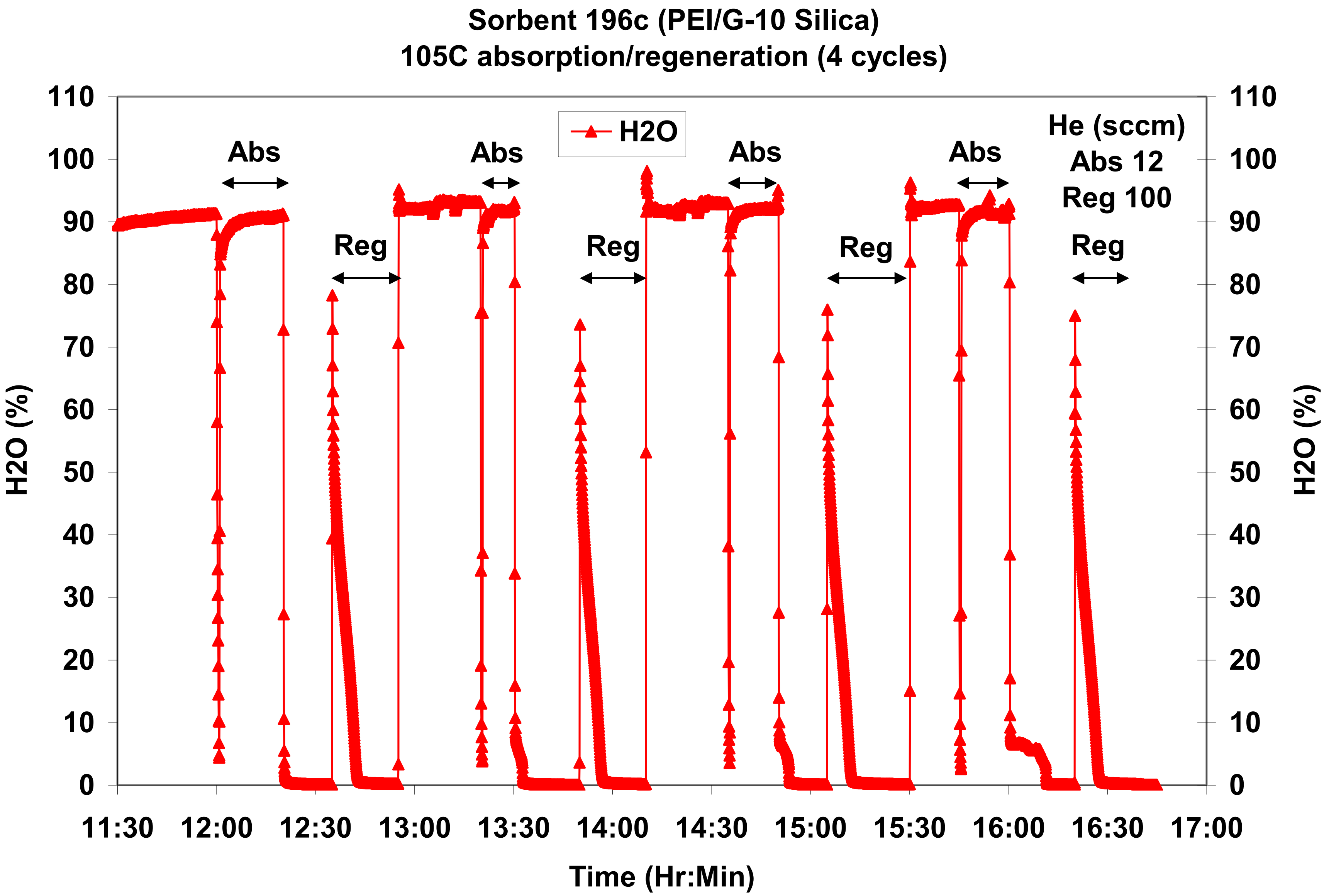
Sorbent 196c (PEI/G-10 Silica)
105C absorption/regeneration (4 cycles)
H2O
He (sccm)
Abs 12
Reg 100
Abs
Reg
Abs
Reg
Abs
Reg
Abs
Reg
H2O (%)
H2O (%)
0
10
20
30
40
50
60
70
80
90
100
110
11:30
12:00
12:30
13:00
13:30
14:00
14:30
15:00
15:30
16:00
16:30
17:00
Time (Hr:Min)

Figure 30

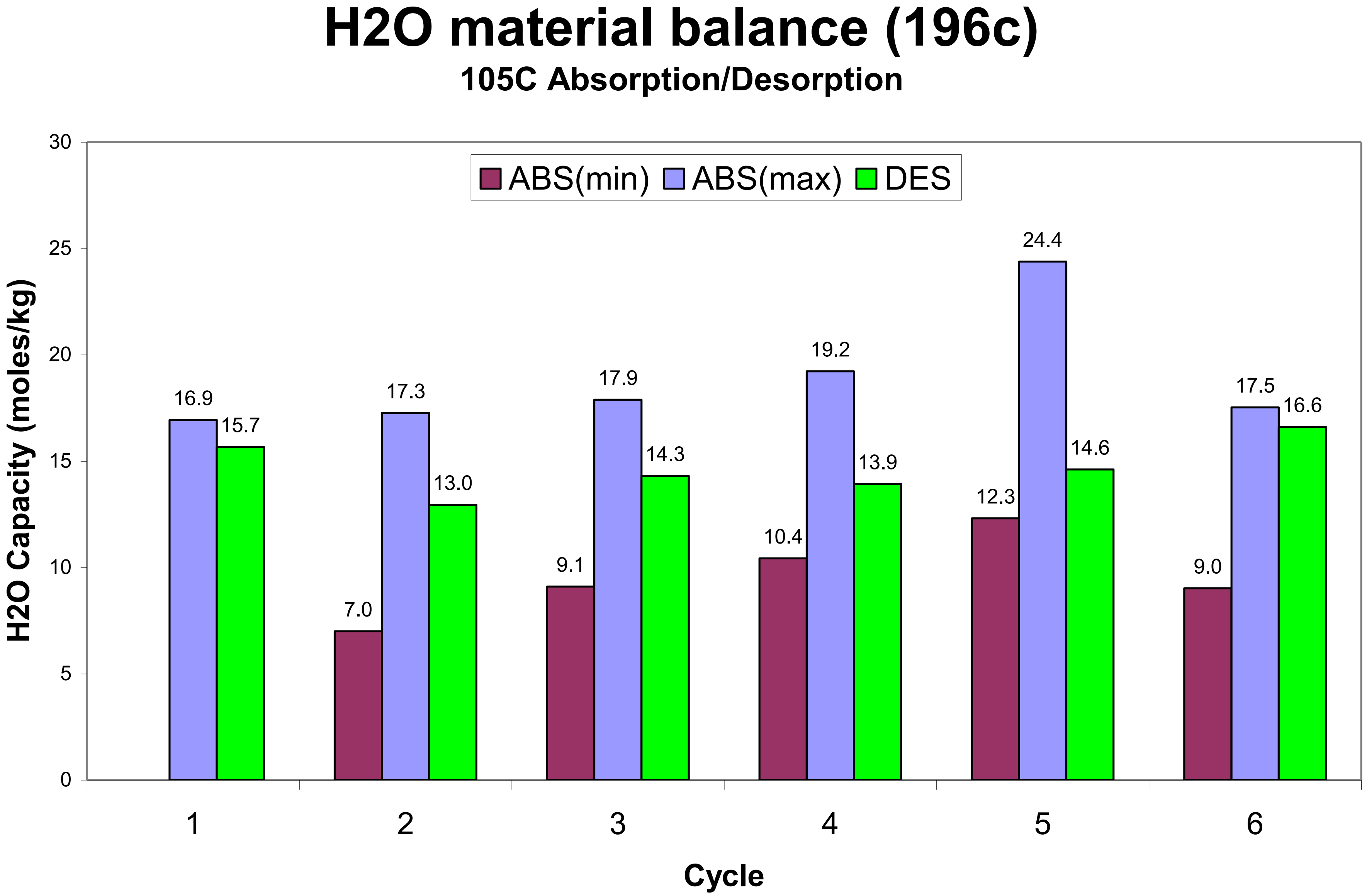
H2O material balance (196c)
105C Absorption/Desorption
ABS(min)
ABS(max)
DES
H2O Capacity (moles/kg)
0
5
10
15
20
25
30
Cycle
1
2
3
4
5
6
16.9
15.7
7.0
17.3
13.0
9.1
17.9
14.3
10.4
19.2
13.9
12.3
24.4
14.6
9.0
17.5
16.6

Figure 31

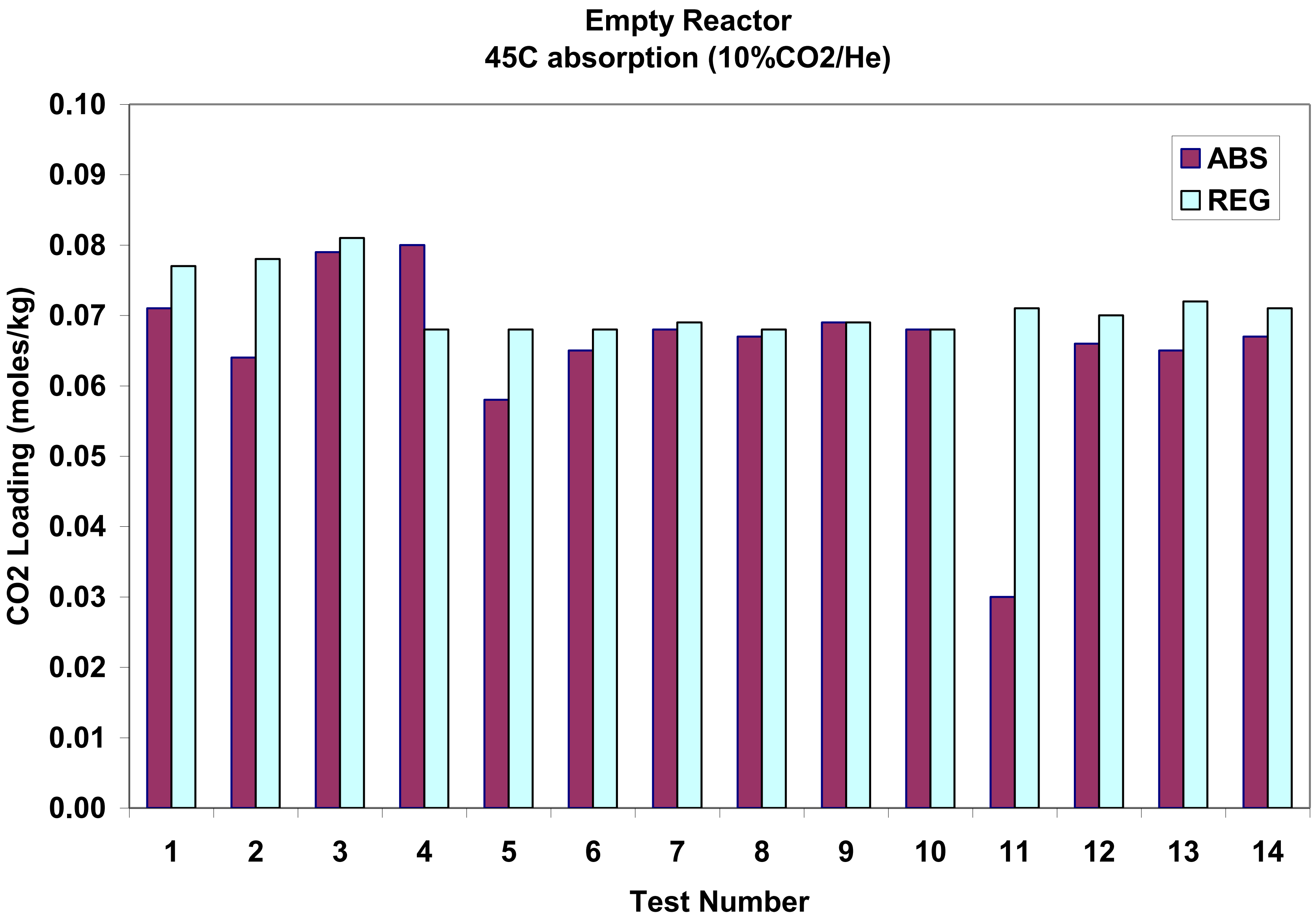
Empty Reactor
45C absorption (10%CO2/He)
0.10
0.09
0.08
0.07
0.06
0.05
0.04
0.03
0.02
0.01
0.00
CO2 Loading (moles/kg)
ABS
REG
1
2
3
4
5
6
7
8
9
10
11
12
13
14
Test Number

Figure 32

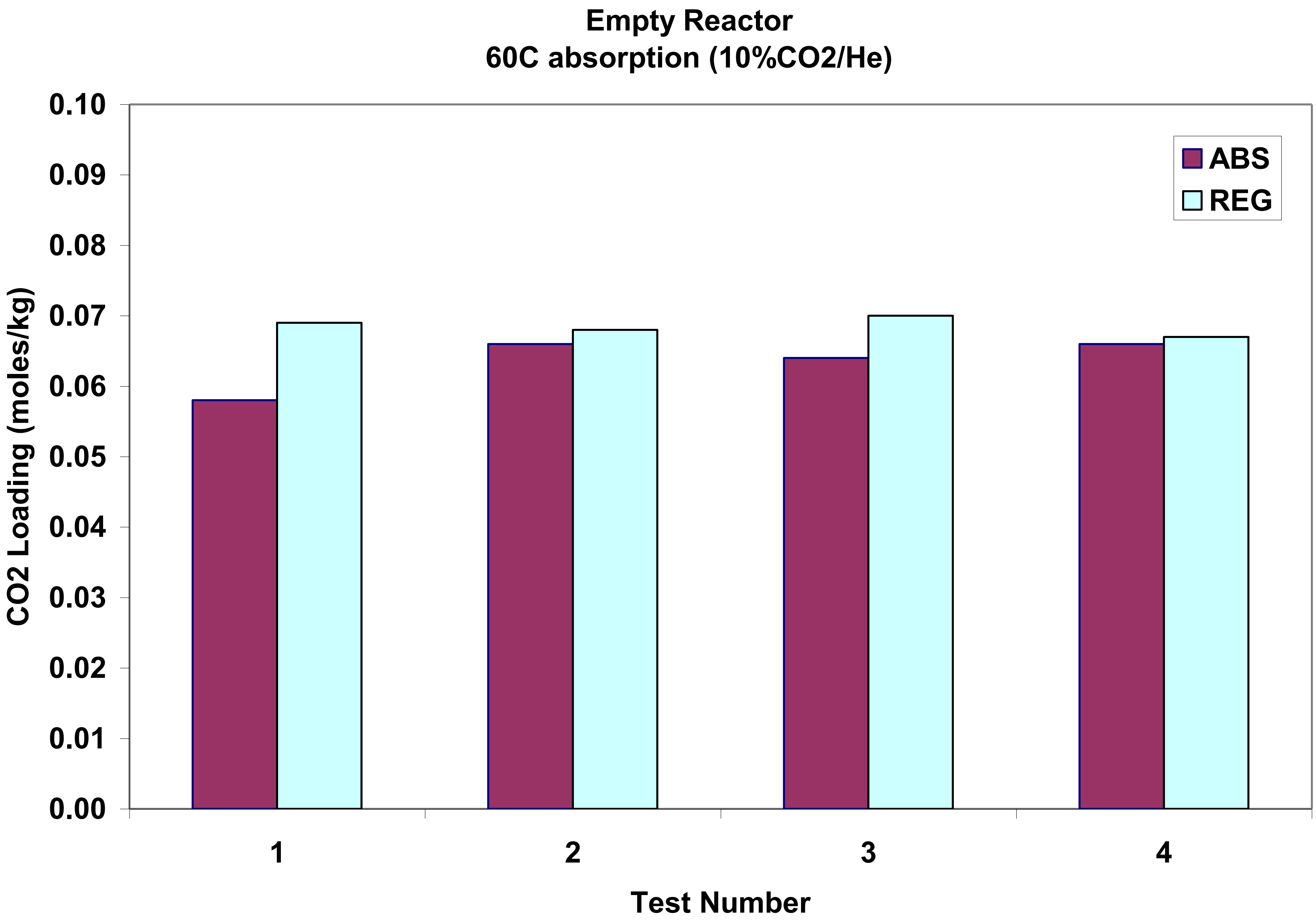
Empty Reactor
60C absorption (10%CO2/He)
CO2 Loading (moles/kg)
0.10
0.09
0.08
0.07
0.06
0.05
0.04
0.03
0.02
0.01
0.00
ABS
REG
1
2
3
4
Test Number

Figure 33

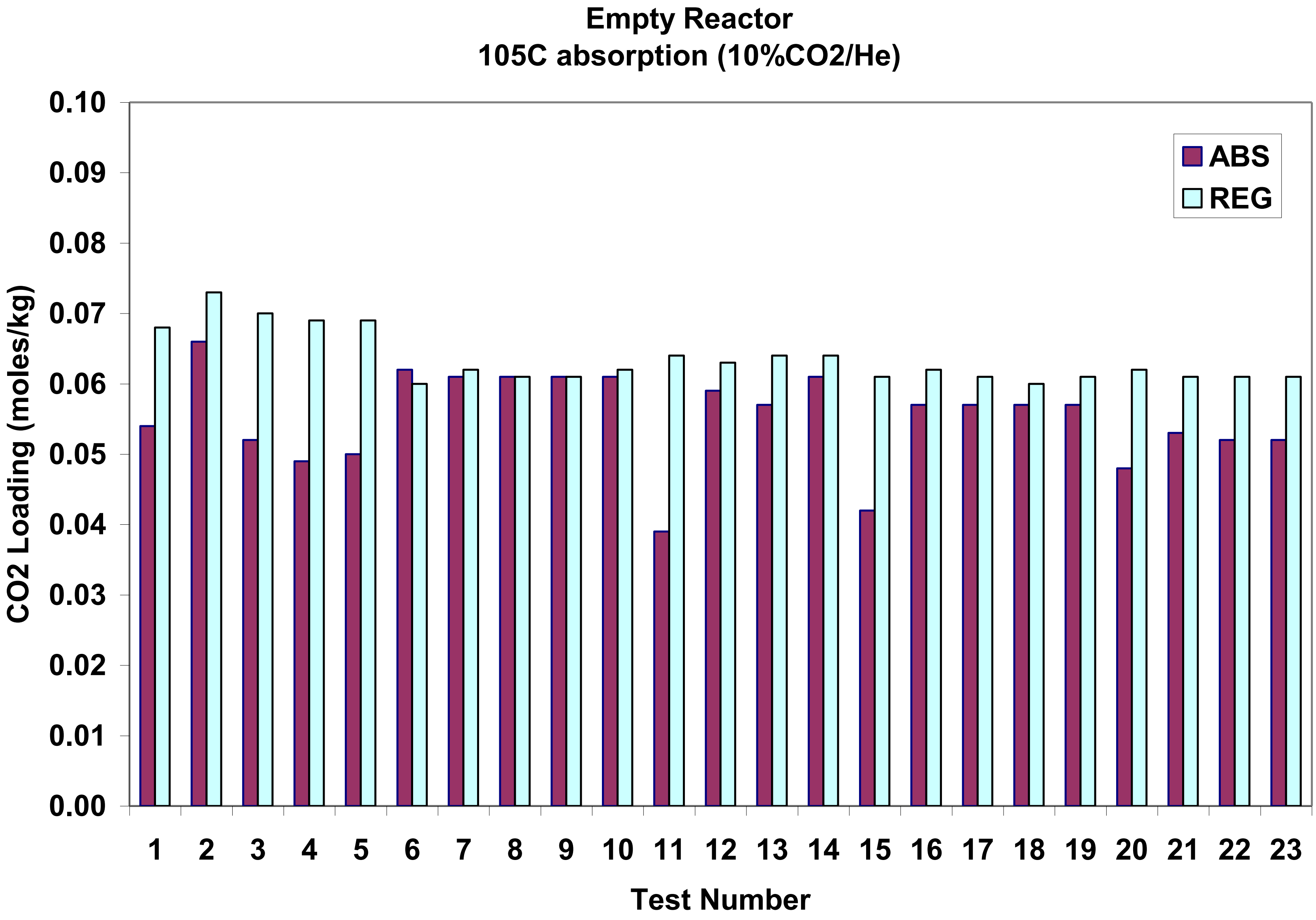

Empty Reactor
105C absorption (10%CO2/He)
CO2 Loading (moles/kg)
0.10
0.09
0.08
0.07
0.06
0.05
0.04
0.03
0.02
0.01
0.00
ABS
REG
1
2
3
4
5
6
7
8
9
10
11
12
13
14
15
16
17
18
19
20
21
22
23
Test Number

Figure 34

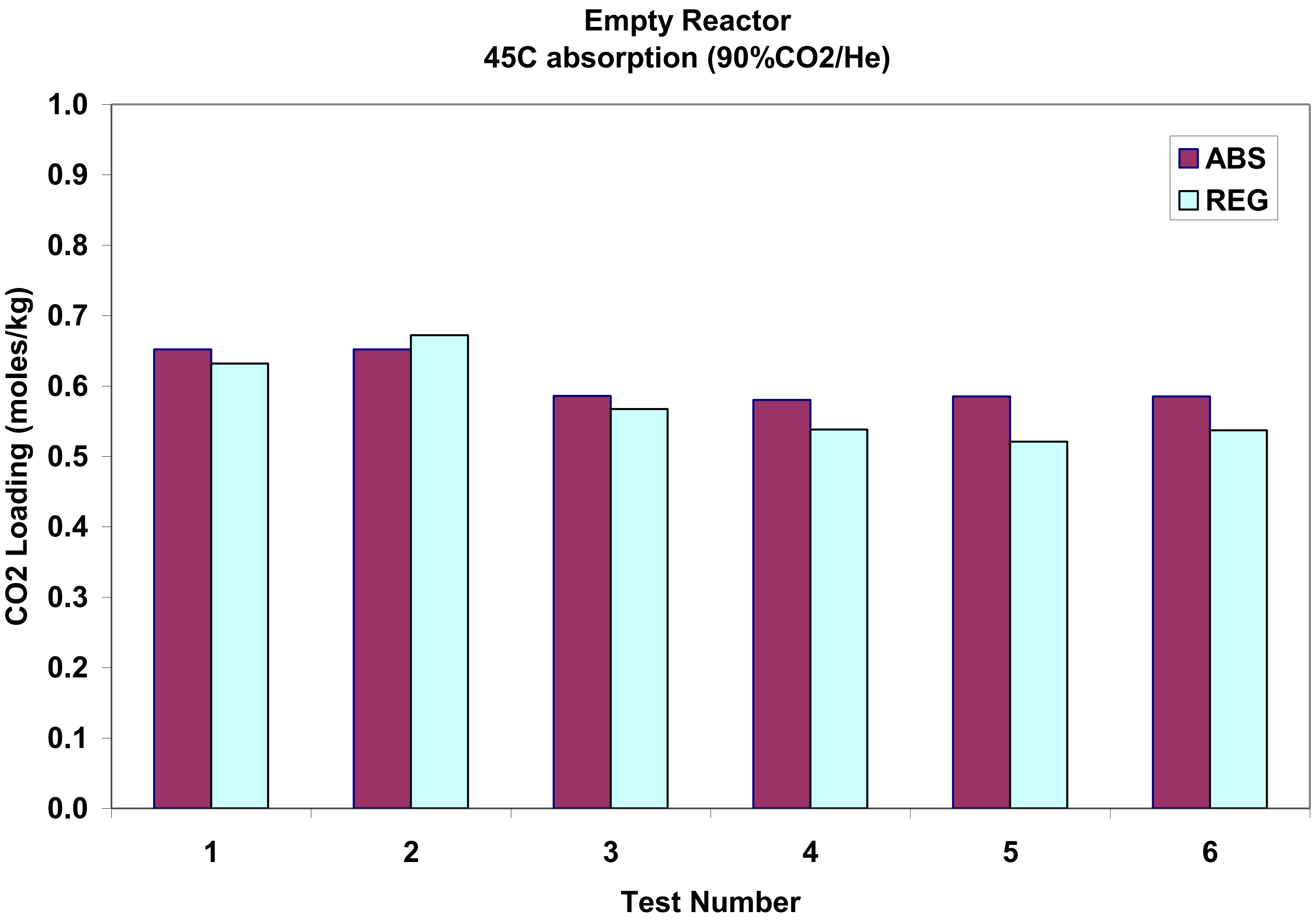
Empty Reactor
45C absorption (90%CO2/He)
CO2 Loading (moles/kg)
1.0
0.9
0.8
0.7
0.6
0.5
0.4
0.3
0.2
0.1
0.0
ABS
REG
1
2
3
4
5
6
Test Number

Figure 35

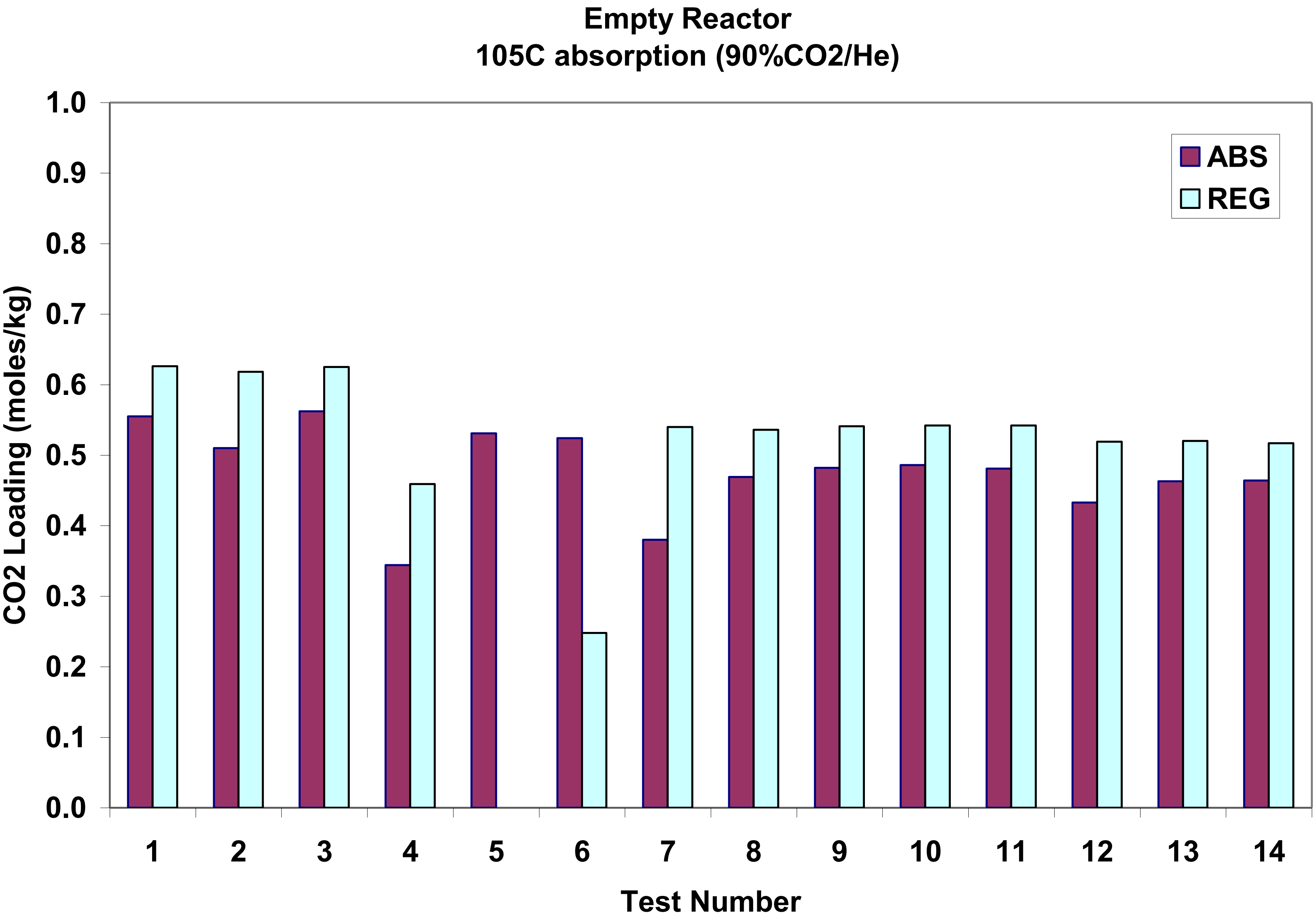
Empty Reactor
105C absorption (90%CO2/He)
CO2 Loading (moles/kg)
1.0
0.9
0.8
0.7
0.6
0.5
0.4
0.3
0.2
0.1
0.0
ABS
REG
1
2
3
4
5
6
7
8
9
10
11
12
13
14
Test Number

Figure 36

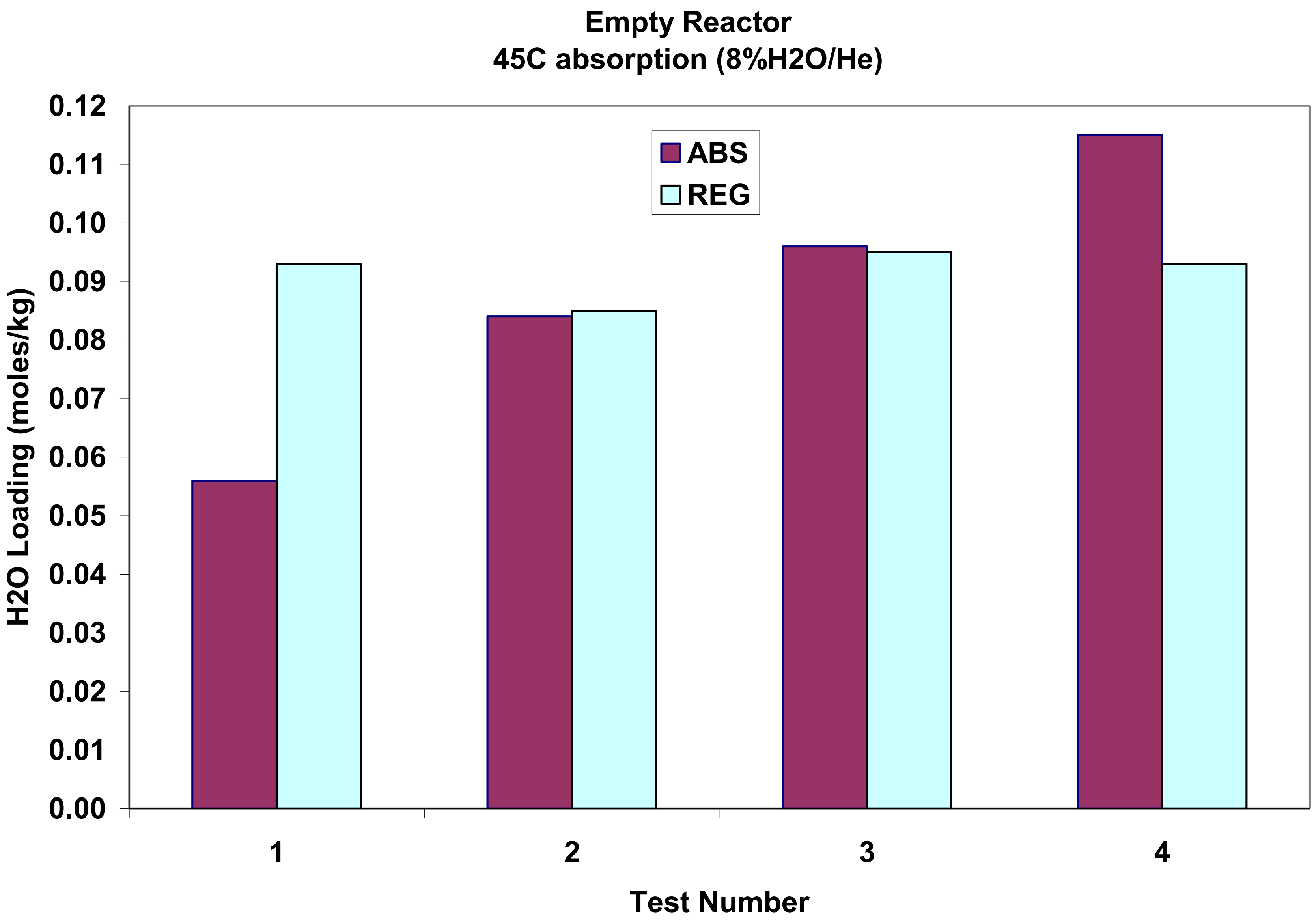
Empty Reactor
45C absorption (8%H2O/He)
H2O Loading (moles/kg)
0.12
0.11
0.10
0.09
0.08
0.07
0.06
0.05
0.04
0.03
0.02
0.01
0.00
ABS
REG
1
2
3
4
Test Number

Figure 37

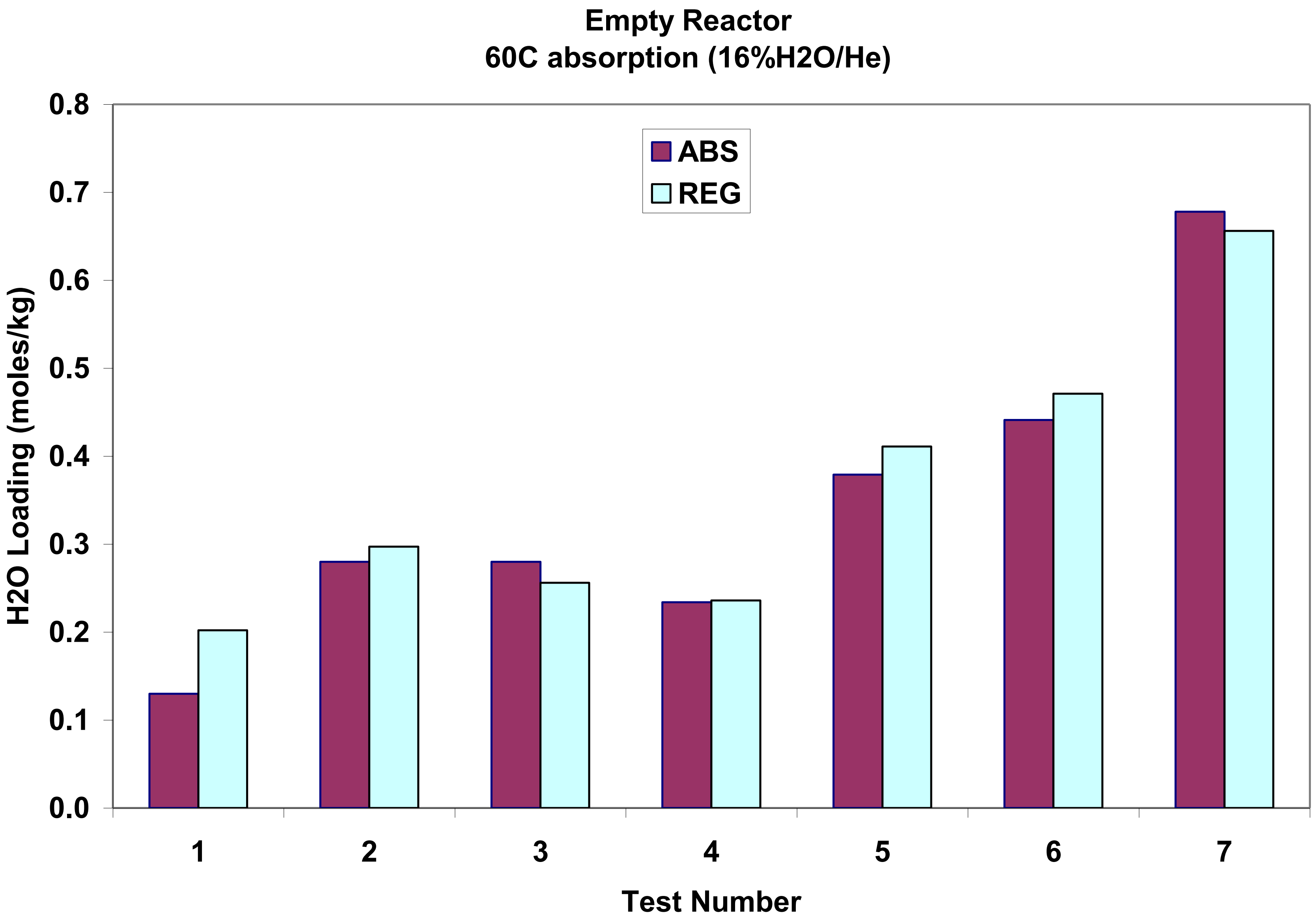
Empty Reactor
60C absorption (16%H2O/He)
ABS
REG
H2O Loading (moles/kg)
0.8
0.7
0.6
0.5
0.4
0.3
0.2
0.1
0.0
1
2
3
4
5
6
7
Test Number

Figure 38

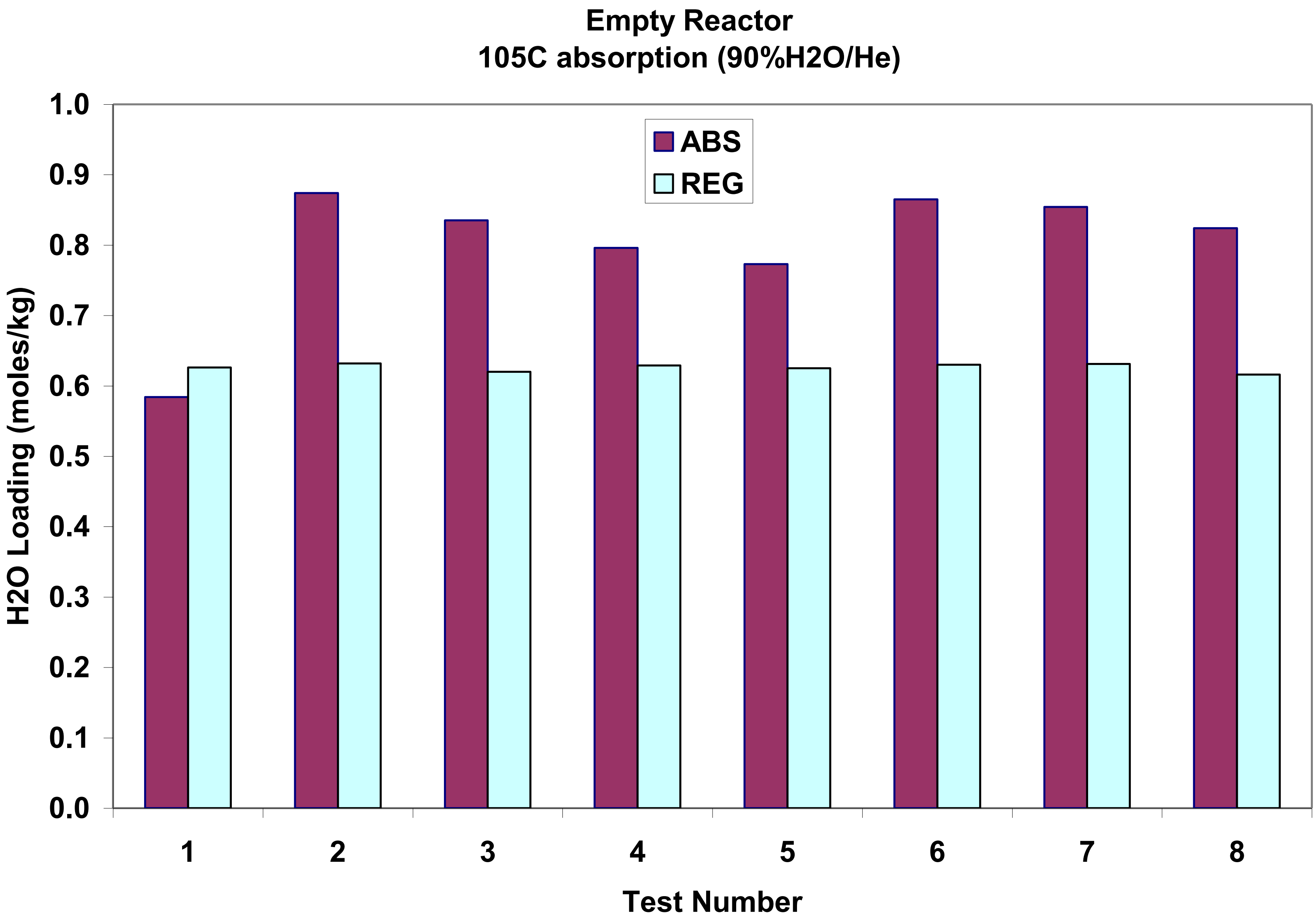
Empty Reactor
105C absorption (90%H2O/He)
ABS
REG
H2O Loading (moles/kg)
1.0
0.9
0.8
0.7
0.6
0.5
0.4
0.3
0.2
0.1
0.0
1
2
3
4
5
6
7
8
Test Number

Figure 39

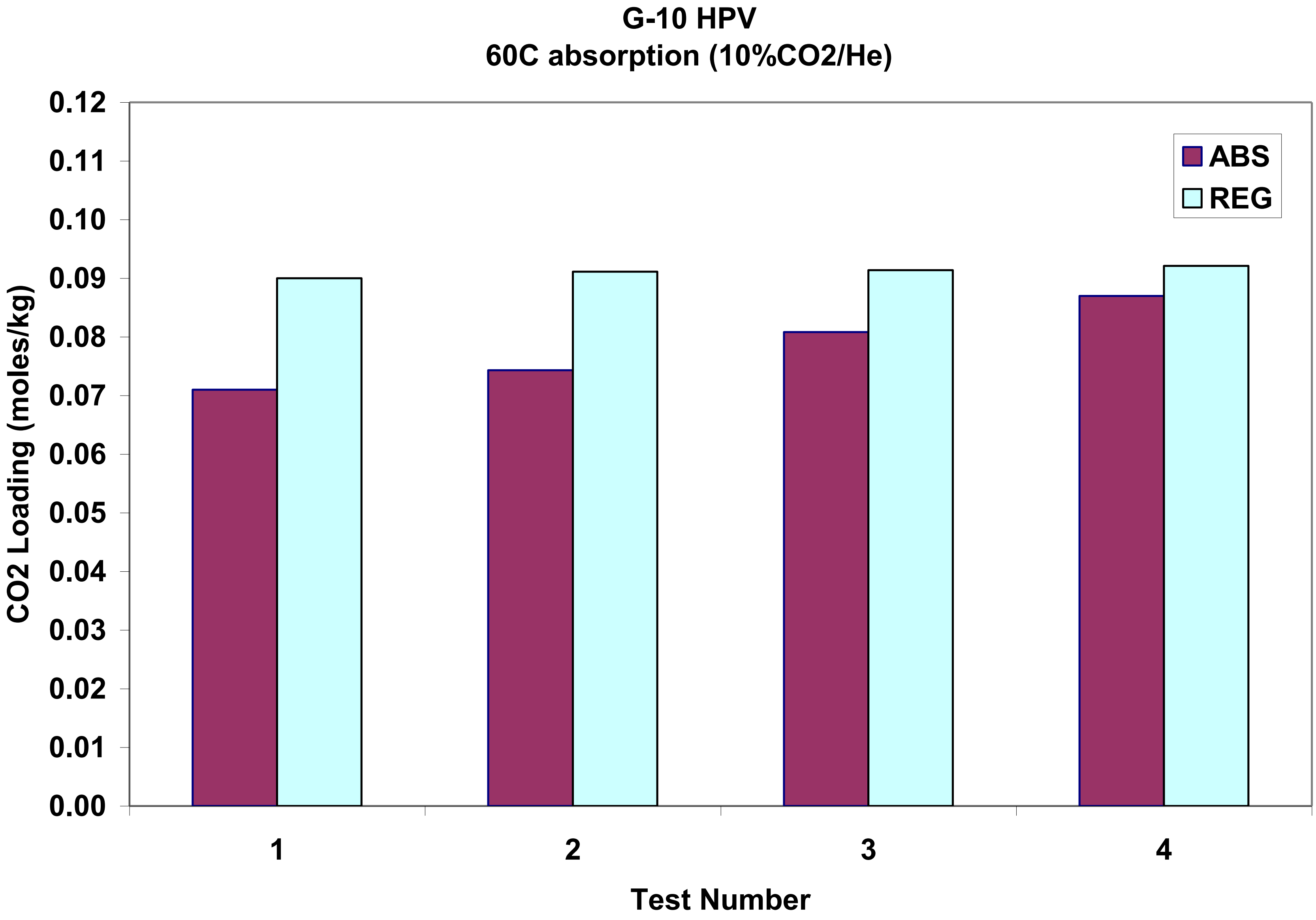
G-10 HPV
60C absorption (10%CO2/He)
CO2 Loading (moles/kg)
0.12
0.11
0.10
0.09
0.08
0.07
0.06
0.05
0.04
0.03
0.02
0.01
0.00
ABS
REG
1
2
3
4
Test Number

Figure 40

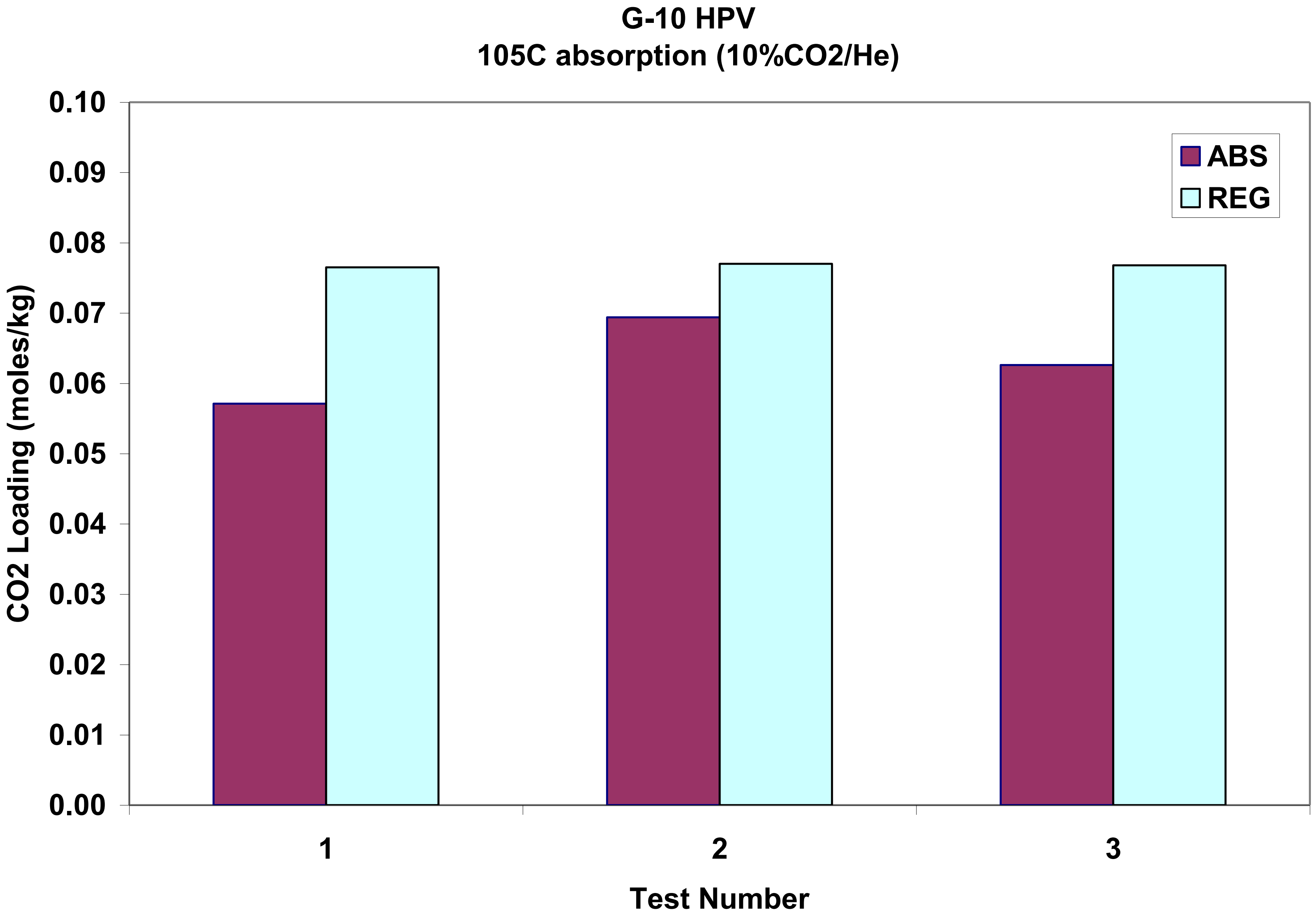
G-10 HPV
105C absorption (10%CO2/He)
0.10
0.09
0.08
0.07
0.06
0.05
0.04
0.03
0.02
0.01
0.00
CO2 Loading (moles/kg)
ABS
REG
1
2
3
Test Number

Figure 41

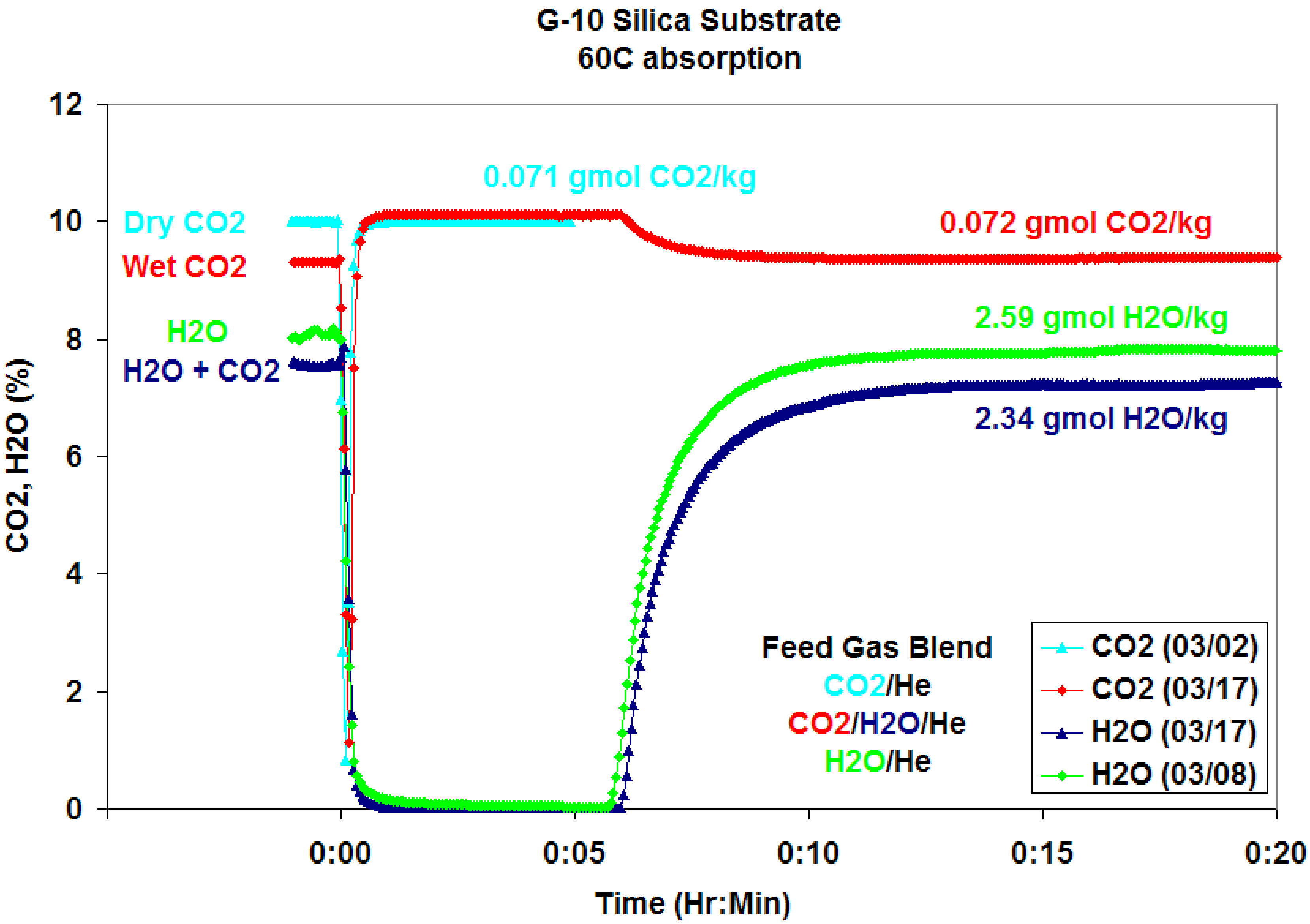
G-10 Silica Substrate
60C absorption
0.071 gmol CO2/kg
Dry CO2
Wet CO2
0.072 gmol CO2/kg
H2O
H2O + CO2
2.59 gmol H2O/kg
2.34 gmol H2O/kg
Feed Gas Blend
CO2/He
CO2/H2O/He
H2O/He
CO2 (03/02)
CO2 (03/17)
H2O (03/17)
H2O (03/08)
CO2, H2O (%)
12
10
8
6
4
2
0
0:00
0:05
0:10
0:15
0:20
Time (Hr:Min)

Figure 42

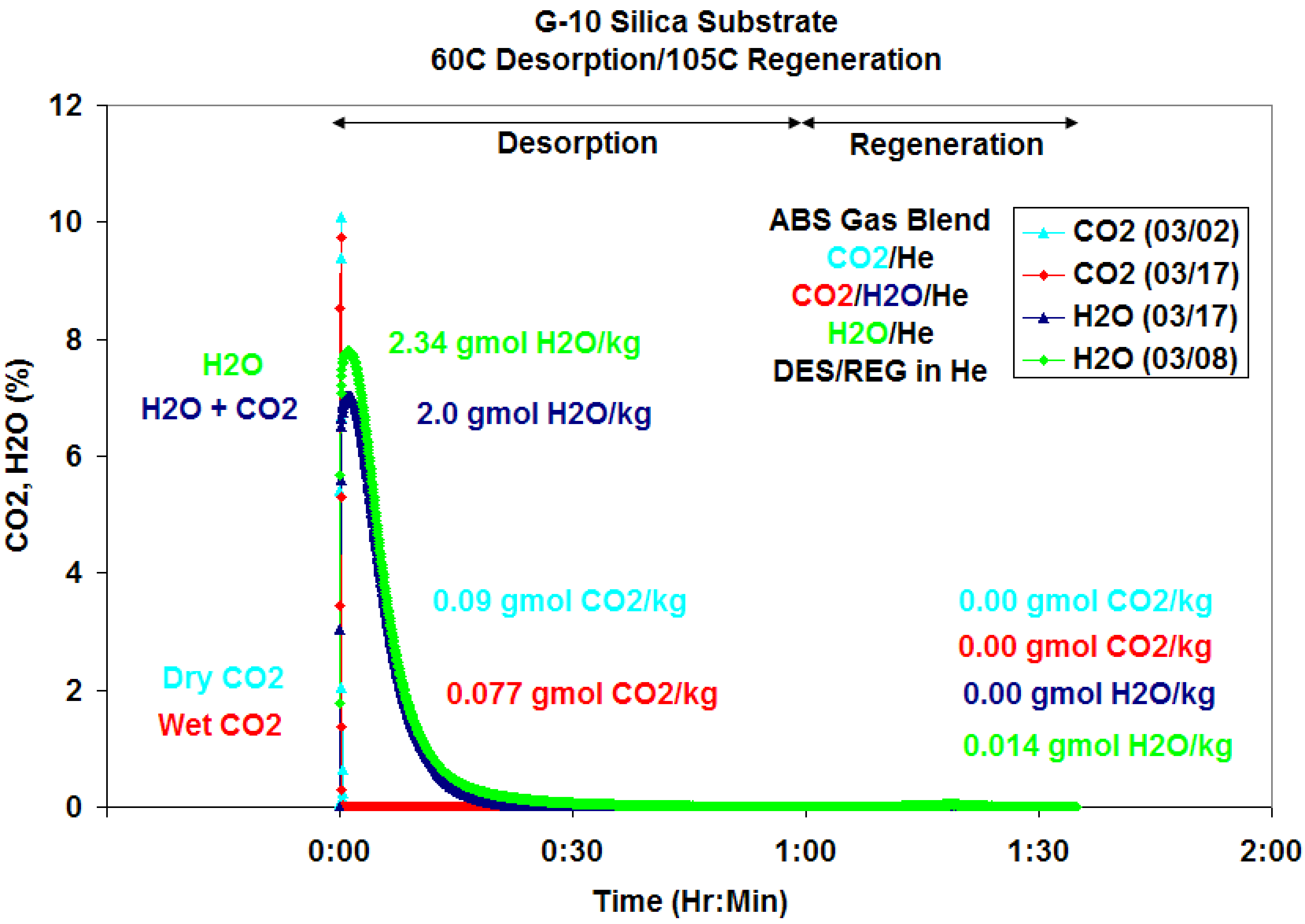
G-10 Silica Substrate
60C Desorption/105C Regeneration
Desorption
Regeneration
ABS Gas Blend
CO2/He
CO2/H2O/He
H2O/He
DES/REG in He
CO2 (03/02)
CO2 (03/17)
H2O (03/17)
H2O (03/08)
H2O
H2O + CO2
2.34 gmol H2O/kg
2.0 gmol H2O/kg
0.09 gmol CO2/kg
0.077 gmol CO2/kg
Dry CO2
Wet CO2
0.00 gmol CO2/kg
0.00 gmol CO2/kg
0.00 gmol H2O/kg
0.014 gmol H2O/kg
CO2, H2O (%)
0
2
4
6
8
10
12
0:00
0:30
1:00
1:30
2:00
Time (Hr:Min)

Figure 43

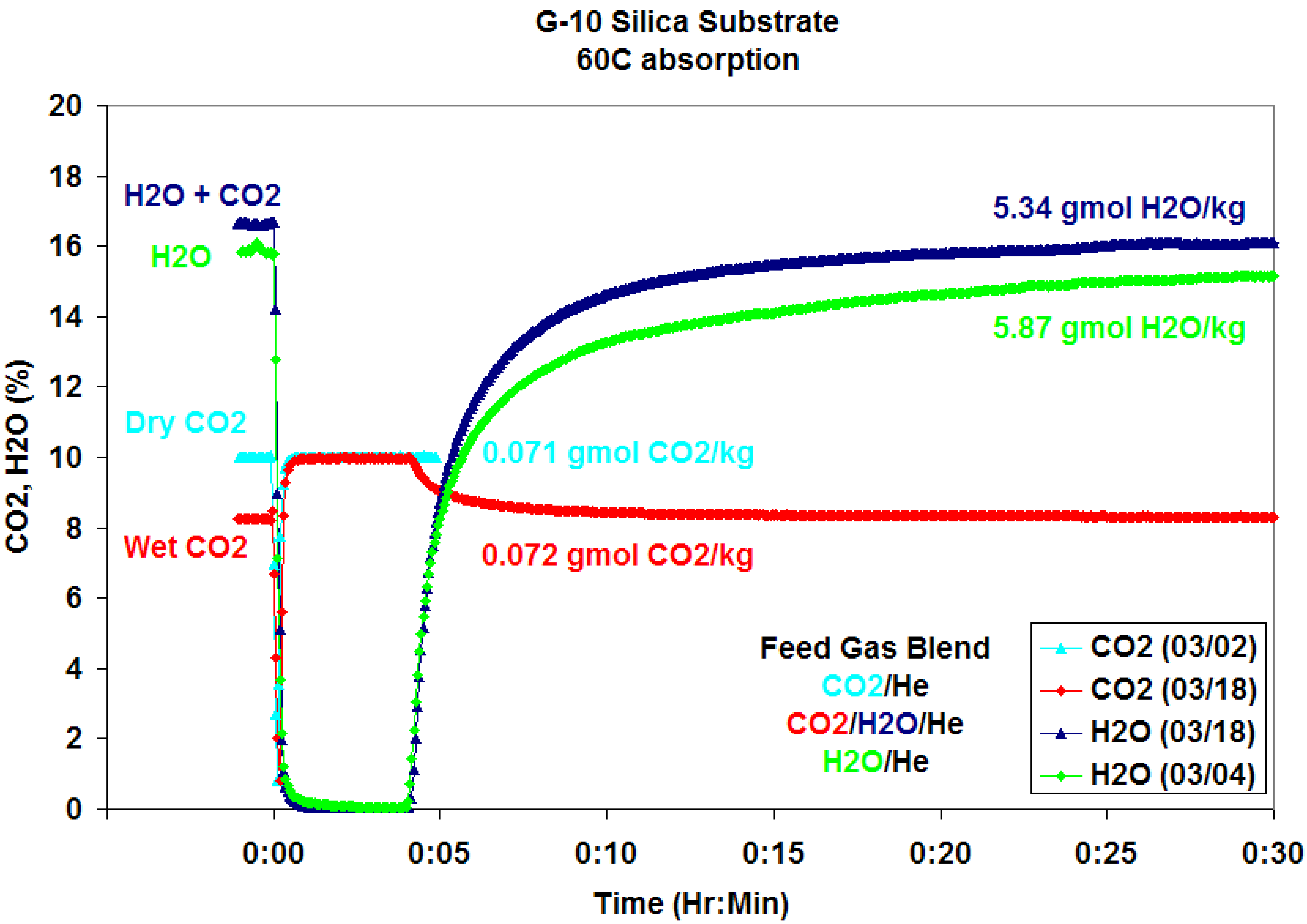
G-10 Silica Substrate
60C absorption
CO2, H2O (%)
20
18
16
14
12
10
8
6
4
2
0
0:00
0:05
0:10
0:15
0:20
0:25
0:30
Time (Hr:Min)
H2O + CO2
H2O
Dry CO2
Wet CO2
5.34 gmol H2O/kg
5.87 gmol H2O/kg
0.071 gmol CO2/kg
0.072 gmol CO2/kg
Feed Gas Blend
CO2/He
CO2/H2O/He
H2O/He
CO2 (03/02)
CO2 (03/18)
H2O (03/18)
H2O (03/04)

Figure 44

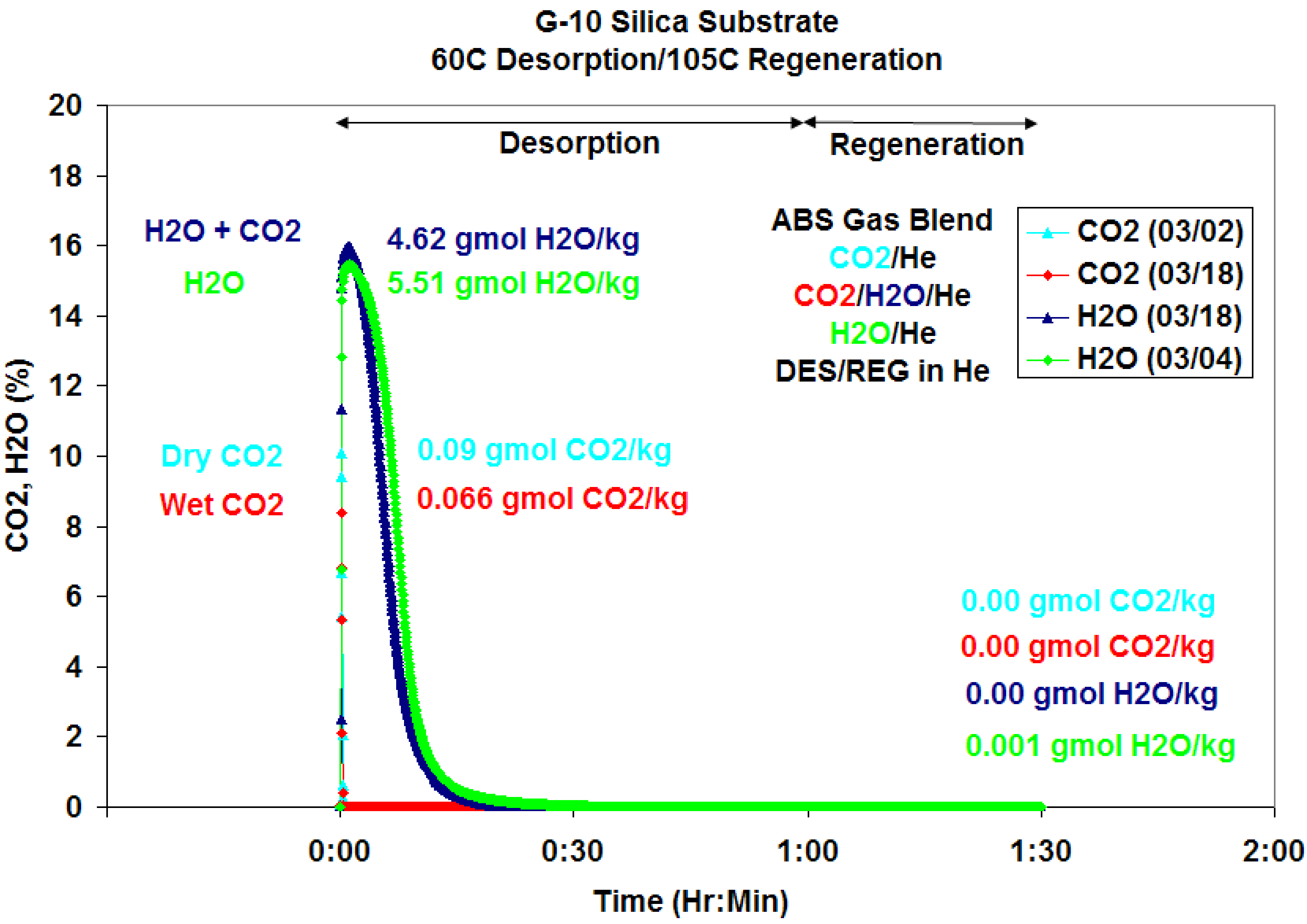
G-10 Silica Substrate
60C Desorption/105C Regeneration
Desorption
Regeneration
H2O + CO2
H2O
4.62 gmol H2O/kg
5.51 gmol H2O/kg
ABS Gas Blend
CO2/He
CO2/H2O/He
H2O/He
DES/REG in He
CO2 (03/02)
CO2 (03/18)
H2O (03/18)
H2O (03/04)
Dry CO2
Wet CO2
0.09 gmol CO2/kg
0.066 gmol CO2/kg
0.00 gmol CO2/kg
0.00 gmol CO2/kg
0.00 gmol H2O/kg
0.001 gmol H2O/kg
CO2, H2O (%)
20
18
16
14
12
10
8
6
4
2
0
0:00
0:30
1:00
1:30
2:00
Time (Hr:Min)

Figure 45

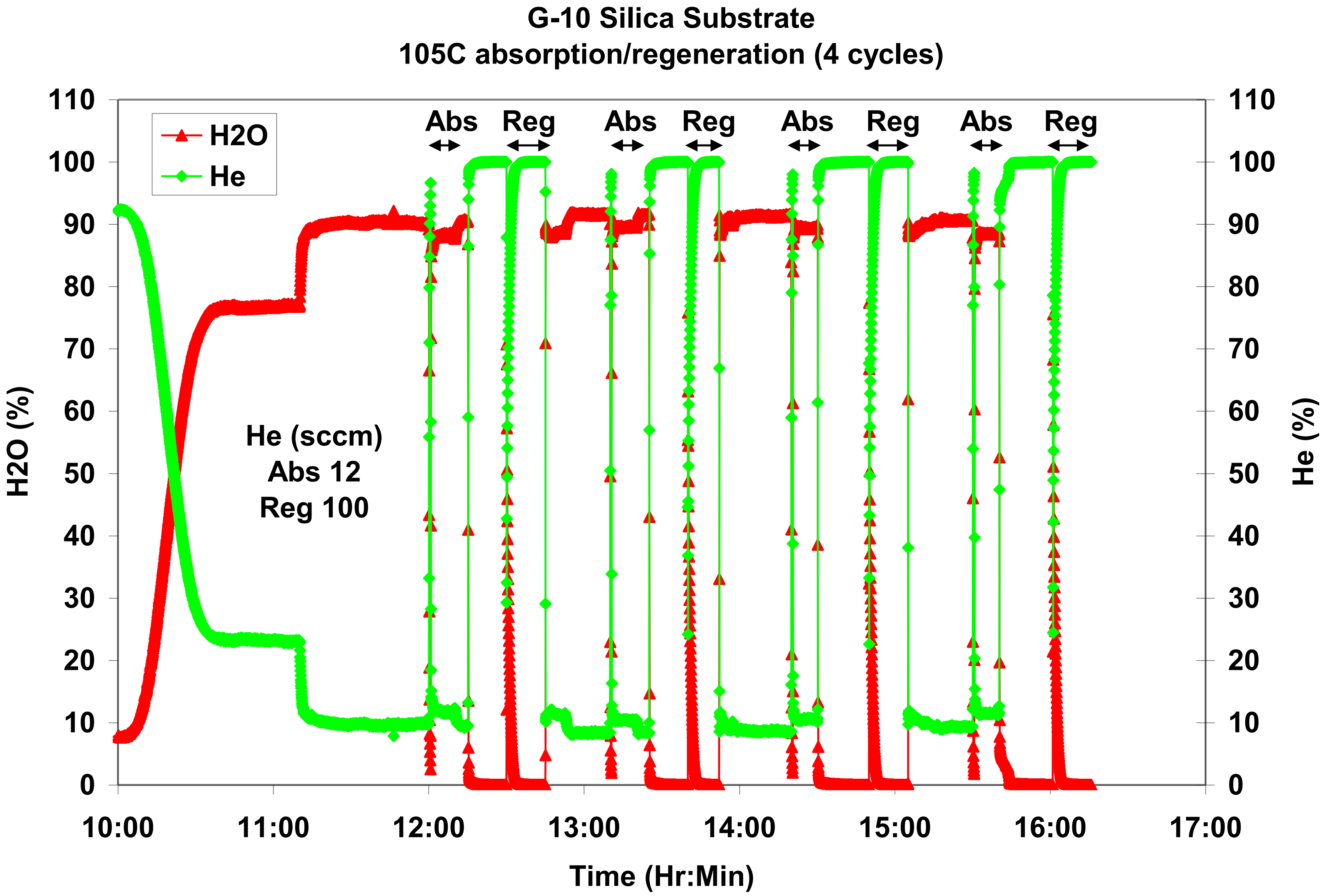
G-10 Silica Substrate
105C absorption/regeneration (4 cycles)
H2O
He
Abs
Reg
Abs
Reg
Abs
Reg
Abs
Reg
He (sccm)
Abs 12
Reg 100
H2O (%)
He (%)
110
100
90
80
70
60
50
40
30
20
10
0
10:00
11:00
12:00
13:00
14:00
15:00
16:00
17:00
Time (Hr:Min)

Figure 46

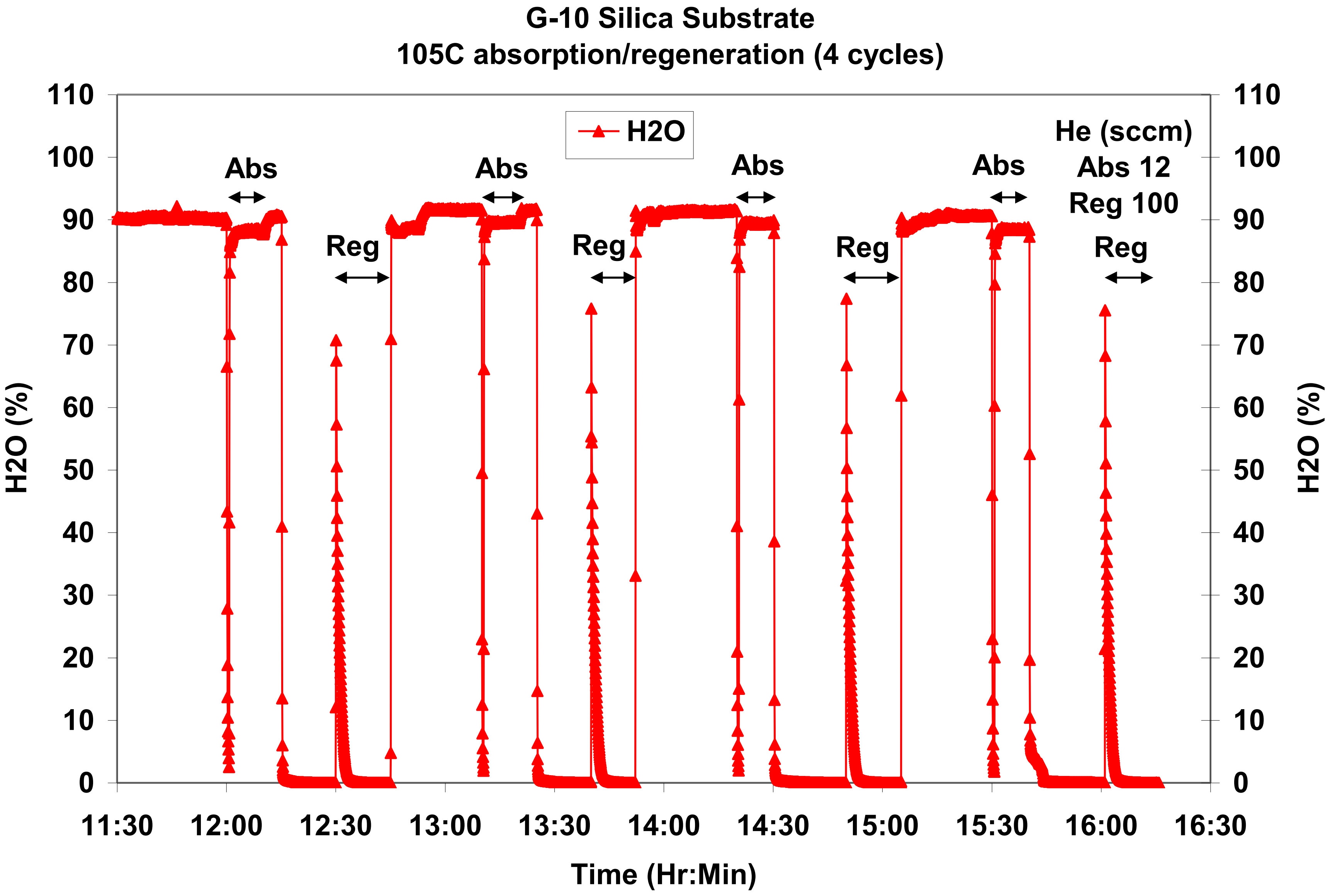
G-10 Silica Substrate
105C absorption/regeneration (4 cycles)
H2O
He (sccm)
Abs 12
Reg 100
Abs
Abs
Abs
Abs
Reg
Reg
Reg
Reg
110
100
90
80
70
60
50
40
30
20
10
0
H2O (%)
H2O (%)
11:30
12:00
12:30
13:00
13:30
14:00
14:30
15:00
15:30
16:00
16:30
Time (Hr:Min)

Figure 47

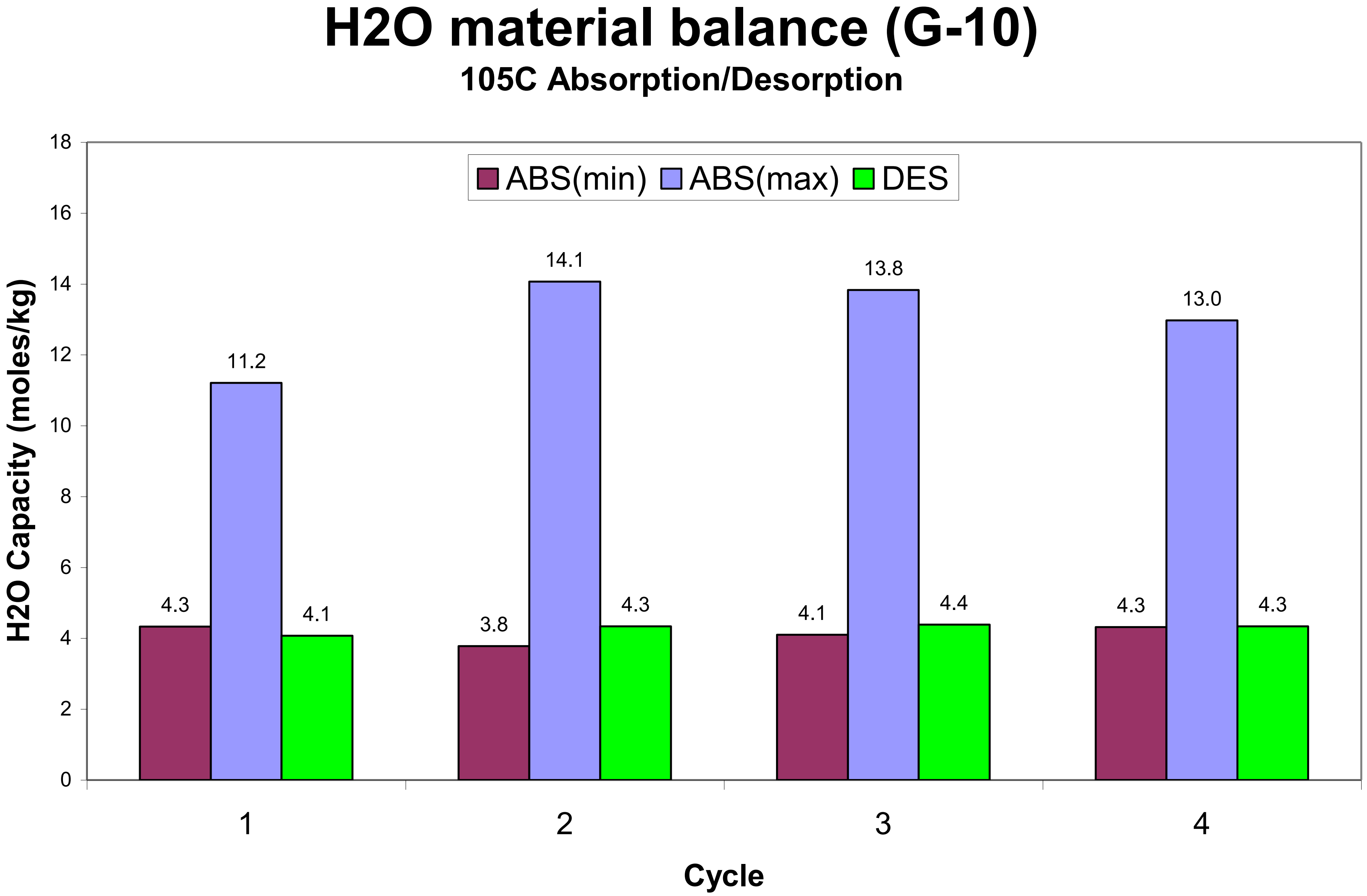
H2O material balance (G-10)
105C Absorption/Desorption
ABS(min)
ABS(max)
DES
H2O Capacity (moles/kg)
0
2
4
6
8
10
12
14
16
18
4.3
11.2
4.1
3.8
14.1
4.3
4.1
13.8
4.4
4.3
13.0
4.3
1
2
3
4
Cycle

Figure 48

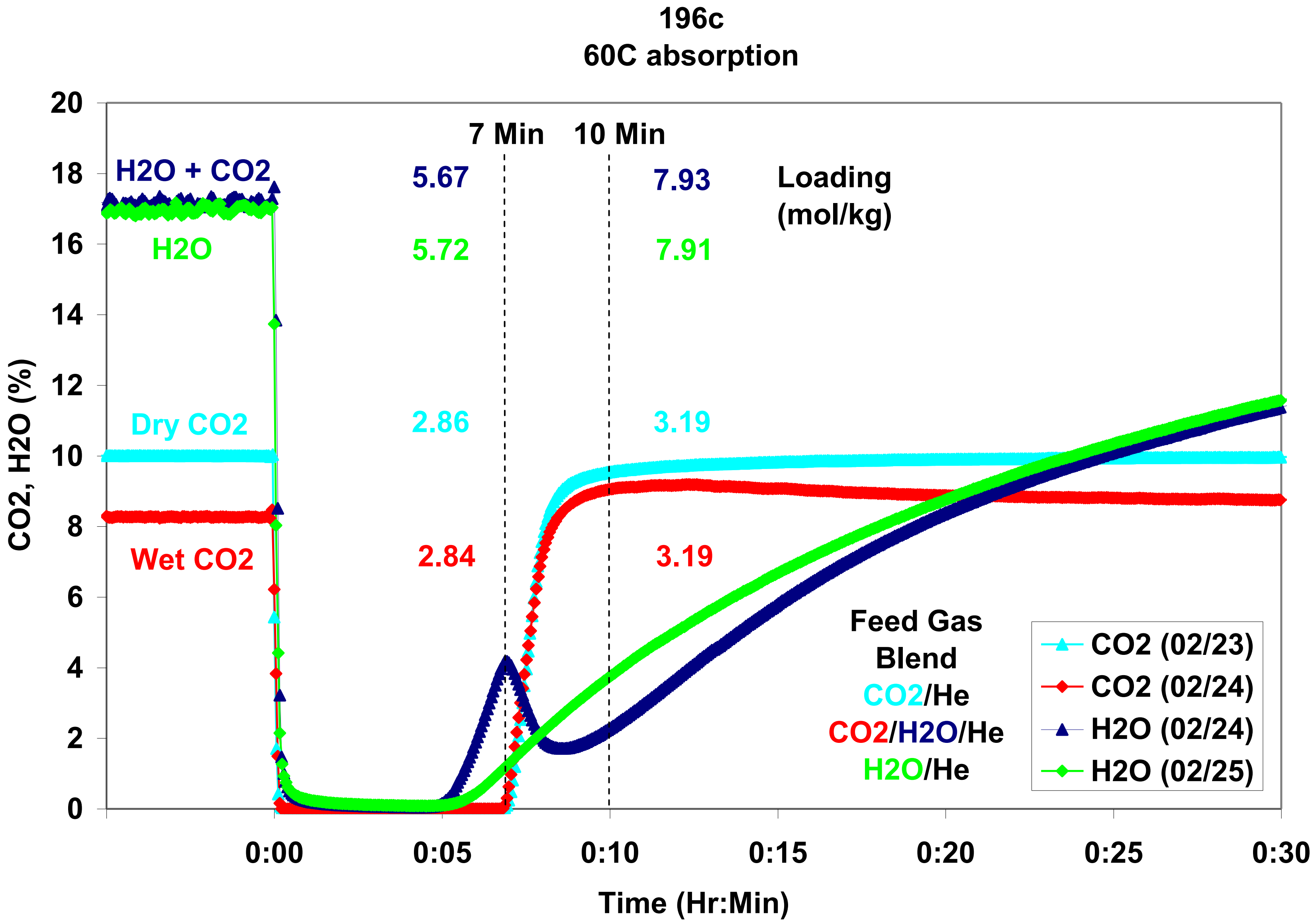
196c
60C absorption
20
18
16
14
12
10
8
6
4
2
0
CO2, H2O (%)
7 Min
10 Min
H2O + CO2
5.67
7.93
Loading (mol/kg)
H2O
5.72
7.91
Dry CO2
2.86
3.19
Wet CO2
2.84
3.19
Feed Gas Blend
CO2/He
CO2/H2O/He
H2O/He
CO2 (02/23)
CO2 (02/24)
H2O (02/24)
H2O (02/25)
0:00
0:05
0:10
0:15
0:20
0:25
0:30
Time (Hr:Min)

Figure 49

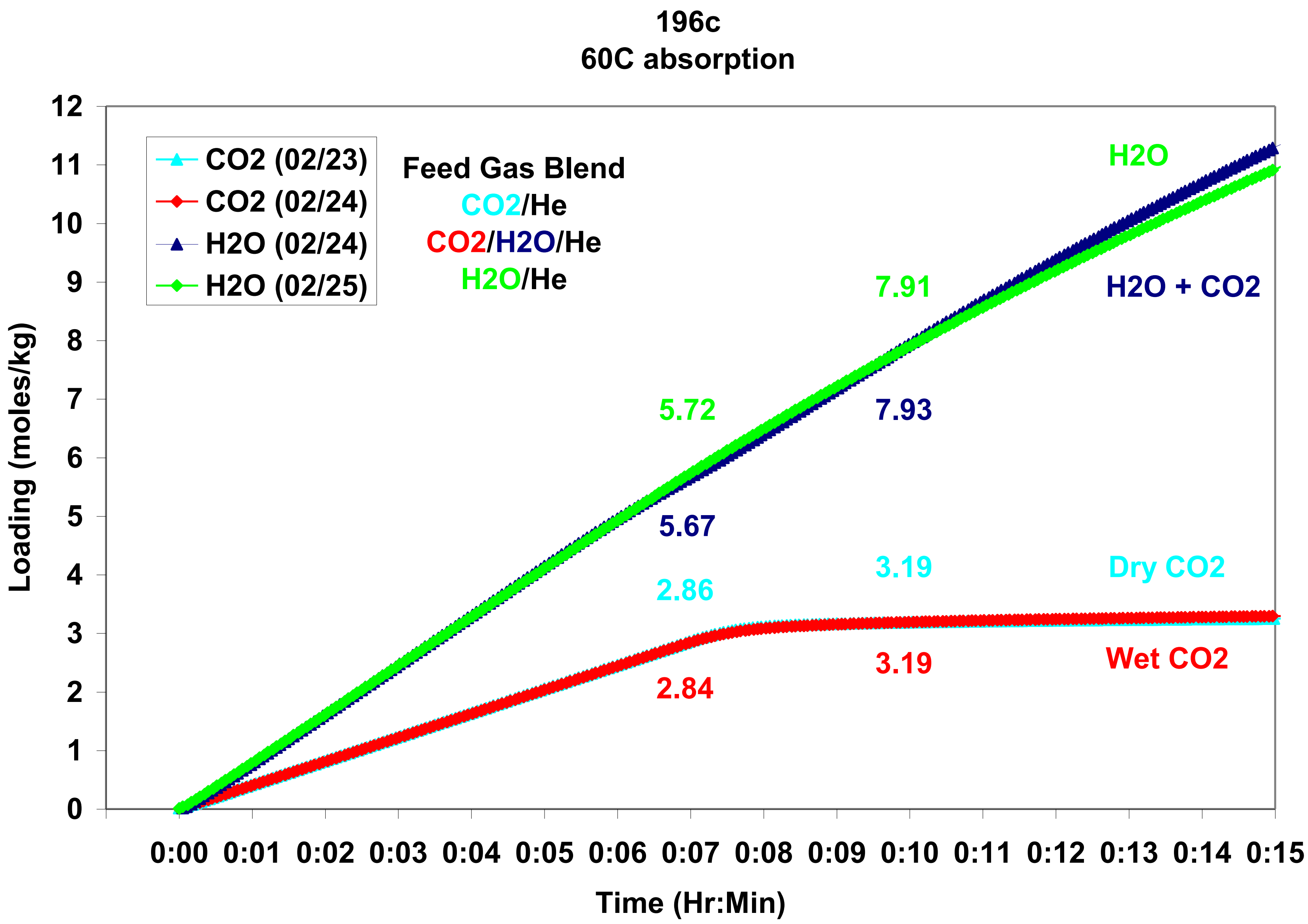
196c
60C absorption
Loading (moles/kg)
0
1
2
3
4
5
6
7
8
9
10
11
12
Time (Hr:Min)
0:00
0:01
0:02
0:03
0:04
0:05
0:06
0:07
0:08
0:09
0:10
0:11
0:12
0:13
0:14
0:15
CO2 (02/23)
CO2 (02/24)
H2O (02/24)
H2O (02/25)
Feed Gas Blend
CO2/He
CO2/H2O/He
H2O/He
H2O
H2O + CO2
7.91
7.93
5.72
5.67
2.86
3.19
Dry CO2
2.84
3.19
Wet CO2

Figure 50

Sorbent Loop: Conceptual BIAS Process with PEI/Silica

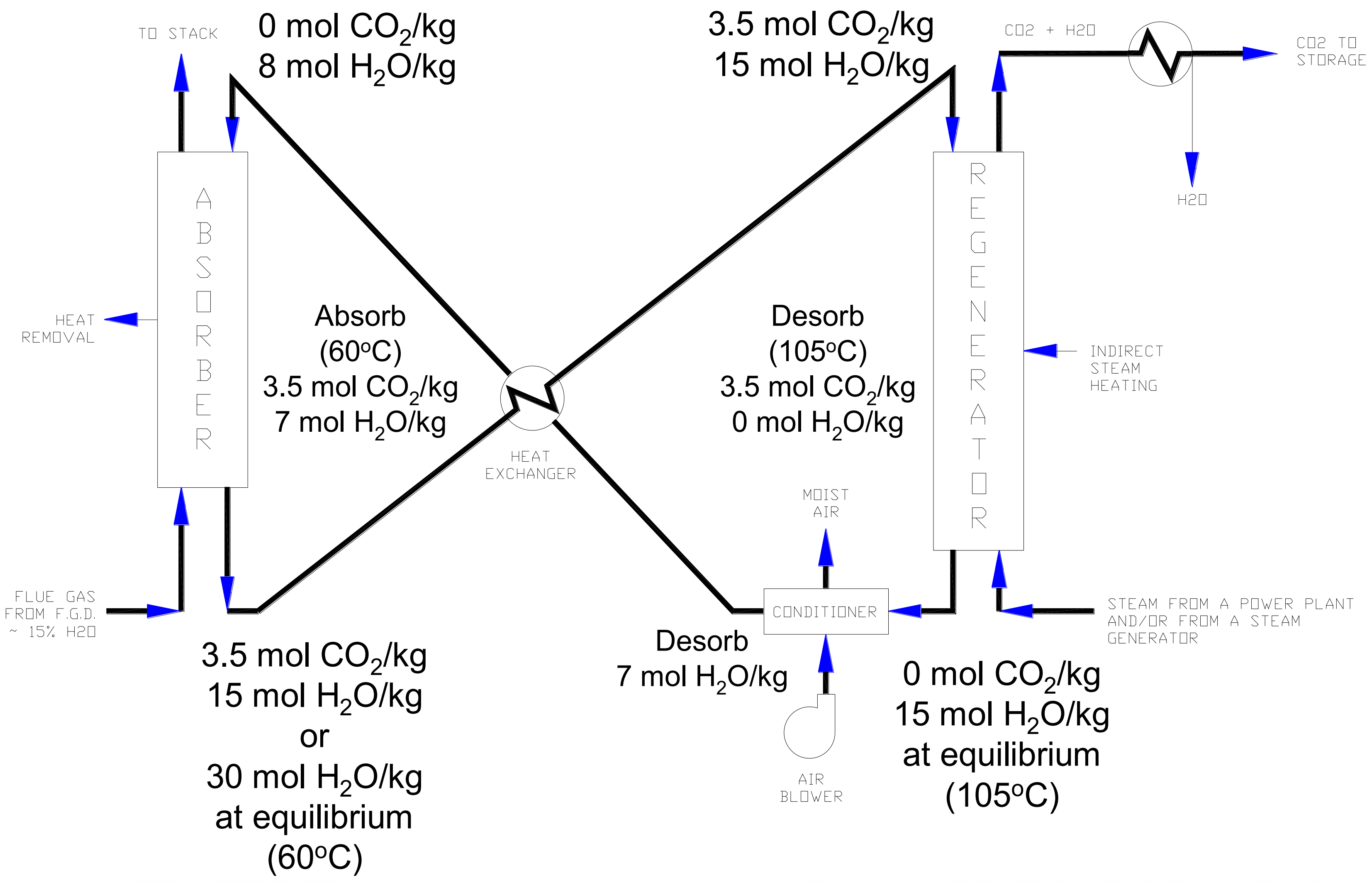

0 mol CO_2/kg
8 mol H_2O/kg

3.5 mol CO_2/kg
15 mol H_2O/kg

Absorb
(60^oC)
3.5 mol CO_2/kg
7 mol H_2O/kg

Desorb
(105^oC)
3.5 mol CO_2/kg
0 mol H_2O/kg

3.5 mol CO_2/kg
15 mol H_2O/kg
or
30 mol H_2O/kg
at equilibrium
(60^oC)

Desorb
7 mol H_2O/kg

0 mol CO_2/kg
15 mol H_2O/kg
at equilibrium
(105^oC)